Studies on Bipedal Robots with Adjustable Whole-Body Dynamics Using Actuator Network System

HUTHAIFA ABEDALLAH MOHAMMAD AHMAD

MARCH 2021

Studies on Bipedal Robots with Adjustable Whole-Body Dynamics Using Actuator Network System

A dissertation submitted to
THE GRADUATE SCHOOL OF ENGINEERING SCIENCE
OSAKA UNIVERSITY
in partial fulfillment of the requirements for the degree of
DOCTOR OF PHILOSOPHY IN ENGINEERING

BY

HUTHAIFA ABEDALLAH MOHAMMAD AHMAD

MARCH 2021

ABSTRACT

A human body functions the best when all the parts operate together as a coherent unit. The natural walking behavior of humans, for instance, results from the interaction among all the parts of the body, and it is not merely a result of the dynamics generated by each leg separately; the synergy between the two legs and the way they interact with each other, along with their interactions with other limbs, plays a major role in the adaptive walking behavior of humans. Therefore, to realize a robot with adaptable behavior, it should be enabled to adjust its morphology accordingly in response to environmental changes. From this perspective, recent studies have considered variable compliant actuation to change the physical characteristics of the robot as it interacts with the environment. Robots with this ability showed a variety of efficient stable motions during contact with the environment. However, having locally variable compliant parts with independent dynamics under the same body may be insufficient for achieving adaptability in diverse environments. To extend the idea of variable compliant actuation, from being used locally to the level of whole-body dynamics, in the present study, we used the principle of Actuator Network System (ANS) in developing our robots.

To test the feasibility of using ANS in legged robots, we started by developing an eight-legged rimless wheel robot with ANS that allows energy transfer among limbs. With this simple mechanism that resembles bipedal robots' dynamics, experiments were conducted to examine how changing the connection patterns between legs will influence the efficient behavior of the robot. As the experimental results showed, to obtain optimum efficiency during the different gate phases, the robot needs to select a different connection pattern respectively.

Since the feasibility of implementing ANS was proven on an approximate representation of bipedal robots, the next step of this study was to develop an actual bipedal robot with ANS. The developed robot utilizes the principle of actuator network system to manipulate its whole-body dynamics. With its adaptive morphology, the current robot is able to adjust the physical characteristics of its legs (compliance and stiffness), as well as changing the way its legs are interacting with each other and the environment. The main finding of the experiments conducted with this robot is that the robot performance in varying environments cannot be at its best with a single body morphology, but it needs to appropriately change its whole body dynamics for better adaptation. For example, a connection pattern that better suits a certain ground material, it does not necessarily suit other ground materials, and what is bad for some ground materials, it might be the best for others. Therefore, exploiting these various dynamics is the way to enable the robot from realizing adaptability to any given situation.

For the next step of our research, we investigated the influence of adding an upper-body to the bipedal robot on its stable walking behavior. The movement pattern of the added upper-body (the way it oscillates) depends on the type of interactions created with other limbs since all body parts are mutually interconnected through an actuator network system. Throughout the experiments, various connection patterns between the lower and upper body parts were tested. The results clearly demonstrated the significance of engaging upper-body movements through its interaction with other body parts during locomotion. The robot with a fixed (motionless) upper-body exhibited unstable walking behaviors, however, once the same upper-body was involved and interacted properly with other body parts, its movement helped to retrieve the stable behavior of the robot.

TABLE OF CONTENTS

CHAPTER 1

INTRODUCTION

In diverse situations, humans produce natural and adaptable bipedal locomotion by cooperatively manipulating the interactions among the different parts of their bodies and the environment. Therefore, to accommodate different environments, the synergy between the two legs and the way they interact with each other, along with their interactions with other limbs, plays a major role in the adaptive walking behavior of humans [1], [2]. Because of these complex tasks performed by the human's body during locomotion, it is hard to augment bipedal robots with human-like locomotion abilities. For this matter, throughout the years, many researchers have conducted intensive studies to build bipedal robots with gait patterns similar to that of humans [3], [4]. They follow in their research two approaches, the numerical computation approach (conventional), and the embodied intelligence approach (modern) [5].

Many of the robots following the conventional approach have demonstrated impressive and versatile motion behaviors, which made them categorized amongst the most advanced humanoid robots. Examples of these robots are the Humanoid Robot Project's HRP series of robots [6] and Honda's ASIMO [7]. However, accurate models of the robot's own body and its surrounding environment are crucial for these robots to achieve adaptability.

On the other hand, researchers following the embodied intelligence approach have developed robots with efficient and more natural walking behaviors. Oftentimes they get their insights into design concepts and ideas for these robots from nature [8], [9]. They utilize the different mechanical dynamics and the material properties of their bodies and exploit its interaction with the environment

to realize efficient behaviors. A common example of these robots are Passive Dynamic Walkers (PDWs) [10], [11], [12]. With their simple mechanical structures, passive dynamic walkers have remarkably shown humanlike motions. It is capable of walking down an incline without any active control or energy input; only gravity and the natural dynamics alone generate the walking cycle. Despite their efficiency, environments in which these robots are capable of operating are confined to inclines of particular slopes. Therefore, these robots are not versatile and lack adaptability to accommodate different environments.

For a robot to realize adaptable behavior, it should be enabled to manipulate its morphology to generate desirable dynamics in response to environmental changes [8], [9]. Based on this view, many studies have addressed this issue by implementing soft materials and variable stiffness actuators [13], [14], [15]. These robots exploited the natural dynamics as it interacts with the environment, and generated more energy-efficient locomotion behaviors [16], [17], [18]. However, while moving within a given environment or during transitioning between different terrains, individually installed parts with variable stiffness actuation may not be sufficient without direct interactions among them. Especially to allow adaptation of opposing dynamic requirements such as stability, maneuverability, efficiency, and speed.

In order to leverage adaptive morphology in robotic systems and allow direct interactions among the different parts of the robot's body, here in this research, we are using the principle of Actuator Network System (ANS). ANS was proposed in previous researches to extend the dynamic performances and provide new functionalities of legged robots by changing the physical characteristics of their bodies [19], [20], [21]. ANS is a closed fluid system. It is composed of mul-

tiple actuators that are connected to each other through tubes and valves with fluid-mediated interaction between them. By changing the connection patterns between the actuators, the fluid flow will change the interaction between them, thus, changing the entire bodys dynamics. Therefore, from a morphological point of view, the robot can change its morphology according to the environment by changing the connection patterns between its actuators. Here in the present study, ANS is used to allow energy transfer among limbs through passive interactions among mutually interconnected air cylinders mounted on the robots' legs.

To investigate the way in which energy transfer between the legs of a robot can improve its walking performance, we developed four different legged robots as shown in figure 1.1. The first robot, called OCTANS, demonstrated in figure 1.1-a, is an eight (OCT)-legged rimless wheel robot with an ANS. This simple mechanism is considered an approximate representation of bipedal robots. After that, we developed a simple structure bipedal robot with ANS as shown in figure 1.1-b. However, this robot required a supporting structure to maintain balance during locomotion. Therefore, we moved to the next step and developed our third robot PedestriANS, as illustrated in figure 1.1-c. It is a self-balanced bipedal legged robot that uses ANS between its legs to adaptively change the type of interactions between its interconnected legs, as well as adjusting their physical characteristics such as compliance and stiffness. Then for our fourth step, as demonstrated in figure 1.1-d, we upgraded the structure design of PedestriANS and extended the actuator network system to include an upper-body. For each of these four robots, experiments were conducted under various environmental conditions to test the effects of different connection patterns among the different body parts of the robots on their adaptive walking behaviors. Afterward,

we built a simulation environment and ran several experiments of PedestriANS on different ground materials to better understand the role of ANS in realizing adaptability. For example, why certain connection pattern X better suits a particular ground material Y. In other words, to further investigate the relationship between the robot characteristics and the environment in which the robot is operating.

The position of our study among other studies on robotics is shown in figure 1.2. As the axes indicate, the distribution of these robots is based on two parameters: a) whether the focus is on morphological computation or numerical computation and b) whether the robot has rigid or compliant legs. For example, the position of Aldebaran NAO [24] in figure 1.2 can be ascribed to its rigid body structure and active control of every joint angle at all times. The Delft biped robot [25], by contrast, is placed on the opposite side because it employs lower levels of control and energy than other powered robots owing to the morphological contribution of its compliant hip actuation and its passive ankle. The shifted-up robots exhibit whole body dynamics.

The rest of the dissertation is organized as follows. Chapter 2 explains the concept of Actuator Network System (ANS) in detail, why we are using it, and its role and contribution in robotic systems. Chapter 3 presents OCTANS's development, structure, tested connection patterns during the experiments, experimental setups and procedures, and the obtained results and discussions. Chapters 4 presents the development of a simple structure bipedal robot, the investigated connections between the robot's legs, experimental setups and procedures, and discussion about the obtained results. Chapter 5 introduces the robot PedestriANS, its structure, the examined types of legs and their various

interactions, the explanation of experimental setups and procedures, and the robot performance evaluation. Chapter 6 presents the updated design of PedestriANS, its added upper-body, the connection patterns between the lower and upper body parts that were tested during the experiments, experimental setups and procedures, and the obtained results and discussions. Chapter 7 sheds light on the experiments conducted in simulation environments, and investigates the relationship between the robot characteristics and the environment in which the robot is operating. Chapter 8 concludes the paper together with some pointers to future areas of research.

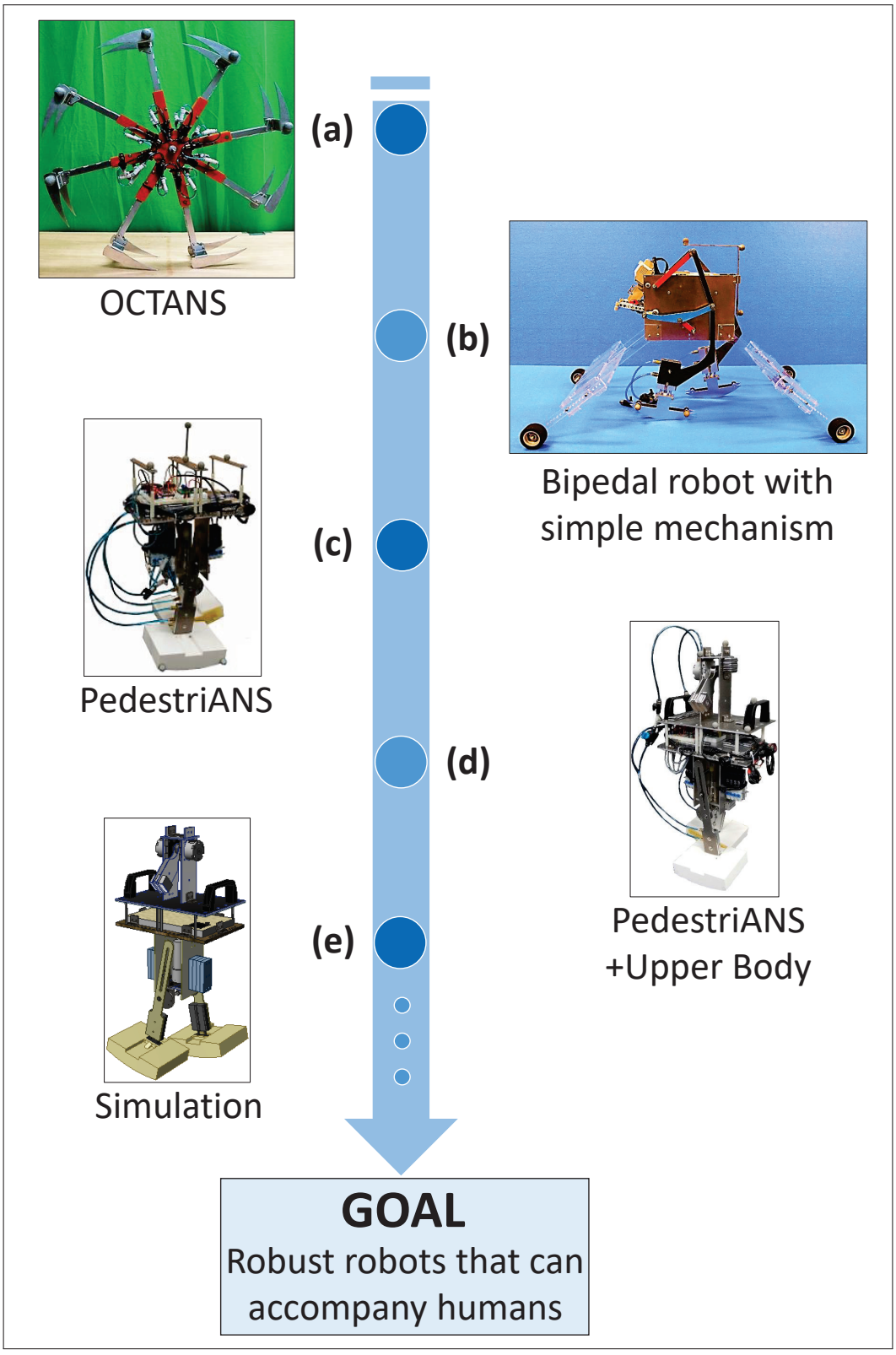

Figure 1.1: The developed legged robots with ANS: Steps taken towards realizing robust robots with adaptive morphology

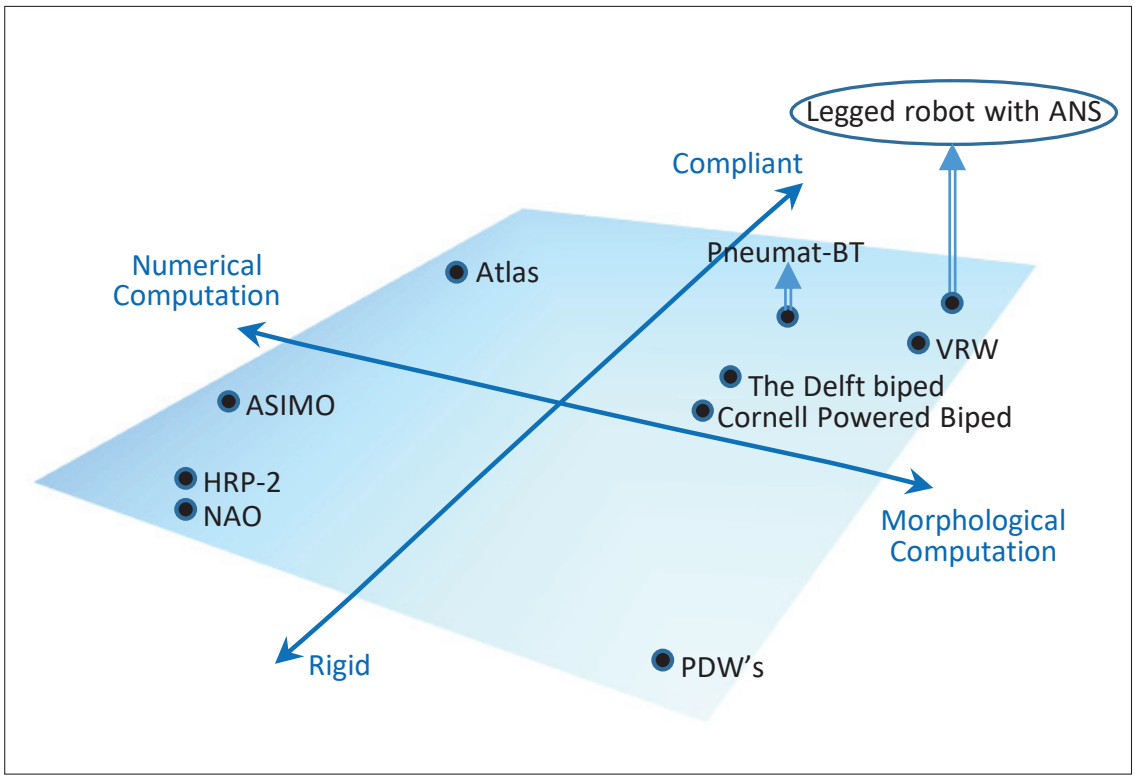

Figure 1.2: Research map showing the position of the developed legged robots with ANS with respect to other robots.

CHAPTER 2

ACTUATOR NETWORK SYSTEM (ANS)

Actuator Network System (ANS) was proposed in previous researches and implemented in different applications, such as building robotic spine [22], arm [23], and multi-legged robots [21]. As the term implies, ANS is composed of multiple actuators that are connected to each other through tubes and valves with fluid-mediated interaction between them. Corresponding to each connection pattern among the actuators, distinct dynamics of the robots body will come out. Therefore, the concept of ANS was proposed in order to leverage adaptive morphology in robotic systems by allowing direct interactions among the different body parts of the robot. ANS can extend the dynamic performances and provide new functionalities of robotic systems by changing the physical characteristics of their bodies to realize adaptability in response to environmental changes.

A simple explanation of how ANS works is presented in figure 2.1. If we have two separate cylinders as shown in figure 2.1-a, it is common sense to notice that the movement of one cylinder will not affect the movement of the other cylinder since they are not connected with each other. In contrast, if these two cylinders are mutually interconnected, as can be seen in figure 2.1-b and c, the movement of one cylinder will affect the dynamics of the other one. In other words, by applying an external force to one of the mutually connected cylinders, the force will be transmitted via fluid to the other cylinder causing it to move. And the movement pattern of these actuators directly depends on the type of connections between them. For example, connecting the upper champers of both cylinders together while connecting the lower chambers together as in the

case of figure 2.1-b, caused the actuators to move in the same direction. On the other hand, when the upper chamber of each cylinder was connected to the other cylinder's lower chamber as in figure 2.1-c, it caused the actuators to move in an opposing direction. Therefore, with different connection patterns of the ANS, different interactions among the actuators will emerge to generate a variety of dynamics for the robots body.

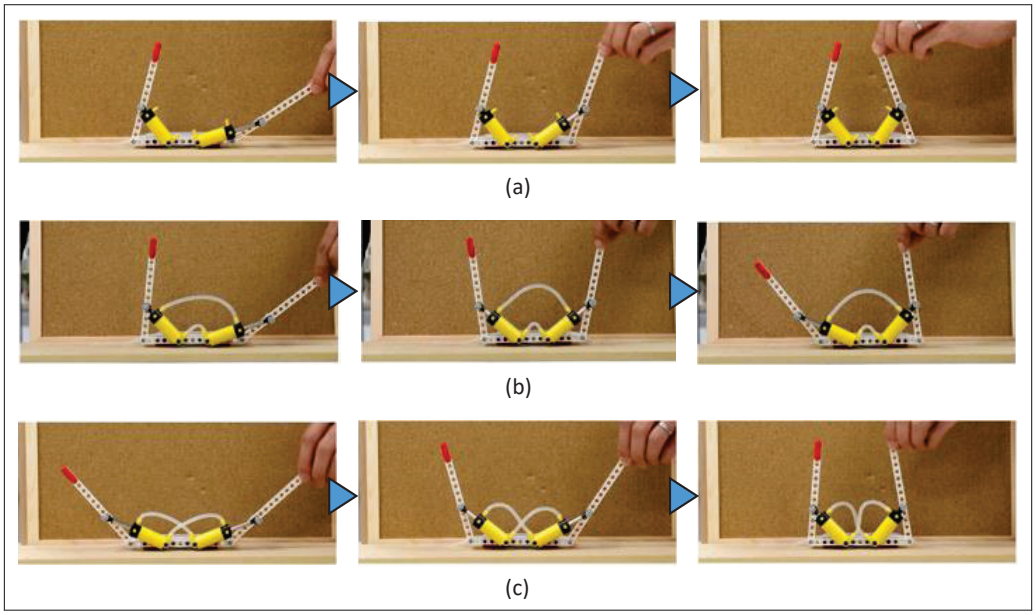

Figure 2.1: Comparison of joint motion in response to external force. Two cylinders are mounted on each joint. (a) The two cylinders are separated. (b) and (c) The two cylinders are mutually interconnected.

To better understand the reasons behind using the concept of ANS in our study, figure 2.2 compares the difference between implementing a hardware network of physical connections among several actuators of a robotic system, and a software network of virtual connections. Under the software networks, as shown in figure 2.2-a, there are no direct interactions among the actuators. Therefore, the controller creates "virtual" connections among the actuators, and then sends control signals to each actuator "separately" to actively control their interactions

with the environment based on the feedback signals received from the mounted sensors. The control process followed in this approach is computationally expensive, and has a slower response (the actuators behave based on the reaction taken by the controller which makes its decision based on the feedback signals). On the other hand, under the hardware networks, which represent the concept of ANS, physical connections are established among the actuators for direct interactions among them as demonstrated in figure 2.2-b. Therefore, the movements of these actuators (the way they interact with each other) are directly influenced by the type of connection pattern among the actuators themselves, as well as their interaction with the surrounding environment. The computational cost for this approach is low, and has a faster response (the actuators spontaneously react to environmental changes).

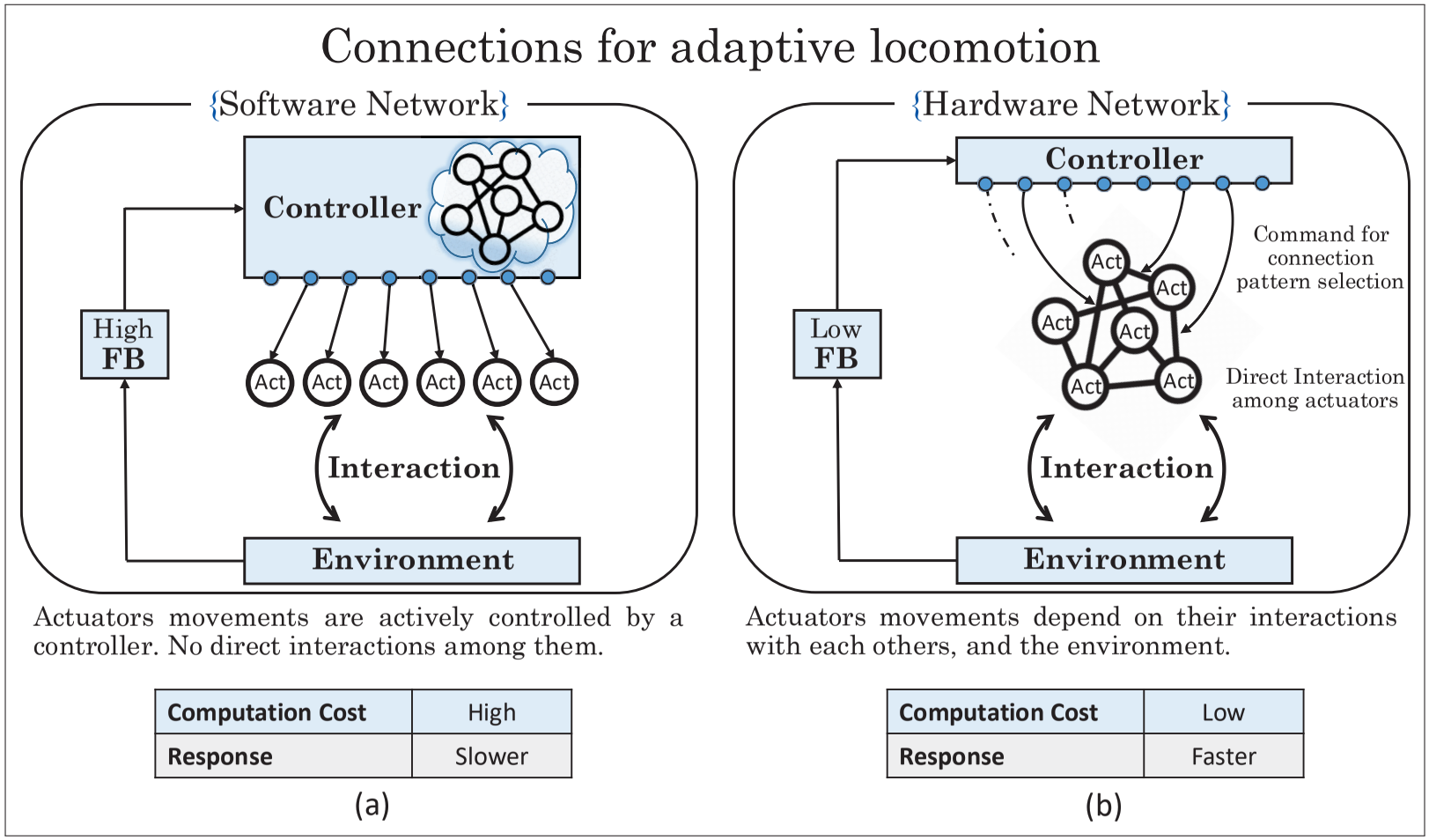

Figure 2.2: Comparison between implementing (a) software network of virtual connections among several actuators of a robotic system, and (b) hardware network of physical connections.

ANS's main contribution in legged robots is to create a stabilizing mechanism; it allows the robots to realize an adaptive morphology and enables them to exploit their whole-body dynamics. The role of ANS can be summarized in two points:

- First: adjusting the physical characteristics of the robot's parts (compliance and stiffness).
- Second: changing the way of interactions among the robot's parts themselves and the environment.

For example, figure 2.3 shows a typical fluid flow diagram of the ANS. The proposed ANS includes two groups of valves: A and B. If the valves in groups A and B are closed as in figure 2.3-a, each cylinder will behave as an independent pneumatic spring due to the sealed air pressure inside each cylinder. The advancing length of each cylinder and their compliance/stiffness can be adjusted by opening the corresponding valve in group A while the corresponding valves in group B are closed. Cylinder c3 in figure 2.3-b shows this behavior. However, if the valves in group B are opened while those in group A are closed, the external force applied to one cylinder is transmitted to the other. For example, by opening valve b1 while valves a1 and a2 are closed as in figure 2.3-b, the external force applied to cylinder c2 will be transmitted to the cylinder c1 via fluid. This process corresponds to the multiarticular muscle functionality, which connects multiple joints to transmit forces from one joint to another. Consequently, the type of interaction between actuators can be modified by opening or closing valves.

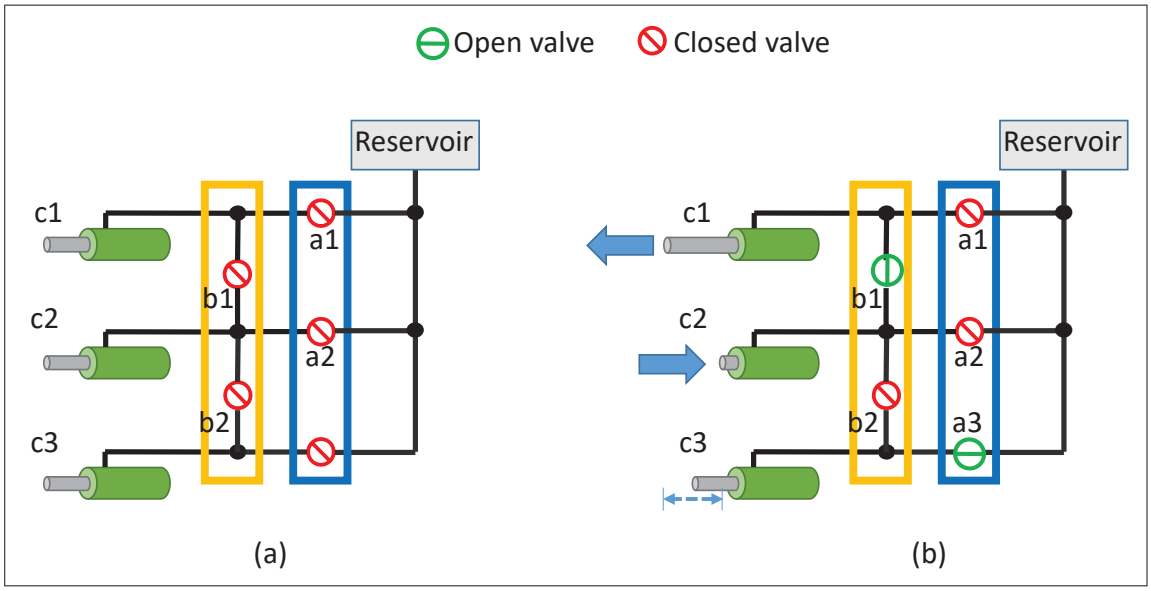

Figure 2.3: Conceptual fluid flow diagram of the ANS for adaptive robot motion.

CHAPTER 3

OCTANS: A RIMLESS WHEEL ROBOT WITH ANS

Researchers who are studying rimless wheel robots can be categorized into two groups. The first group studies rimless wheel robots because it combines the simplicity of the wheel with the obstacle-clearing advantages of the foot. In turn, it allows them to produce a reliable, adaptive, and efficient mode of transportation on rough terrain [26], [27]. The second group of researchers studies rimless wheel robots because it can resemble the behavior of actual human walking, and it can be considered as an approximation of bipedal robots (figure 3.1). In the case of such a robot, one may visually ignore the legs that are not in contact with the ground (swinging legs) and instead consider that another leg is recirculating to prepare for the next step; then the dynamics of its periodic motion relates well to the cyclic motion of bipedal robots. For example, in terms of the hip joint trajectory, the period of the Double Limb Support (DLS), and the gravitational reaction forces (GRF), the Rimless Wheel robot shows a similar behavior compared to that of humans [10], [28], [29], [30].

By considering a rimless wheel robot as a representative of bipedal robots for the purpose of this study, we can focus on the dynamics of the entire body and its role in improving gait patterns without having to concern ourselves with other issues such as balancing and falling down. Therefore, to investigate the way in which energy transfer between the legs of a robot can improve its walking performance, we developed a multi-legged robot, more specifically, an eight (OCT)-legged rimless wheel robot with an ANS, as shown in figure 3.2.

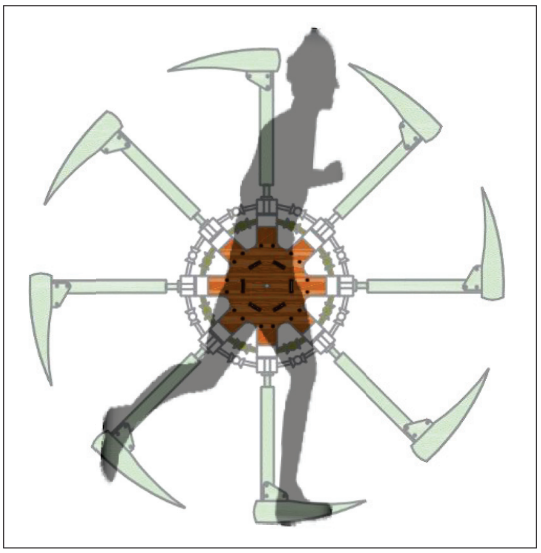

Figure 3.1: Schematic diagram of OCTANS.

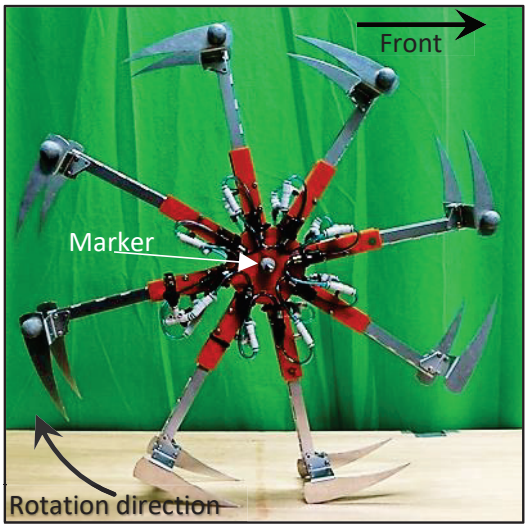

Figure 3.2: Eight-legged rimless wheel robot OCTANS.

3.1 Structure of the robot

The proposed rimless wheel robot OCTANS shown in figure 3.2 is constructed symmetrically with eight identical legs that are attached to the main body through eight pneumatic cylinders. As shown in figure 3.3-a, each leg has a

semicircular foot, and all eight legs together form a circle of 52 cm diameter when all of the robot's legs are set at their half-advanced lengths as shown in figure 3.3-c. This circular shape of the foot helps the robot to achieve a smoother movement by reducing the collision impact forces against the ground. A linear motion guide unit comprising two plates elongated from the robot's main body, as shown in figure 3.3-a guides the robot's legs, allows it to move linearly along the cylinder axis, and prevents it from rotating during the robot's locomotion.

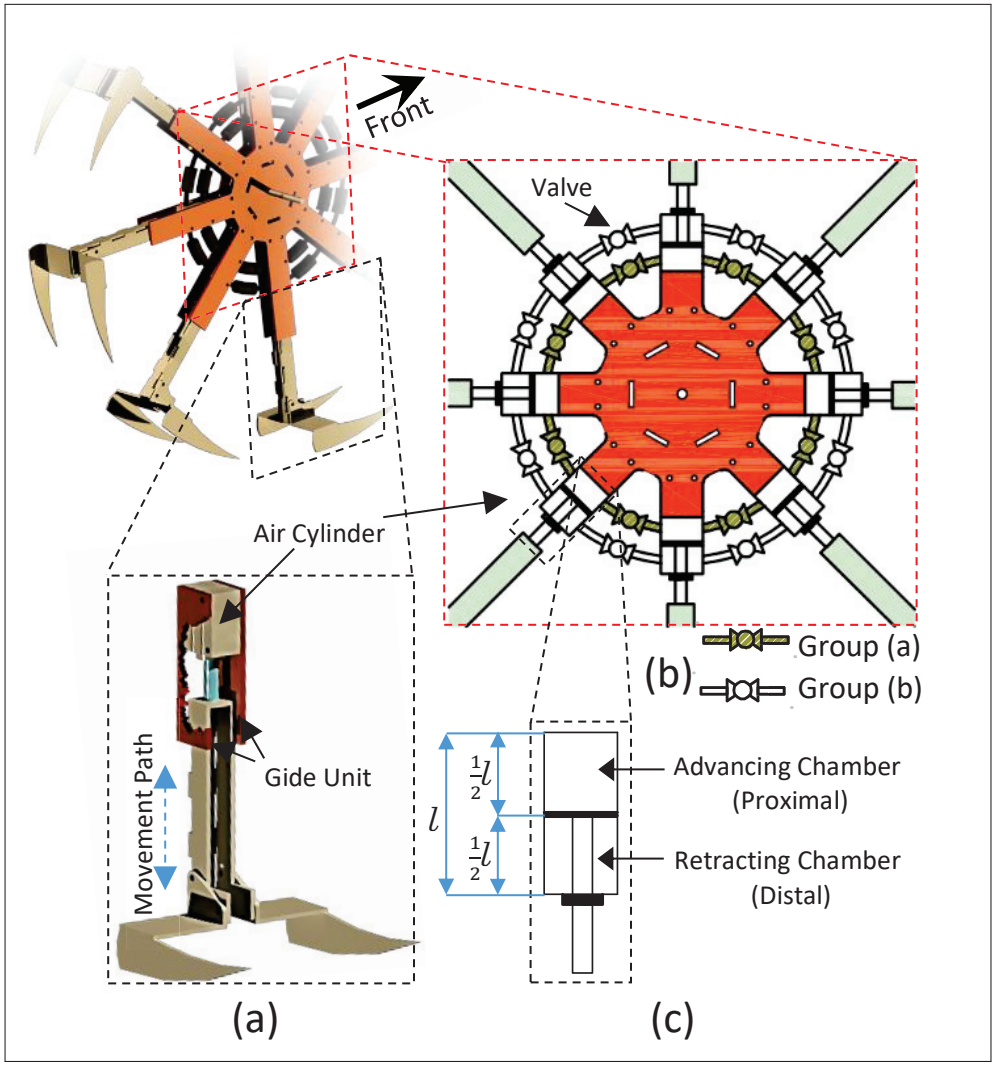

Figure 3.3: (a) Structure of each leg; (b) Valve system of the ANS; (c) Cylinder's initial condition, with piston set at its half advanced-length.

3.2 OCTANS's valve system

As shown in figure 3.3-b, a valve system of two groups (a) and (b) is built using 16 "hand"[1] valves to form the ANS of our robot OCTANS. This valve system connects the robot's legs with each other. Group (a) connects the advancing (proximal) chambers of all cylinders, while group (b) connects the retracting (distal) chambers of all cylinders. With different sets of opened/ closed valves, different connection patterns among the robot's legs can be realized, and with these different connection patterns, different robot behaviors can be achieved.

3.3 Mechanism of energy transfer among limbs

In the present study with OCTANS, we expect to find a connection pattern that will allow energy transfer among the robot's legs to realize a walking behavior similar to the sequence of motion shown in figure 3.4. A connection pattern where actuators implemented to the successive legs are mutually connected (e.g., condition 2 mentioned in section 3.4). Just before placing the robot on the ground to start its locomotion, as in figure 3.4-1, all robot legs are made to have the same advancing lengths by setting all the cylinders to their mid stroke. Once the fore leg (L2) hits the ground, as in figure 3.4-2, it will fully retract, causing the air in the attached cylinder to be transmitted to the successive rear cylinder attached to leg (L1); at this moment, (L1) will expand, kick the ground, and push the robot forward in the rolling direction to prepare for the next step (figure 3.4-3). During the robot's locomotion, the same process will be repeated

[1]Hand valve: is a hand-operated valve, with a quarter turn movement lever to manually change the (open/ close) status of the valve.

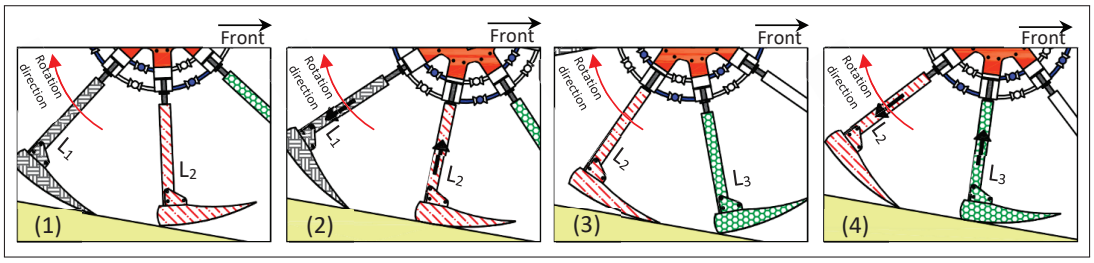

Figure 3.4: Mechanism of energy transfer among robot limbs during locomotion.

along the way on every step the robot takes, helping to keep it moving.

In addition to the energy transfer among the limbs of the robot during locomotion by using the ANS, as shown in figure 3.4, if our expectations are right, the robot will push off the ground with its rear leg just before it enters the swing phase. This behavior is similar to human walking during the terminal stance and pre-swing phases, where the foot applies a posteriorly directed force to the ground to propel the body forward and prepare it for the next step [31].

3.4 Connection patterns

To test our hypotheses, the robot's behaviors were compared under three different connection patterns, as shown in figure 3.5. Under condition 1, all 16 valves of both groups of the ANS are kept open, ensuring that the advancing chambers of all cylinders are connected to each other, and the retracting chambers of all cylinders are connected to each other. In this condition, the movement of one leg will affect the behavior of all other legs, for example, in an ideal case (ignoring the friction and pressure loss during air transmission), if one of the legs is retracted by 10 mm, each of the remaining seven legs will advance by 1.43 mm.

Under condition 2, eight valves are opened, four from each group, and connected alternatively, as shown in figure 3.5-b. In this condition, the advancing chamber of cylinder *i* will be connected to the advancing chamber of cylinder *i*+1, while the retracting chamber of cylinder *i* will be connected to the retracting chamber of cylinder *i*-1. Once the leg attached to cylinder *i* hits the ground and fully retracts, the high pressure generated in the advancing chamber of cylinder *i* will transmit the air to the advancing chamber of cylinder *i*+1, which will cause the leg attached to it to expand. At the same time, the low pressure generated in the retracting chamber of cylinder *i* will suck the air from the retracting chamber of cylinder *i*-1, causing the leg attached to it to expand as well. In other words, here in this condition there are two groups of legs, odd-numbered legs and even-numbered legs as shown in figure 3.5-b. The retraction of one leg for a certain distance, will cause the other three legs of the same group to retract the same distance, while the other four legs from the second group will advance the same distance. For example, in the ideal case, if one of the odd-numbered legs retracted by 10 mm, each of the odd-numbered legs will retract by 10 mm as well, while each of the even-numbered legs will advance by 10 mm.

Under condition 3, all 16 valves are left closed, as shown in figure 3.5-c. There is no interaction among the robot's legs, and the air sealed inside the cylinders will make each leg to behave as if it is attached to an independent pneumatic spring. Note that this condition corresponds to standard PDWs with compliant legs.

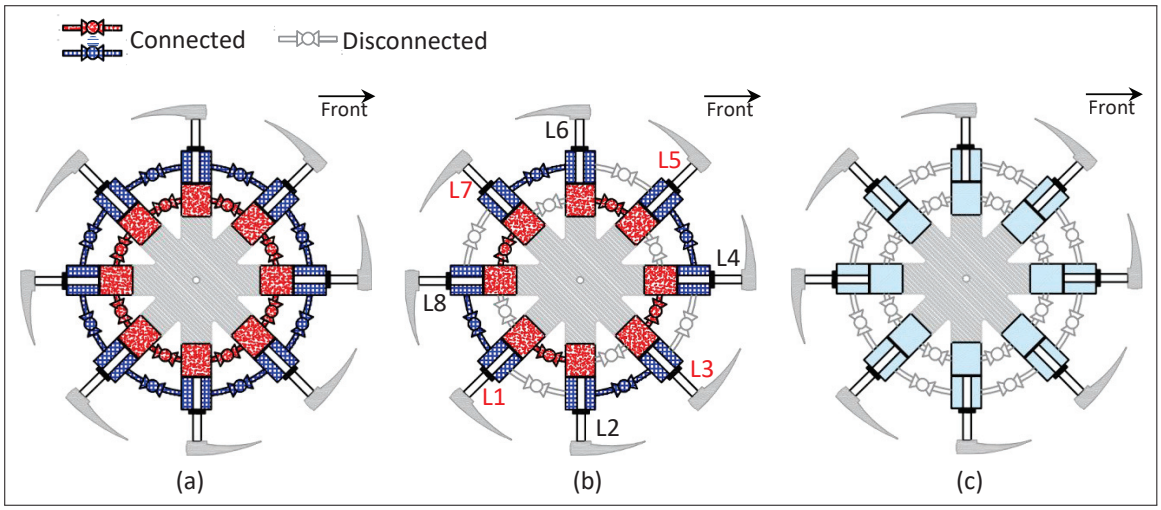

Figure 3.5: Connection patterns used in experiments. (a) Condition 1: all valves of the ANS are kept open to ensure mutual interaction among all legs. (b) Condition 2: eight valves of the ANS are opened, four from each group allowing to create two groups of legs, odd- and even-numbered legs. (c) Condition 3: no interaction among the legs since all valves of the ANS are left closed.

3.5 Experiments:

Two experiments were conducted to investigate the effect of the three previously mentioned connection patterns on the robot's behavior in terms of the driving force required to start robot locomotion, which is represented by the slope angle, and the efficiency of the robot, which represented by the distance traveled.

3.5.1 Experimental setups:

Given that OCTANS is fully passive and gravity is the only power source for its locomotion, both experiments herein were conducted by placing the robot on

an inclined board with a variable slope angle controlled using a screw jack, as shown in figures 3.6-a and b. Before starting the trials of the two experiments, the following three preparation steps were performed on the robot:

1. Pressurizing the ANS with air by using an air compressor.
2. Adjusting the pressure in ANS groups (a) and (b) to the appropriate values to set all legs at mid stroke.
3. Changing the connection patterns manually to one of the three previously mentioned conditions and fixing it during the robot's locomotion.

... More details are given in Appendix A.

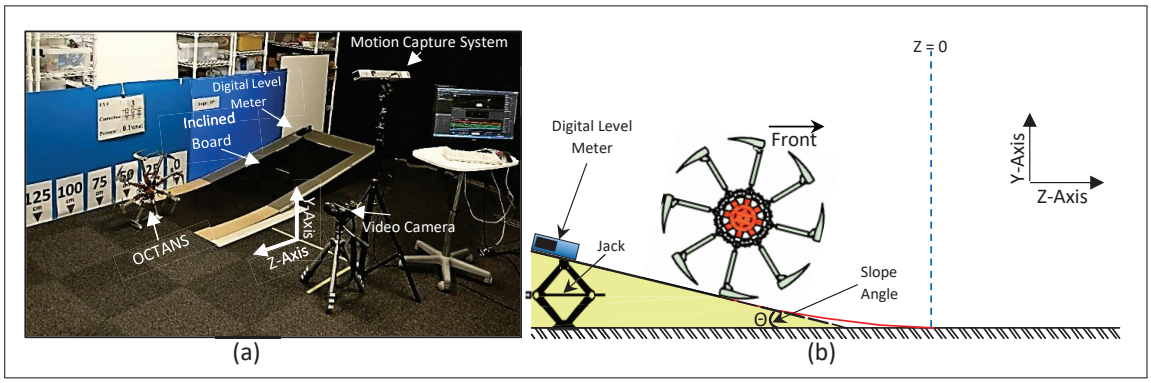

Figure 3.6: (a) Experimental environment; (b) Schematic of experimental setup.

3.5.2 Traveling Distance Experiment [TD]

In this experiment we investigate the effect of the three previously mentioned connection patterns on the distance traveled by the robot after leaving the inclined board. The experiment was conducted with two slope angles, $\Theta = 10^{\circ}$ and

$\Theta = 15^{\circ}$, and the ANS pressurized to 0.10 MPaG. Ten trials were conducted for each connection pattern. In each trial, and after going through the experimental setups mentioned in section 3.5.1, the following procedures were performed:

1. The robot was placed on an inclined board with a fixed slope angle ($\Theta = 10^{\circ}$, $\Theta = 15^{\circ}$).
2. The robot was passively rolled down the inclined board, as shown in figure 3.6.
3. The distance traveled and the number of steps walked by the robot after leaving the inclined board were measured.

To track the robot's movement, a motion capture system (V120: Trio tracking system, NaturalPoint, Inc. DBA OptiTrack) was used. The robot position was defined by a reflective marker attached to the center point of the robot, as shown in figure 3.2.

Results:

For the ten trials conducted for each connection pattern, the average distance traveled in addition to the number of steps walked by the robot are listed in table 3.1. Regardless the value of the slope angle, as the results show, the robot with independent spring-like legs under condition 3 was able to walk a greater number of steps after leaving the inclined board compared to the other two connection patterns that use the ANS to mutually interconnect the robot's legs with each other; therefore, under this condition, the robot traveled a significantly ($p < 0.001$) longer distance compared to those under the other two conditions according to a t-test performed with 18 degrees of freedom, as shown in figure 3.7.

The robot relatively travelled a longer distance under condition 2 compared to condition 1, although it was not a significant difference ($p = 0.006 > 0.001$).

Table 3.1: Average of distance traveled [m] and number of steps walked by robot after leaving inclined board ± S.D at slope angles of Θ = 10° and Θ = 15°.

		Condition 1	Condition 2	Condition 3
Θ = 10°	**Traveled Distance**	1.00 ± 0.23	1.11 ± 0.15	1.64 ± 0.13
	Number of Steps	5.20 ± 1.03	5.70 ± 0.67	8.40 ± 0.84
Θ = 15°	**Traveled Distance**	1.21 ± 0.19	1.43 ± 0.18	1.97 ± 0.13
	Number of Steps	6.10 ± 0.86	7.30 ± 0.82	9.90 ± 0.57

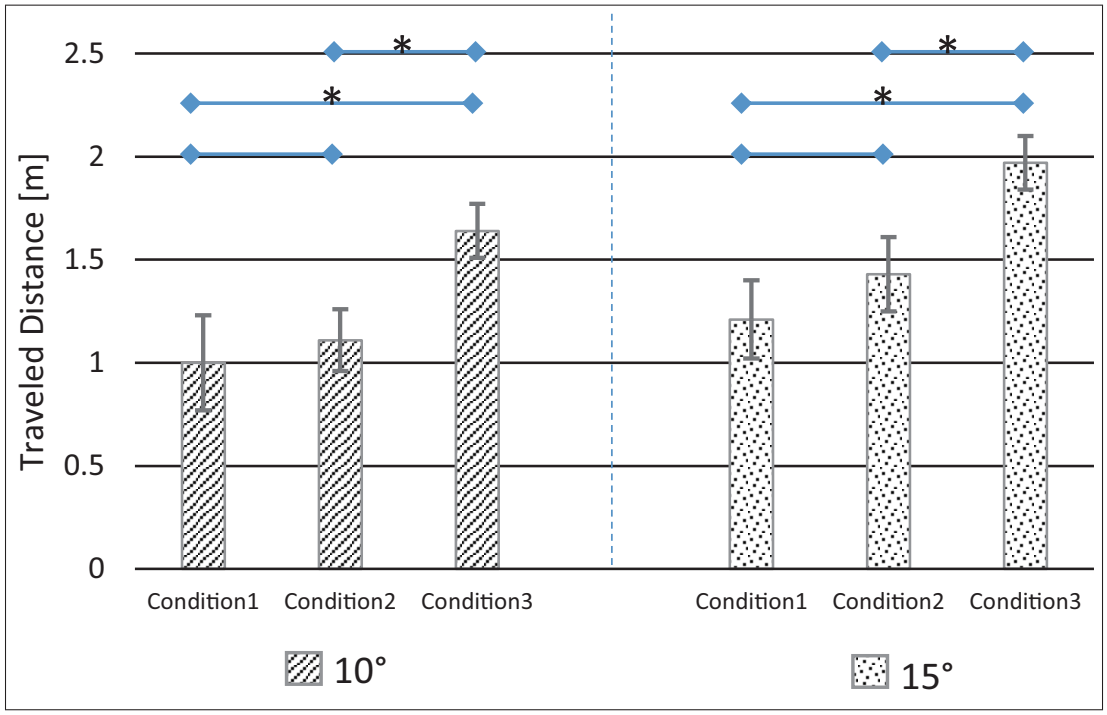

Figure 3.7: Average distance traveled ± S.D. at slope angles of Θ = 10° and Θ = 15°. (*) indicates $p < 0.001$.

The results of the TD experimental trials are summarized in figures 3.8-a and b, which compare the distance traveled and the speed of the robot under the three

conditions and two different slope angles of $\Theta = 10^\circ$ and $\Theta = 15^\circ$. The black line represents one of the commonly occurring behaviors across the 10 trials under each condition. After the robot reaches its maximum speed at the end of the inclined board (at z = 0) and leaves it to move on level ground, as shown in figure 3.8-b, under condition 3, the robot decelerates at a lower rate compared to that under the other two conditions, helping it retain its energy and travel a longer distance.

As an example, time-series photographs of OCTANS during locomotion (figure 3.9) show the motion sequence of the robot under the three connection patterns and slope angle of $\Theta = 15^\circ$, as denoted by the black lines in figure 3.8.

Under the three conditions, figure 3.10 shows the changes happened to the lengths of the robot's legs during the first three steps of its locomotion (the period from the moment leg L2 hits the ground until leg L5 hits the ground as shown in figure 3.10-d). With no interaction between the legs under condition 3, a robot's leg partially retracts during its contact with the ground before it returns to its initial length once it enters the swing phase as shown in figure 3.10-c. Under condition 1, as shown in figure 3.10-a, with all legs being mutually connected with each other, once one of the legs hits the ground, it fully retracts to affect the lengths of the other legs. A clear interaction between the robot's legs is happening under condition 2 as shown in figure 3.10-b. Once a leg hits the ground as the figure shows, it fully retracts, causing the successive rear leg to relatively fully expand and pushing the robot forward in the rolling direction, to realize a behavior similar to the expected sequence of motion shown in figure 3.4.

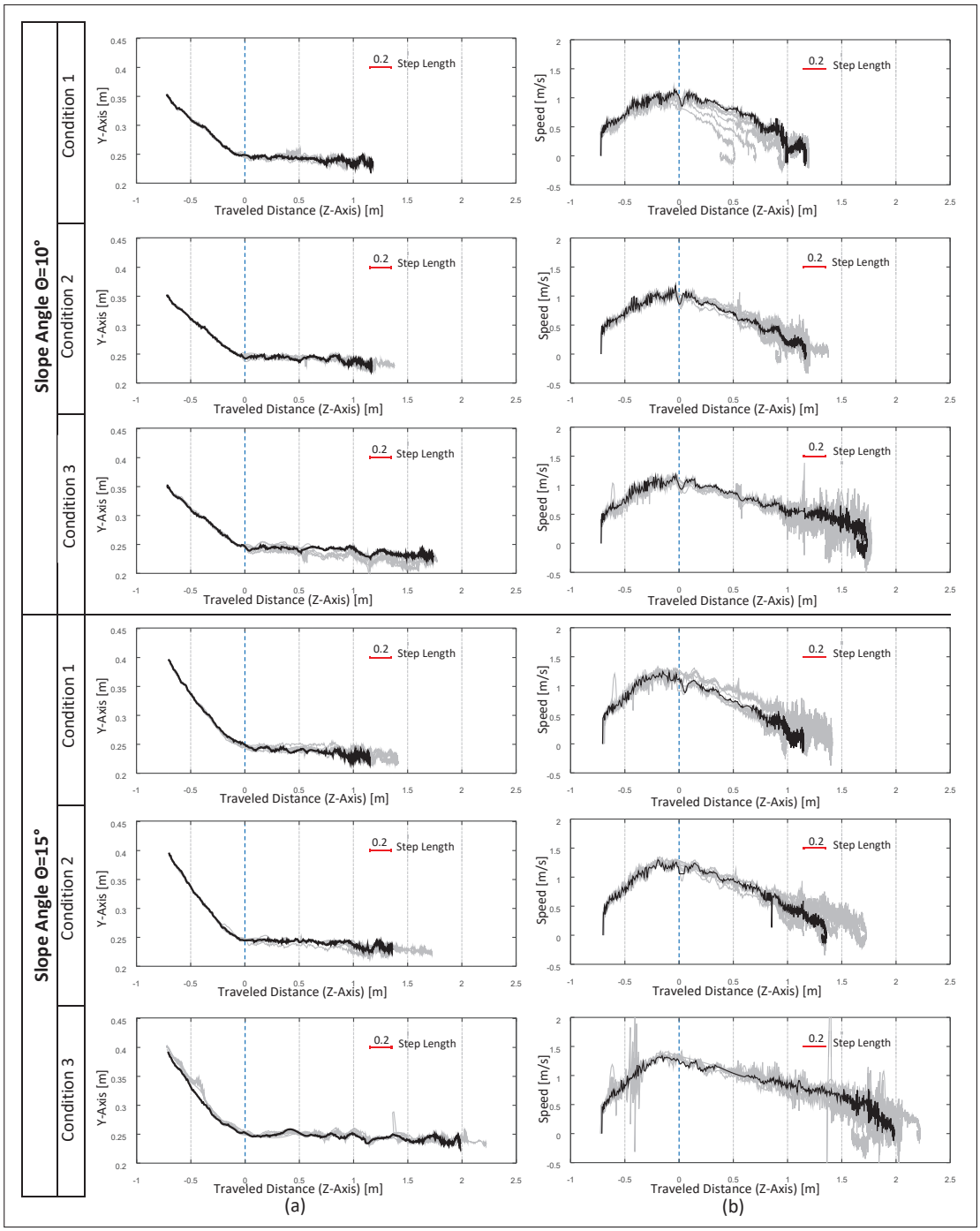

Figure 3.8: Comparison of distance traveled and robot speed under three conditions and two different slope angles of 10° and 15°. (a) Distance traveled and (b) speed. The black line represents a typical behavior (Median) across 10 trials under each condition. The dashed line (z = 0), represents the end of the slope and the beginning of horizontal ground.

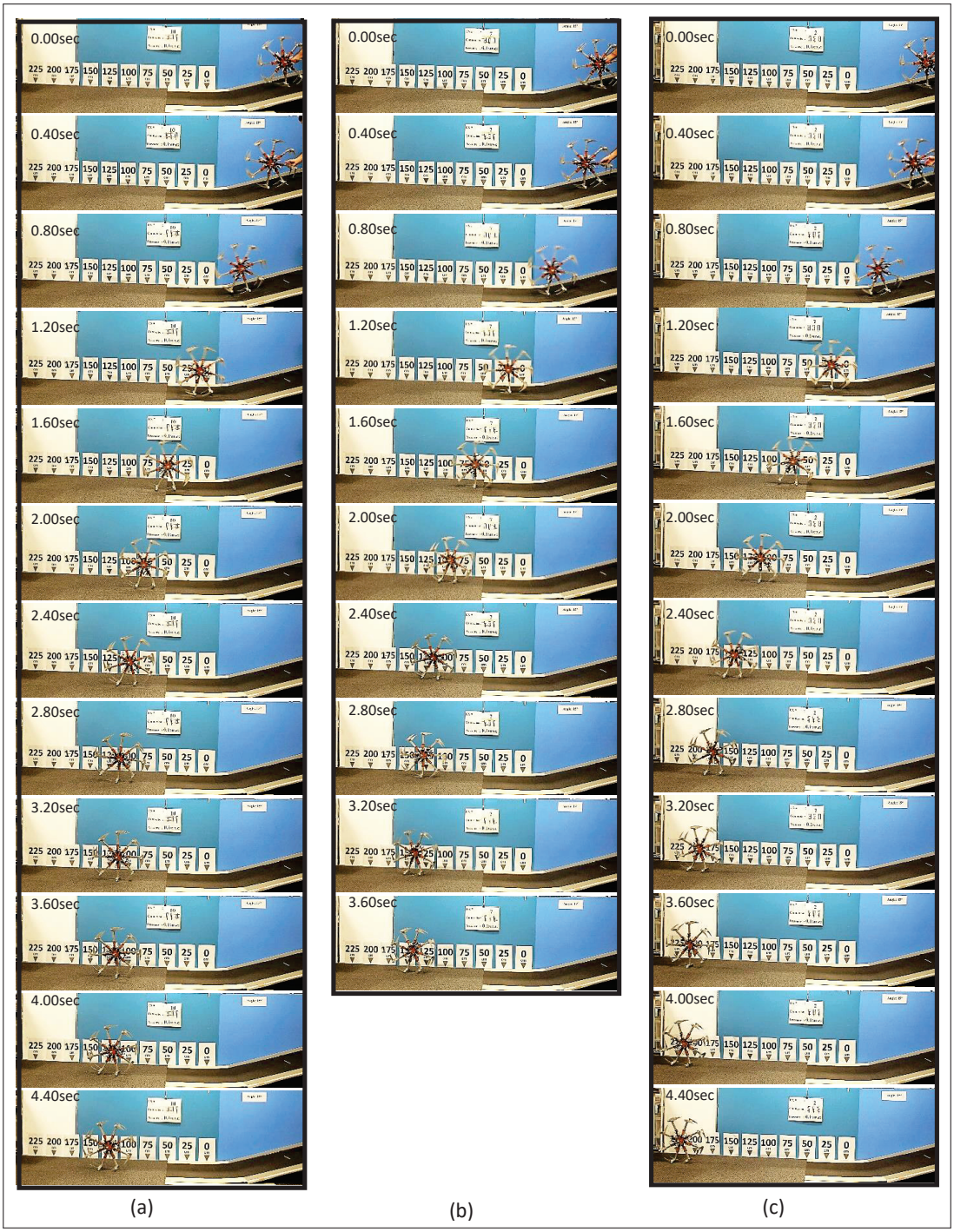

Figure 3.9: (a), (b), and (c) show time-series photographs of OCTANS during locomotion, representing the black lines of figure 3.8 on board with a slope angle of 15° under conditions 1, 2, and 3, respectively. The interval between the two pictures is 0.40 s.

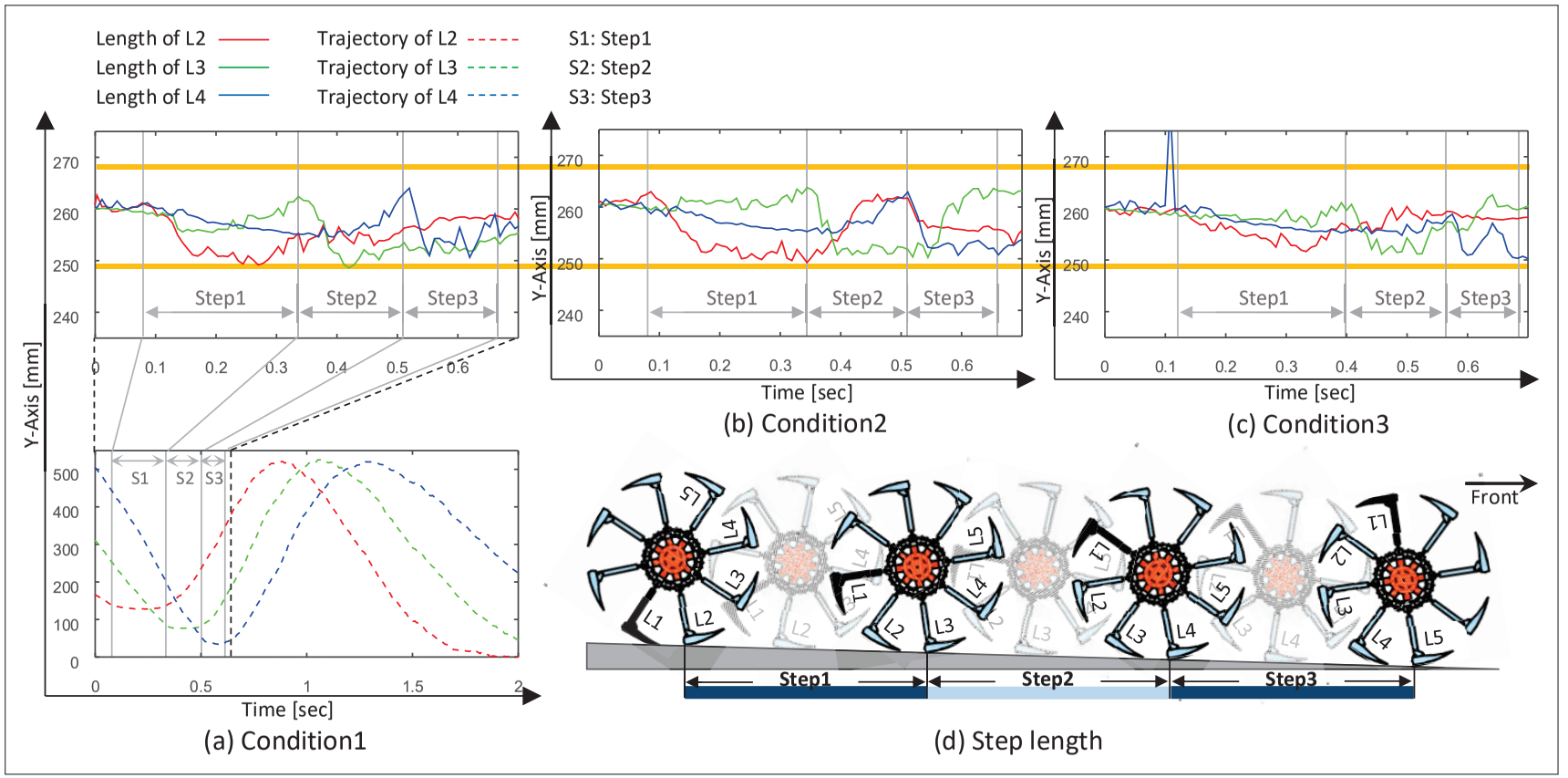

Figure 3.10:

(a), (b) and (c) show the changes in length happening to the robot's legs L2, L3 and L4 during the first three steps of the robot's locomotion, under the conditions 1, 2 and 3 respectively. The lower part of figure (a), shows the trajectories of the legs L2, L3 and L4 during the first two seconds (almost one cycle) of the robot's locomotion. As shown in figure (d), a step is defined by the period between the moment a leg hits the ground until the next following leg hits the ground. The two horizontal orange lines indicate the shortest/ longest possible lengths due to the hardware limitations.

3.5.3 Driving Force Experiment [DF]

In this experiment, we investigated the effect of the three previously mentioned connection patterns on the driving force required by the robot to start locomotion. To this end, we measured the minimum slope angle of the inclined board that caused the robot to start moving. This minimum slope angle was called the Motion Initiation Slope Angle (MISA). The experiment was conducted with two different pressure values for the ANS, 0.10 MPaG and 0.20 MPaG. For each connection pattern, 10 trials were conducted. In each trial, after going through the experimental setups mentioned in section 3.5.1, the following procedures were performed:

1. The robot was placed on a horizontally laid board with the slope angle of $\Theta = 0^{\circ}$.
2. The slope angle was increased gradually by using a screw jack, as shown in figure 3.6, until the robot started moving.
3. The MISA was measured using a digital level meter (DI-230M) that measures the exact angle of the inclined board with respect to the horizontal ground with a resolution of 0.05°.

Results:

Table 3.2 presents a comparison of the average MISA over 10 trials for each connection pattern and two different values of air pressure (0.10 MPaG and 0.20 MPaG) inside the ANS. Regardless the value of the air pressure inside the ANS, as the results show, the robot with mutually interconnected legs under conditions 1 and 2, which realizes energy transfer among the robot's legs during

locomotion, needed smaller MISA for the robot to start moving compared to the robot under condition 3, which has independent spring-like legs. In other words, under conditions 1 and 2, the robot needed lower driving force to start its locomotion compared to that under condition 3.

Table 3.2: Average of MISA [deg] ± S.D. for three connection patterns at pressure values of 0.10 MPaG and 0.20 MPaG.

	Condition 1	**Condition 2**	**Condition 3**
0.10 MPaG	3.49 ± 0.52	1.61 ± 0.22	6.00 ± 0.58
0.20 MPaG	3.23 ± 0.56	1.79 ± 0.40	5.73 ± 1.12

The results of the DF experimental trials are summarized in figure 3.11. For the two pressure values (0.10 MPaG and 0.20 MPaG) inside the ANS, the MISAs of the robot under the three conditions are significantly different ($p < 0.001$) from one another, as indicated by the results of a t-test with 18 degrees of freedom.

As an example, time-series photographs of OCTANS with 0.10 MPaG pressurized ANS during locomotion, as in figure 3.12, show one of the commonly occurring MISA across the 10 trials of the robot conducted under conditions 1, 2, and 3 after increasing the slope angle gradually until the robot started moving.

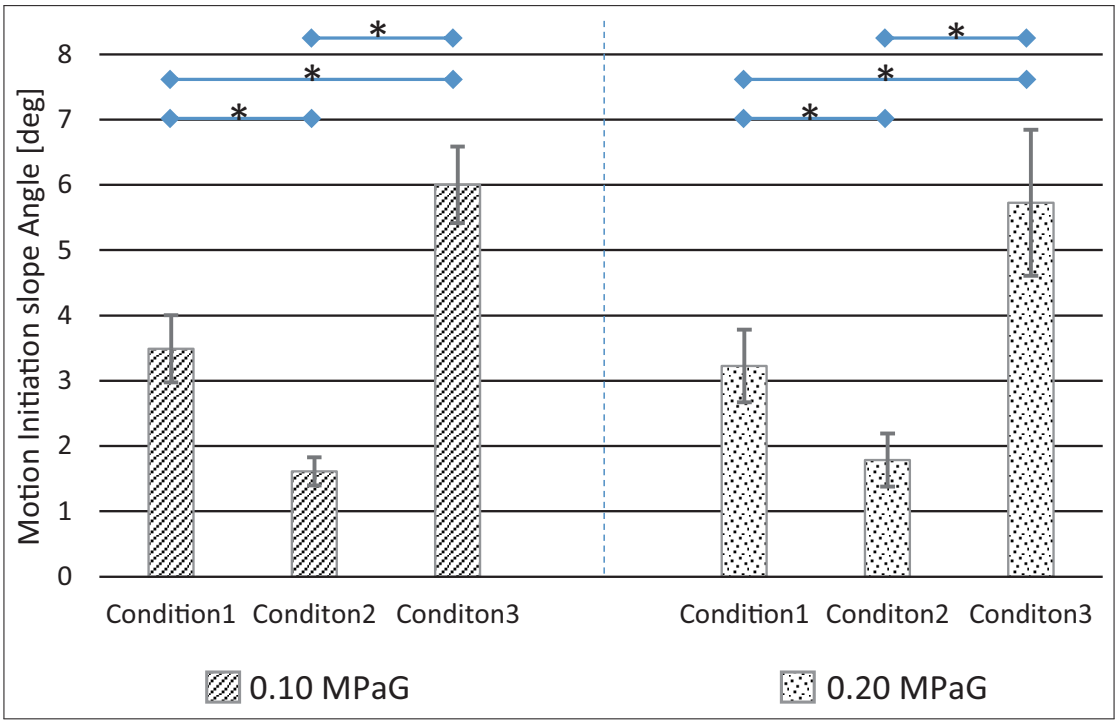

Figure 3.11: Average of MISA [deg] ±S.D. for three connection patterns at pressure values of 0.10 MPaG and 0.20 MPaG. (*) indicates $p < 0.001$.

Figure 3.12: Time-series photographs of OCTANS with 0.10 MPaG pressurized ANS during locomotion, showing one of the commonly occurring MISAs across 10 trials under (a) condition 1, (b) condition 2, and (c) condition 3, after increasing the slope angle gradually until the robot started moving. The interval between two pictures is 0.47 s.

3.6 Discussion

For the DF experiment, it is reasonable to find that under conditions 1 and 2, the robot with ANS requires lower driving force to start locomotion compared to that in condition 3, in which the robot has independent spring-like legs. The underlying reason is that because the ANS allows for energy transfer among legs, especially under condition 2, where the air transmission between legs as the fore leg hits the ground, causes the successive rear leg to relatively fully expand while the fore leg is fully retracted as shown in figure 3.4-2 and figure 3.10-b. In response, the robot's center of mass is raised and pushed forward. The robot then falls in the rotation direction with potential energy being converted to kinetic energy. It is worth noting that these changes in potential and kinetic energies during walking are very similar to the changes that occur in a human during walking [32].

In the TD experiment, we can see that under conditions 1 and 2, the robot travels shorter distances compared to that under condition 3, although they all started their locomotion from the same height with same potential energy (mgh). The robot's behavior in this case can be explained by the dissipation of energy that takes place as a result of the friction between the legs and their guide units during retraction and expansion of the robot's legs, as well as because of the pressure loss due to the friction between the tubes and air during the transmission of air from one leg to another. Therefore, by increasing the air pressure in the ANS, the interaction among the robot's legs can be improved and by enhancing the design of both the legs and their guide units, this behavioral limitation can be mitigated, and the robot would be more energy efficient.

With a closer look to the results of both TD and DF experiments, we can notice that the robot under condition 2 seems to have a better behavior in all cases compared to the robot under condition 1. From the TD experiment at slope angle of $\Theta = 15^{\circ}$, the robot under condition 2 has travelled longer distance compared to condition 1, although it was not a significant difference ($p = 0.006$) based on the performed t-test. From the DF experiment, the robot under condition 2 needed smaller MISA to start moving compared to condition 1 with a significant difference ($p < 0.001$) as indicated by the performed t-test with 18 degrees of freedom. This superiority in performance in case of condition 2 over condition 1 can be related to the way the robot's legs are interacting with each other under each condition. If a leg retracted a certain distance under condition 2, in the ideal case, it would cause all other legs to retract/ advance the same distance. On the other hand, if one of the legs under condition 1 retracted a certain distance, in the ideal case, each of the remaining seven legs would advance by one-seventh that distance.

The connection pattern of the robot was changed manually before starting each trial by switching (open/ close) the hand valves of the ANS that mutually connect the robot's legs with each other. Thus during the robot's locomotion, it retained the predetermined connection pattern without having the ability to change it. As can be inferred from the experiment results, the connection pattern that is suitable for starting the robot's gait differs from the connection pattern that is best for the stationary gait phase. Based on these observations and to improve the robot's performance to generate an efficient gait through all locomotion phases, in future work, we will replace the manually actuated hand valves with electronically actuated ones. This would allow the robot to automatically change the connection pattern of its ANS during locomotion based on the given

situation. Moreover, to ensure movement continuity on a level ground, a simple actuation mechanism, such as a rotary motor, will be installed.

CHAPTER 4

A SIMPLE STRUCTURE BIPEDAL ROBOT WITH AN ENERGY TRANSFER MECHANISM BETWEEN ITS LEGS

Since the feasibility of implementing ANS was proven on an approximate representation of bipedal robots, the next step of this study was to develop an actual bipedal legged robot with ANS. Therefore, in this chapter, we investigate the way in which energy transfer between the legs of a simple bipedal robot can improve its walking performance. The developed bipedal robot, shown in figure 4.1, has a simple mechanical structure based on Klann mechanism, and its legs are mutually connected via an actuator network system.

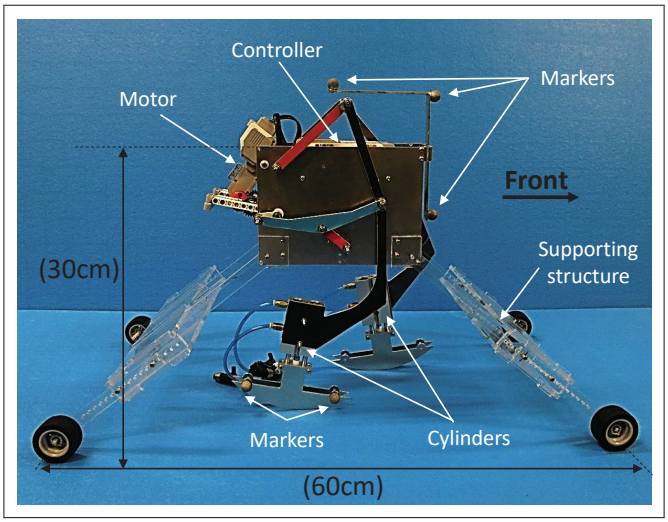

Figure 4.1: Bipedal robot with ANS.

4.1 Structure of the robot

With a pneumatic cylinder attached to each leg of the proposed bipedal robot, the compliance of each leg in addition to the energy transfer between them be-

come adjustable. The 30 cm height robot is built with a simple structure based on Klann linkage (figure 4.2) that is mechanically coordinated by a single-degree-of-freedom [33]. The robot consists of a servomotor (LEGO MINDSTORMS EV3 large servomotor) responsible for the robot's locomotion, two identical Klan linkages coupled together at the crank and one-half cycle out of phase with each other are representing the robot's legs, allowing the robot's body to travel parallel to the ground. Each of the linkages consists of the robot's body frame, a crank, two grounded rockers, and two couplers all connected by pivot joints. A supporting structure is also added to the robot to ensure stability and to prevent the robot from falling down. The length of the supporting structure is set in a way that all of its four wheels are touching the ground when the robot is in its initial posture as shown in figure 4.5-c.

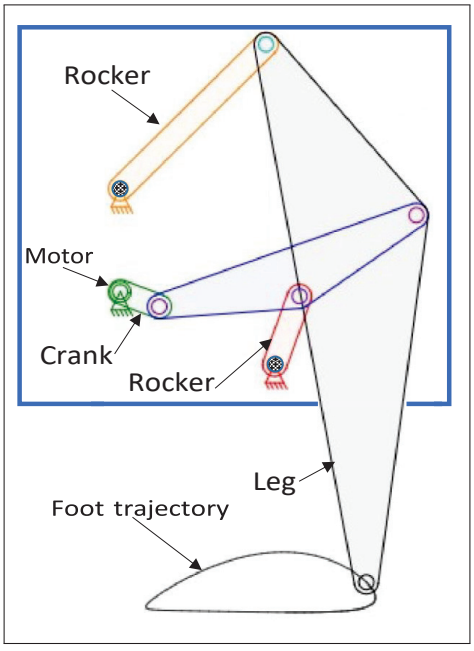

Figure 4.2: Diagram of Klann linkage.

4.2 Connection patterns

A simple valve system of two hand-valves forms the ANS of our bipedal robot. It connects the robot's legs as shown in figure 4.3. Valve (a) links the advancing chambers (proximal) of the two cylinders together, while valve (b) links the retracting chambers (distal) together. By opening/ closing the valve system with various combinations, different interactions between the actuators will emerge to generate a variety of dynamics for the robot's body.

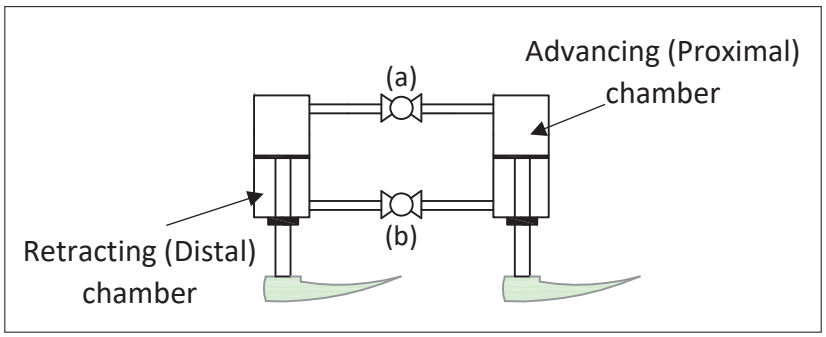

Figure 4.3: The valve system of the ANS.

During the conducted experiments, the robot's movement was examined with three different types of legs as illustrated in figure 4.4. Under type 1, both of the hand-valves are kept open to allow energy transfer between the two legs. For example, once the robot steps on its right leg, the piston of the cylinder attached to this leg will fully retract. In response to that, the left leg will fully expand due to the air transmission between the two legs. Under type 2, both of the valves are kept closed as illustrated in figure 4.4-b, to prevent the direct interaction between the robot's legs. In this case, the robot has compliant legs; its legs are attached to air springs created by the locked air inside the chambers of each actuator. As shown in figure 4.4-c, under type 3, the robot has stiff legs, since the pistons of both cylinders are locked-up at their half-advanced lengths.

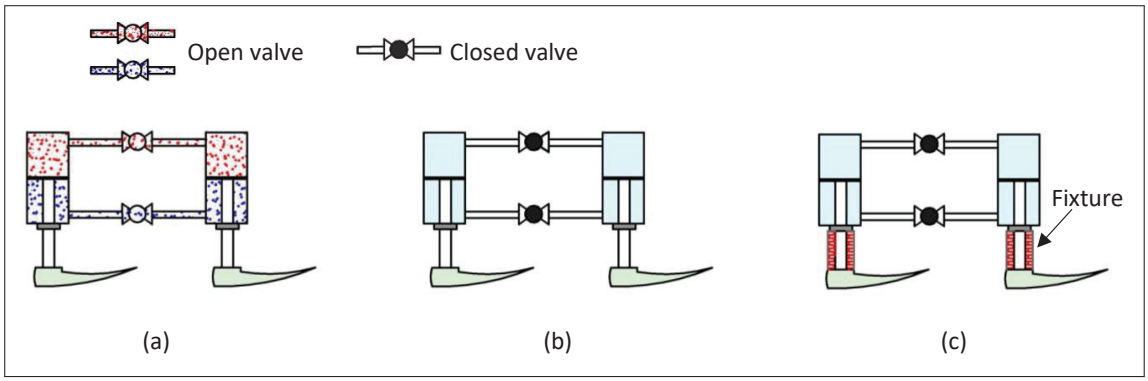

Figure 4.4: Applied connection patterns during the experiments. (a) Type 1: Mutually interconnected legs, (b) Type 2: Compliant independent legs, and (c) Type 3: Rigid legs.

4.3 Experiments

4.3.1 Procedure and experimental settings

To examine the effect of the three different types of legs (mentioned earlier) on the stable walking behavior of the robot, both of the roll motion (shown in figure 4.5-a), and the vertical oscillation of the robot's body (shown in figure 4.5-b) were observed and measured during the conducted experiments.

The steps below are the performed preparation procedures before starting any trial:

- Pumping air into the ANS using an air compressor.
- Setting the air pressure inside the cylinders with proper values to get the legs at their half-advanced lengths.
- Selecting one of the three previously mentioned connections by manually

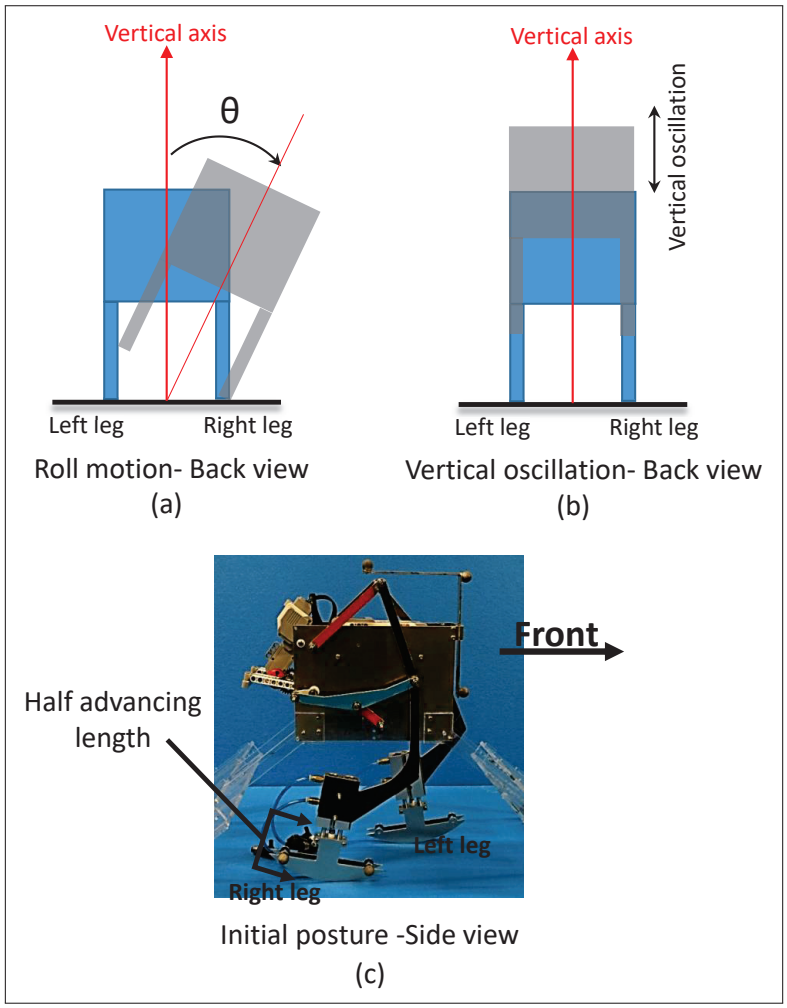

Figure 4.5: (a) Demonstration of the roll motion, (b) Demonstration of the vertical oscillation of the robot's body, and (c) The initial posture of the robot: both of its legs are at their half-advanced lengths. The left leg is in the front, and the right one is in the back.

open/ close the valves respectively, and fixing it during the robot's locomotion.

After that, we start the experiment with the robot having the same posture for all trials. Its right leg is in the back while the left one is in the front as shown in figure 4.5-c. For each connection, three trials were conducted. The motion of the robot was analyzed by placing reflective markers on the robot as shown

in figure 4.1. To track those markers, a motion tracking system (OptiTrack-V120:TRIO) was used.

4.3.2 Results

For the three trials conducted for each connection, the roll motion in addition to the vertical oscillation of the robot's body during locomotion are graphed in figures 4.6-a and b. As can be inferred from the graphs, With connected legs to allow energy transfer between them, the robot realizes the lowest oscillation amplitude of both the roll motion and the vertical oscillation of the robot's body, with ranges of (2.06°), and (4.32 mm) respectively. On the other hand, the robot with rigid legs had the shakiest behavior with oscillation amplitude ranges within (7.34°) for the roll motion, and within (10.27 mm) for the vertical oscillation of the robot's body. The robot with compliant legs (type 2) has amplitude values that lie between the other two types of legs, closer to type 3. Based on the applied t-test with 4 degrees of freedom, the experimental results showed a significant difference ($p <= 0.001$) in behavior between the three connections, as shown in figure 4.7. Table 4.1 summarizes the results of the conducted experiments. It compares the average of both, the roll motion and the vertical oscillation of the robot's body for the three types of legs.

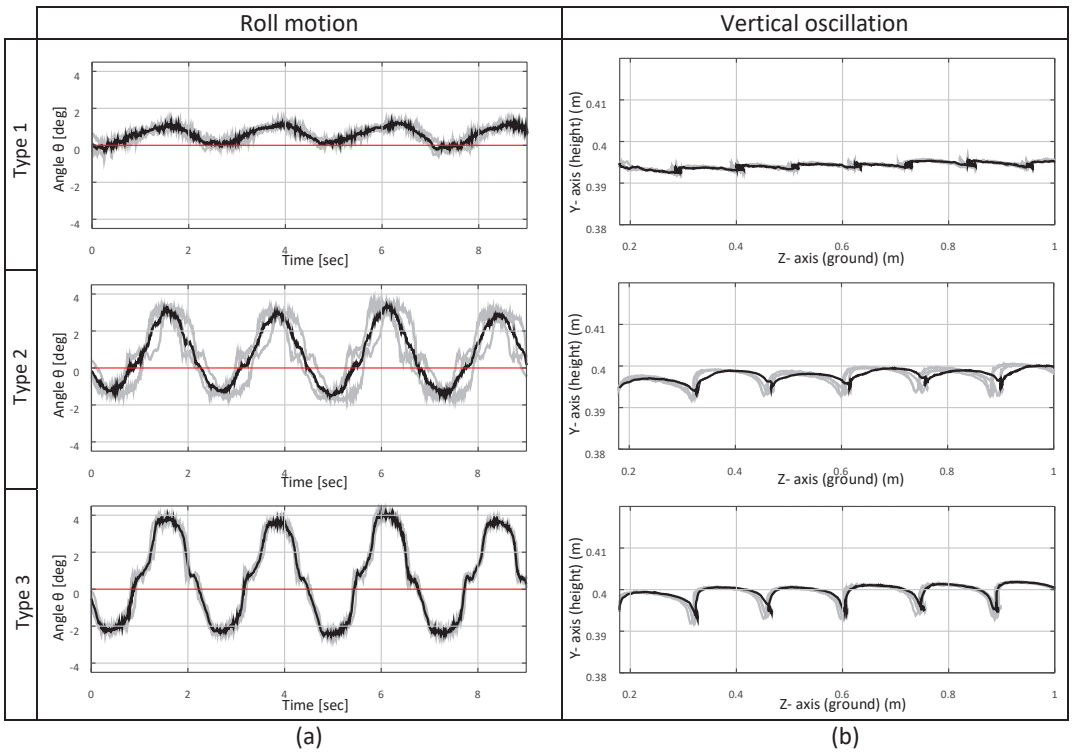

Figure 4.6: Comparison of (a) the roll motion and (b) the vertical oscillation of the robot's body under the three types of legs. The black lines represent the average behavior among the three conducted trials of each type, which are drawn in gray colors. The horizontal red lines ($\Theta = 0°$) of the roll motion graphs, represents the vertical axis shown in figure 4.5-a.

The snapshots of figure 4.8 display one of the three conducted trials for each type of legs. It shows the bipedal robot during the first gait cycle of its locomotion.

Table 4.1: Average range of both the roll motion's angle [deg] ± S.D, and the vertical oscillation [mm] ± S.D.

	Range of the roll motion [deg]	**Range of the vertical oscillation [mm]**
Type 1	2.06 ± 0.18	4.32 ± 0.34
Type 2	5.47 ± 0.11	8.92 ± 0.11
Type 3	7.34 ± 0.45	10.27 ± 0.16

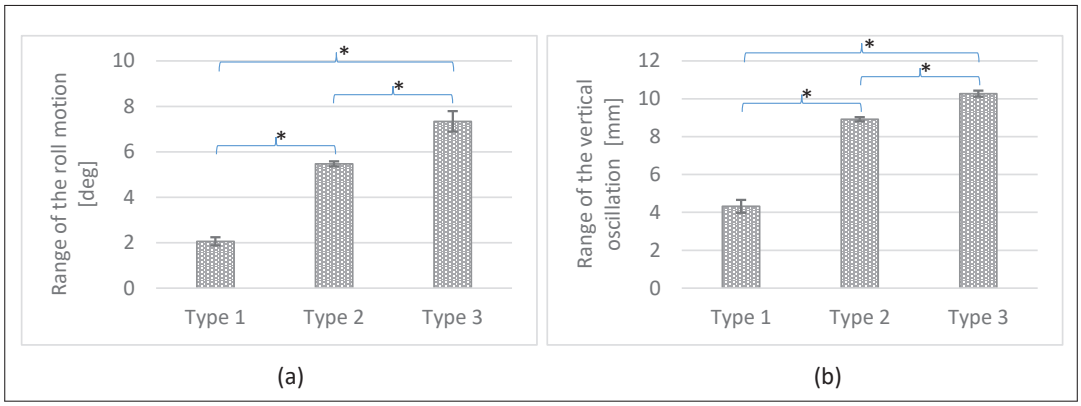

Figure 4.7: (a) Average range of the roll motion's angle [deg] ± S.D. (b) Average range of the vertical oscillation [mm] ± S.D. * indicates $p <= 0.001$.

Figure 4.8: Time-series photographs of one gait cycle of the bipedal robot during locomotion, showing one of the conducted trials of each connection pattern. (a) Type 1, (b) Type 2, and (c) Type 3. The interval between every two successive pictures is 0.37 s.

4.4 Discussion

As the experimental results showed, by changing the interaction between the actuators of the ANS, the robot's walking behavior was also changed even though all of the other experimental settings remained the same. Whereas can be inferred from the conducted experiments with three types of connections, the robot showed a noticeable difference in behaviors regarding the vertical oscillation of the robot's body and the roll motion. These differences in behaviors could be exploited to enhance the robot's adaptability based on the given situation.

During the robot's locomotion with mutually interconnected legs (which allows energy transfer between them), the robot was able to move in a smoother and more stable way compared to the other two connections of the rigid and compliant legs. It showed low oscillation amplitudes of both the roll motion and the vertical oscillation of the robot's body. However, the experiments here were conducted to test the robot's behavior on one type of ground materials (carpet on a leveled ground). Therefore, these results might get changed on other ground materials with different texture and different inclinations. And there, different connection patterns might be required to realize better performance.

Although the obtained promising results show possible improvements on the robot's walking behavior by applying ANS, our robot (introduced in this chapter) is just a prototype that has some drawbacks and limitations that need to be addressed. For example, the robot's demands to an extra supporting structure to keep it in balance and preventing it from falling down during locomotion, affects the robot's gravitational reaction force. Another thing, the robot was more

leaning to the right side during locomotion compared to the left side, which indicates the asymmetrical distribution of the robot's mass. Therefore, in the next chapter, improving the design of the robot would be the first thing to be done, to realize a self-balanced bipedal robot.

With this robot, the experiments were conducted to investigate the improvements that can be realized by utilizing ANS. However, the experiments were only done on one type of ground materials, and with only three types of legs. Thus, in the comming chapters, and after upgrading the robot's design, the robot's performance with different connection patterns will be examined on different ground materials with different inclinations. The effect of different types of independent legs with adjustable elasticity will also be considered. In addition to that, we will look for other emerged differences in behaviors that might occur by changing the way the robot's legs interact with each other. For example, the pitch and roll motions, walking speed, stability, the period of swing phase, stance phase and double limb support during the gait cycle, and how the robot will adapt to the variations of loads weights.

CHAPTER 5

PEDESTRIANS: A BIPEDAL ROBOT WITH ADAPTIVE MORPHOLOGY

Here in this chapter, we introduce the development of our third robot, PedestriANS, shown in figure 5.1-a. It is a self-balanced bipedal legged robot that uses ANS between its legs to adaptively change the type of interactions between its interconnected legs, as well as adjusting their physical characteristics such as compliance and stiffness. Contrary to other studies that applied ANS on legged robots, here in this part of our research, instead of using manually actuated valves for the ANS, which prevented the robots from switching to different connection patterns during locomotion, we are using electronically actuated valves to test how changing the connection patterns during the robot's locomotion will enhance its performance. The developed bipedal robot, PedestriANS, uses ANS to change the physical characteristics of its legs and the way they interact with each other. This allows it to overcome the limitations imposed by fixed body structures, broaden its body dynamics, and expand its ecological niche. Hence, the purpose of this study can be summed up under the following hypothesis: The performance of a bipedal robot (that has telescopic legs and semicircular shaped feet) cannot be at its best with a single body morphology whilst operating on different ground materials (slippery, hard, and soft). A robot should realize diverse levels of variable compliance actuation that include not only each part of the robot individually, but exceeds it to the level of whole-body dynamics. Therefore, to achieve optimal robustness of its locomotion gait, a robot needs to adapt its body with different elasticity, stiffness, and interactions among its parts to attain better behaviors in the face of changing environments.

5.1 PedestriANS: a bipedal robot with ANS

5.1.1 Structure of the robot

The developed bipedal robot "PedestriANS", shown in figure 5.1-a, is built with a simple structure based on Inverted Slider-Crank mechanism [34]. It is a four-link mechanism with three revolute joints and one prismatic joint as demonstrated in figure 5.1-b. Two of this mechanism, coupled at the crank and one-half cycle out of phase with each other, create the robot's legs. As both of the cranks rotate, the robot's legs oscillate up and down generating the walking behavior. A 24V DC motor is responsible for the robot's locomotion. The battery, as well as the microcontroller (Mbed), are mounted on top of the robot as illustrated in figure 5.1-a.

To obtain adjustable compliant legs in addition to mutual interactions between them; a dual rod pneumatic cylinder is added at the end of both legs. Attached to each of the pneumatic cylinders is a semicircular shaped foot, as shown in the figure. This particular shape of the feet was chosen to control the step size and to allow ground clearance during the swing phase of the robot's gait. It also provides a smooth walking behavior as it helps to reduce the collision impact forces against the ground. With these feet, and the symmetrical distribution of the robot's mass, the robot realizes self-balance during locomotion that prevents it from falling down.

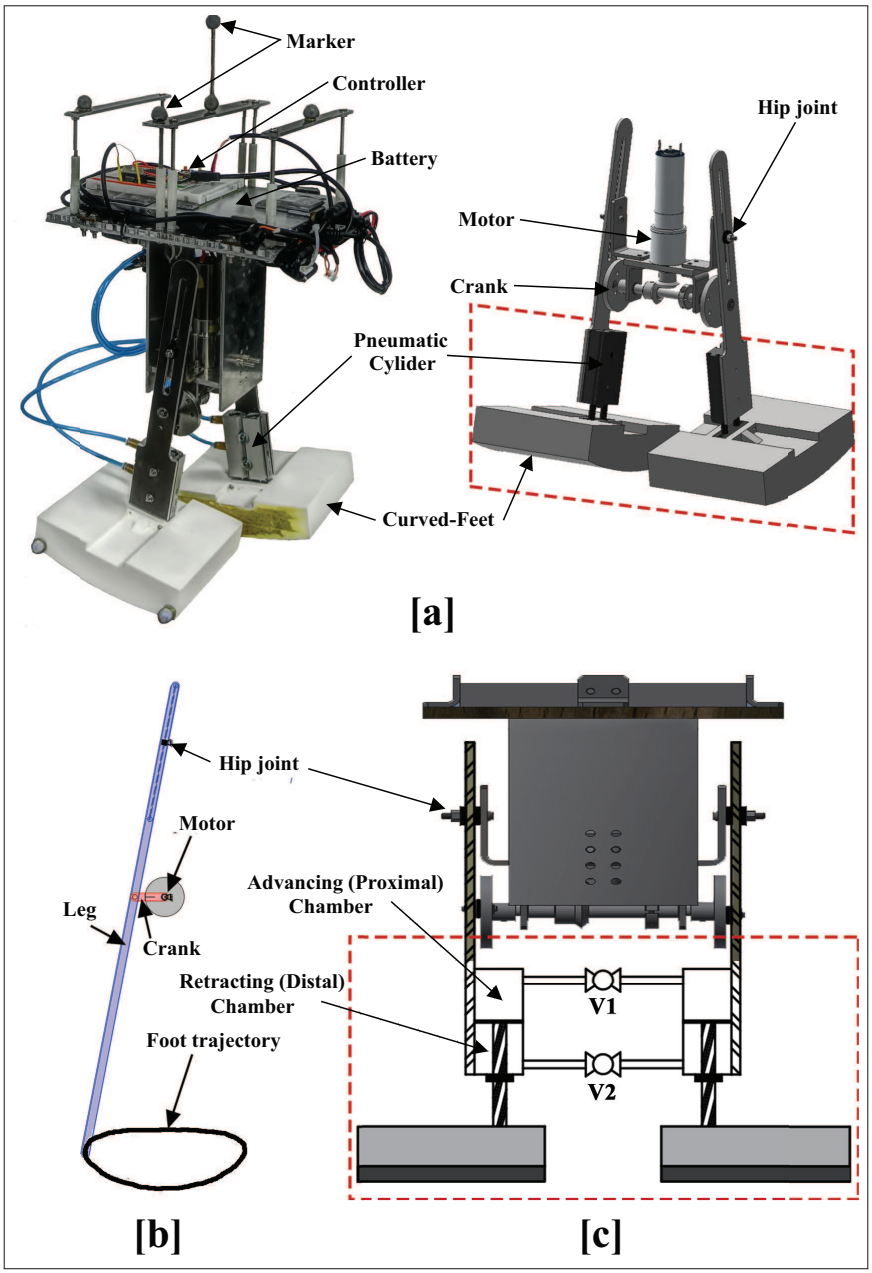

Figure 5.1: The developed bipedal robot "PedestriANS". [a] Mechanical structure illustration of the robot. [b] Inverted Slider-Crank mechanism. [c] Valve system diagram of the ANS.

5.1.2 Valve system of the robot

A simple valve system of two manually actuated hand-valves forms the ANS of our bipedal robot "PedestriANS". It connects the robot's legs as illustrated in figure 5.1-c. Valve V1 links the advancing chambers (proximal) of the two cylinders together, while valve V2 links the retracting chambers (distal) together. The difference in air pressure between the two chambers of a cylinder affects the net force applied on its piston; therefore, this pressure difference is the reason behind the extension, retraction, and compliance adjustment of a robot's leg. For example, higher pressure in the advancing chamber compared to the retracting chamber will result in an extension of the robot's leg, and vice versa.

The different combinations of open/ close valves are what define the interactive nature between the robot's legs themselves and the environment. If both valves are closed, independent legs will be created with compliance determined by the sealed air pressure inside each cylinder. On the contrary, mutually interconnected legs will be created if both valves are kept open, allowing force transmission between the two legs. As a result of these different connection patterns of the ANS between the robot's legs, the robot can modify its whole body dynamics through its interactions with the environment, providing a wide range of behaviors that could be exploited for better adaptation.

Although the robot has rigid feet that are not compliant themselves, the whole body dynamics and its compliance can be manipulated and adjusted by using the different connection patterns of the ANS.

5.2 Analyzing the robot's behavior at different connections of the ANS and on different ground materials

To evaluate the robot's locomotion behavior and investigate its adaptability to various environments, we have conducted our experiments on different ground materials, such as slippery, rigid, and soft ones. Throughout the experiments, we examined how the different connection patterns of the ANS affect the robot's behavior.

5.2.1 Connection patterns

During the conducted experiments, the robot's movement was examined with three different types of legs, as illustrated in figure 5.2. Under type 1, we set the air pressure inside the cylinders with proper values to get the legs at their half-advanced lengths. Then, we keep both of the valves open to allow energy transfer between the two legs. For example, in this case, once the robot steps on its right leg, the piston of the cylinder attached to this leg will fully retract. In response to that, the left leg will fully expand due to the air transmission between the two legs.

To get compliant legs under type 2, we only pressurize the advancing (proximal) chambers of both cylinders, while keeping the retracting (distal) chambers under atmospheric pressure. After that, we close both of the valves to prevent any direct interaction between the robot's legs, as illustrated in figure 5.2-b. In this case, the locked air inside the chambers of each actuator will create independent spring-like legs.

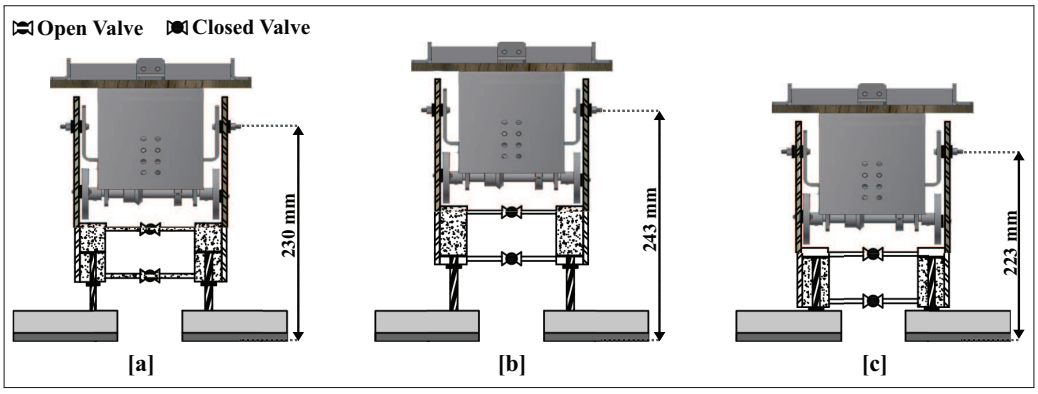

Figure 5.2: The applied connection patterns during experiments. [a] Type 1: Mutually connected legs; both cylinders are set at their half-advanced lengths, and the valves are kept open to allow energy transfer between legs. [b] Type 2: Independent compliant legs; both cylinders are fully extended by pressurizing the advancing chambers, and the valves are kept closed to prevent any direct interaction between legs. [c] Type 3: Rigid legs; both cylinders are fully retracted by pressurizing the retracting chambers, and the valves are kept closed to prevent any direct interaction between legs. * Leg length: is the distance from the hip joint of the robot to the bottom of its feet during its initial posture.

Contrary to type 2, in the situation of type 3 legs, we only pressurize the retracting (distal) chambers of both cylinders, while keeping the advancing (proximal) chambers under atmospheric pressure. Consequently, the robot's legs will fully retract to create rigid legs with no interaction between them, as shown in figure 5.2-c.

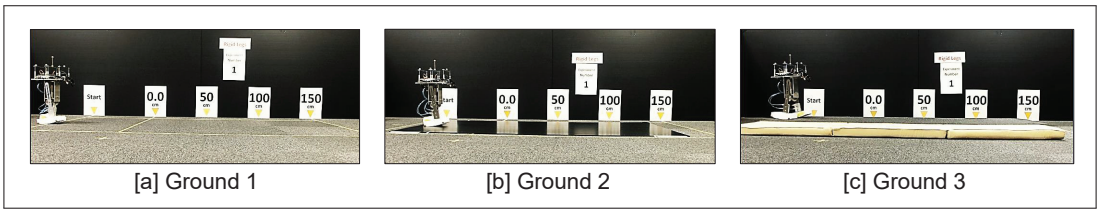

Figure 5.3: The ground materials of the conducted experiment. [a] Ground 1: Carpet on a leveled ground. [b] Ground 2: Plastic cardboard. [c] Ground 3: Carpet on a sponge.

5.2.2 Procedure and experimental settings

To examine how changing the robot's dynamics (through changing the connection patterns of ANS) will affect the stable/ adaptable walking behavior of the robot, experiments were conducted on three different ground materials.

- Ground 1: Carpet on a leveled ground, as shown in figure 5.3-a; to test the robot's behavior on a rigid ground surface.
- Ground 2: Plastic cardboard, as shown in figure 5.3-b; to test the robot's behavior on a slippery ground surface.
- Ground 3: Carpet on a sponge, as shown in figure 5.3-c; to test the robot's behavior on a soft ground surface.

For each type of legs mentioned earlier in this section, ten trials were conducted on each of these three ground materials to investigate the robot's locomotion. After preparing the robot and selecting one of the three legs types, the following procedures are performed during every trial on all ground materials:

1. Run the robot, place it on the ground and guide its movement direction during the first (0.40 ~ 0.50 m) to make sure that the robot is moving in a straight path alongside the Z-axis, as demonstrated in figure 5.4.

2. Release the robot to move by its own for the next (1 ~ 1.5 m).
3. If the robot falls down during a trial before traveling 1 m by its own, the trial is canceled, and one failed trial is registered.
4. Repeat these procedures until completing ten successful trials.

By placing reflective markers on the robot, as shown in figure 5.1-a, the movement of the robot was analyzed and recorded using a motion tracking system (OptiTrack-V120: TRIO) with a capture frame rate of 120 fps.

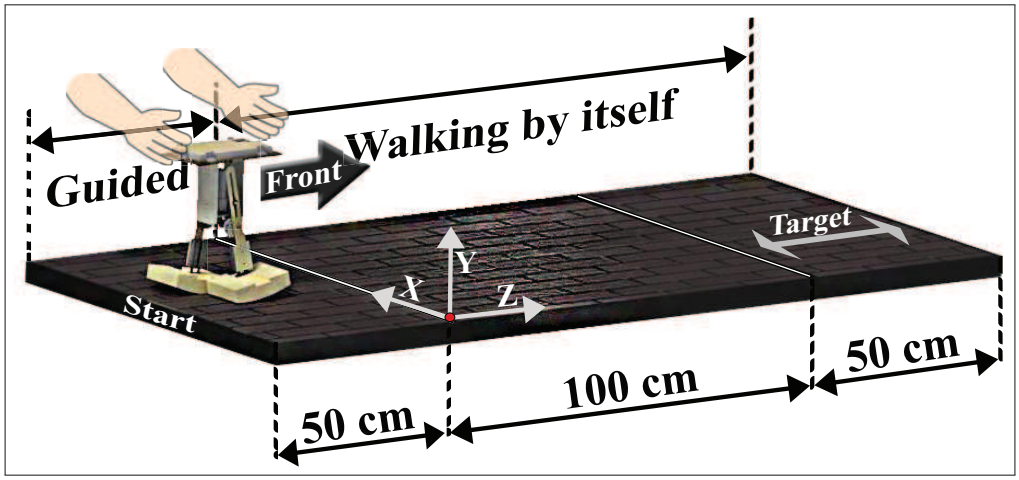

Figure 5.4: Schematic diagram of the experimental settings.

5.2.3 Results

For each of the conducted trials, the robot's behavior was evaluated by looking into four aspects:

- Direction: whether the robot keeps moving in the same direction or not.

This is investigated by observing the walking path of the robot during locomotion.

- Walking style: whether the robot walks in a smooth and gentle way, or have a rough and shaky walking style. This is evaluated by measuring the roll motion, pitch motion, yaw motion, and vertical oscillation of the robot's body, as illustrated in figure 5.5.
- Stability: whether the robot loses its balance and falls down, or maintains its balance until the end of the trial. The number of trials the robot falls down before reaching the target destination used as an indication for the robot's stability.
- Speed: how fast the robot can reach the target destination. To make sure that the difference in performance does not result from the fact that the three types of legs have effectively different lengths, as shown in figure 5.2, the speed results are measured after normalizing the lengths of the robot's legs.

Results of the trials conducted on Ground 1

By checking the graphs of figure 5.6, for the experiments conducted on carpet ground material, we can clearly compare the robot's behavior under the different types of legs. With mutually connected legs (type 1) which allows energy transfer between legs during locomotion, the robot maintained its moving direction as it kept walking straight along the z-axis, as shown in the first row of figure 5.6. On the other hand, with compliant legs (type 2) and rigid legs (type 3), once the robot was released to walk by its own without guidance, its walking paths started to diverge into random directions as evident in the figures.

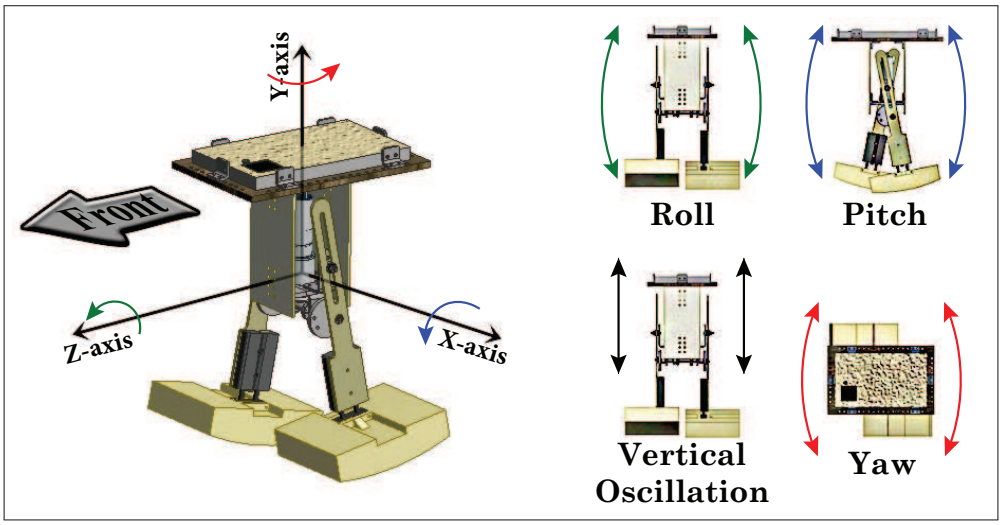

Figure 5.5: Illustration diagram of the body motions. *Roll motion: rotation of the robot's body around its front-to-back axis (Z-axis). *Pitch motion: rotation of the robot's body around its side-to-side axis (X-axis). *Yaw motion: rotation of the robot's body around its vertical axis (Y-axis). *Vertical oscillation of the robot's body.

On this ground material, the robot with mutually connected legs did not only have the advantage of moving straight during locomotion, but also exhibited other preferences. The robot walked more gently and smoothly compared to the other types of legs. Referring to the graphs of figure 5.6, counter to the other legs types, the roll motion under type 1 demonstrated periodic oscillation with almost constant amplitude and frequency. In addition to that, the pitch motion, yaw motion, and vertical oscillation of the robot's body had regular oscillations with low amplitudes compared to the other two types of legs, compliant and rigid ones, as illustrated in table 1 of figure 5.7.

The robot with type 1 legs also showed more stable and adaptable walking behavior on this ground material. As table 2 of figure 5.7 indicates, the robot with connected legs did not fall down in any of the ten conducted trials. However, the robot fell down one time in case of the compliant legs and six times in case

of the rigid legs before completing ten successful trials.

As figure 5.7-a shows, the robot with type 1 legs was the fastest to reach the target destination among the three types of legs. At the same time, the robot with compliant legs (type 2) and rigid legs (type 3) had slower walking behaviors on this ground material.

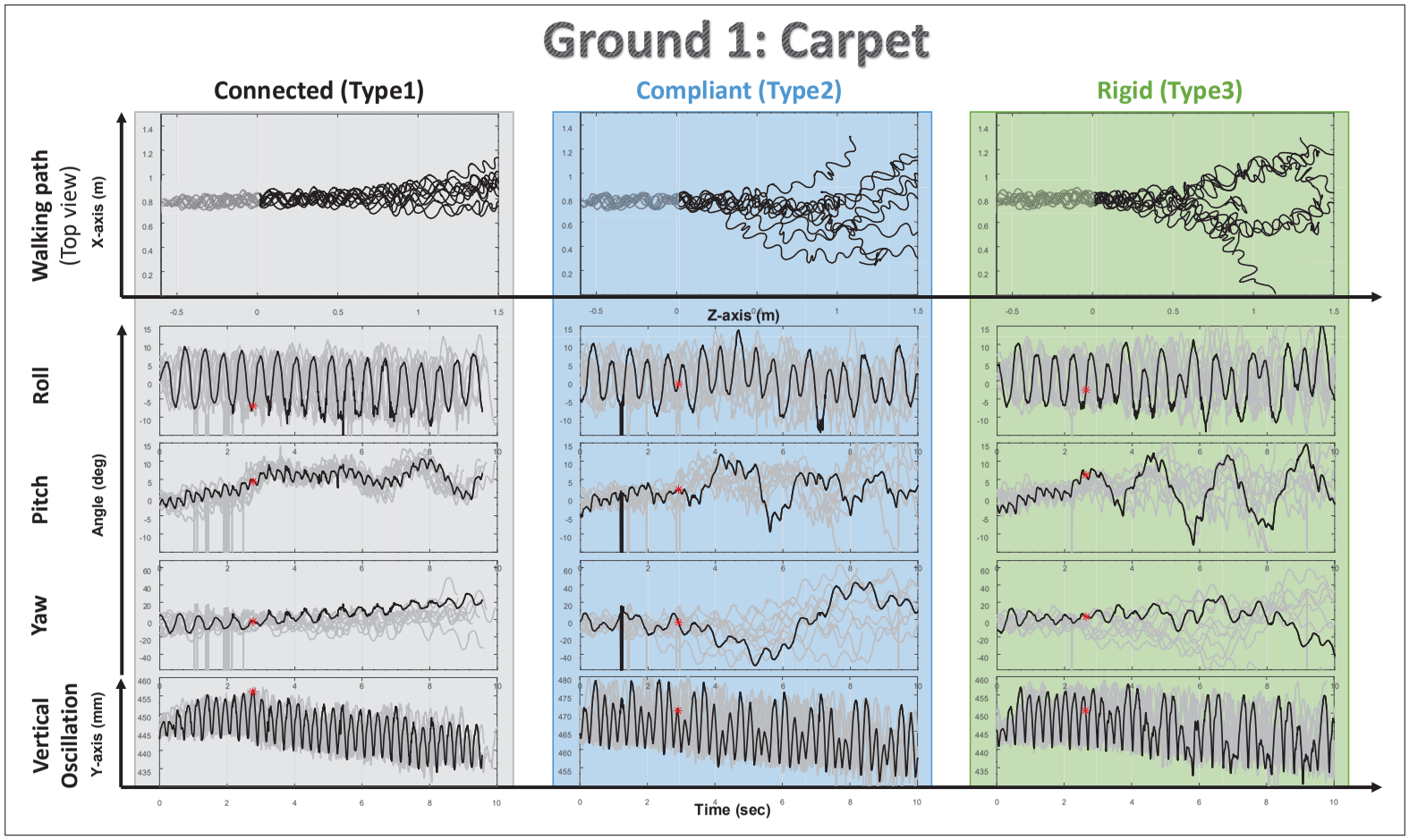

Figure 5.6: Results of the experiment on a carpet ground material.

Graphs of the Roll, Pitch, Yaw and Vertical oscillation of the robot's body under the three types of legs. The faded part at the beginning of walking path graphs represents the guided period of the robot. The highlighted black lines represent a typical behavior among the ten conducted trials under each type of legs. "*" Indicates the end of the guided period.

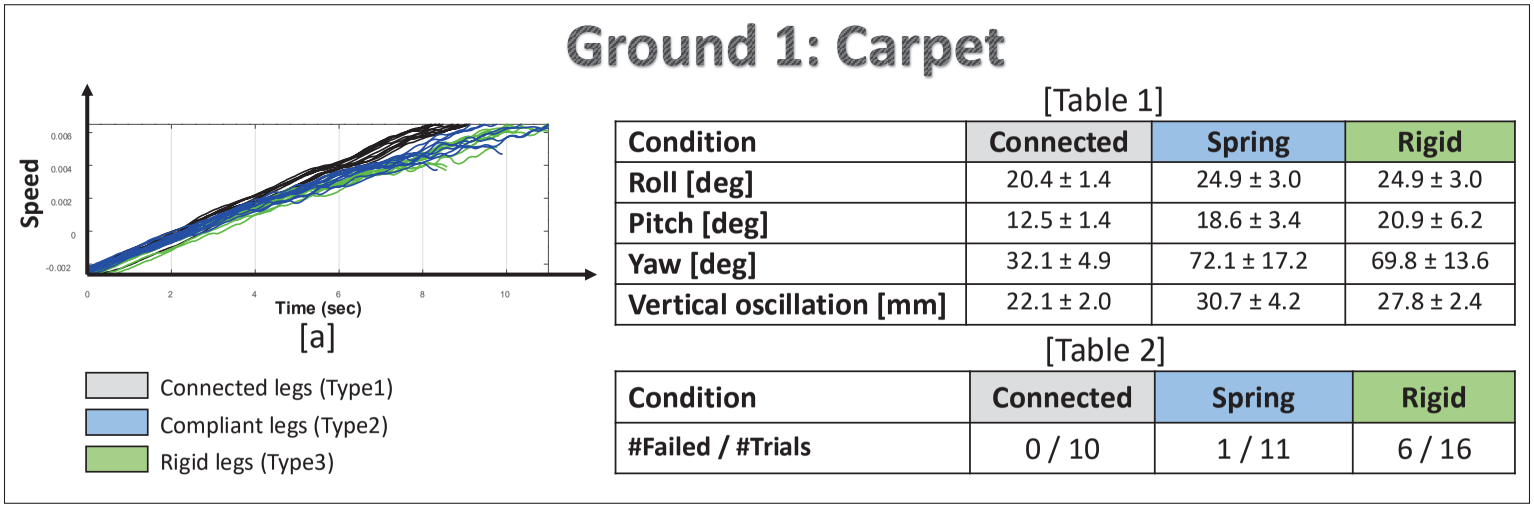

[Table 1]

Condition	Connected	Spring	Rigid
Roll [deg]	20.4 ± 1.4	24.9 ± 3.0	24.9 ± 3.0
Pitch [deg]	12.5 ± 1.4	18.6 ± 3.4	20.9 ± 6.2
Yaw [deg]	32.1 ± 4.9	72.1 ± 17.2	69.8 ± 13.6
Vertical oscillation [mm]	22.1 ± 2.0	30.7 ± 4.2	27.8 ± 2.4

[Table 2]

Condition	Connected	Spring	Rigid
#Failed / #Trials	0 / 10	1 / 11	6 / 16

Figure 5.7: Results of the experiment on a carpet ground material.

[a] Comparison of the robot speed under the three types of legs. The vertical axis of figure [a] is an indication of the traveled distance after normalizing the lengths of the robot's legs. [Table 1] The average range (difference between the highest and lowest values) of the Roll, Pitch, Yaw motions [deg] ± S.D, and the Vertical oscillation of the robot's body [mm] ± S.D. [Table 2] The number of trials the robot fell down before reaching the target destination

Results of the trials tonducted on Ground 2

Plastic Cardboard was selected to examine the robot's locomotion on a slippery ground surface. As can be inferred from table 2 of figure 5.9, regardless of the connection pattern between the robot's legs, the robot on this ground material has shown a stable walking behavior without falling down during any trial. However, there are still other differences in the robot's behavior among the three types of legs.

While the walking paths of the robot with rigid legs have scattered onto different directions as depicted in figure 5.8, the robot with both connected and compliant legs has kept moving in the same direction even after it was left to walk by itself without guidance.

As can be deduced from the motion graphs of roll, pitch, yaw and vertical oscillation of the robot's body; the robot with connected legs (type 1) had relatively better walking style compared to the other two types of legs. For example, from the pitch motion graphs under type 2, the robot kept leaning forward and backward after it was left to walk by itself as shown in figure 5.10. By taking the difference between its highest and lowest inclination angles, it had an oscillation range of (12.2 ± 1.5 deg) as demonstrated in table 1 of figure 5.9. However, it had the lowest oscillation range of (10.4 ± 2.6 deg) under type 1 legs.

On this ground material, the robot with compliant legs (type 2) was the fastest to reach the target destination among the three types of legs, as shown in figure 5.9-a. By contrast, the robot with rigid legs (type 3) was the slowest among them.

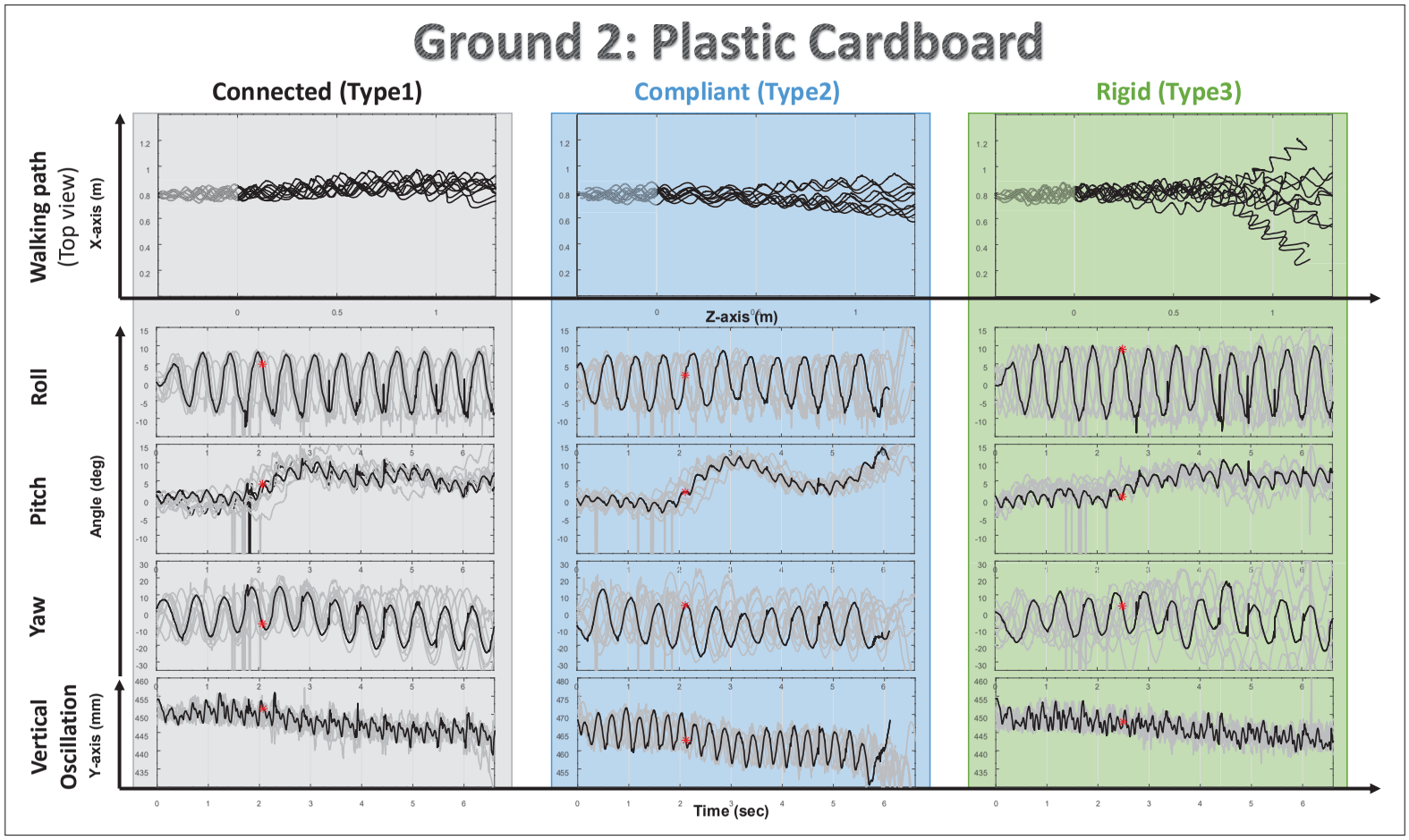

Figure 5.8: Results of the experiment on a plastic cardboard material.

Graphs of the Roll, Pitch, Yaw and Vertical oscillation of the robot's body under the three types of legs. The faded part at the beginning of walking path graphs represents the guided period of the robot. The highlighted black lines represent a typical behavior among the ten conducted trials under each type of legs. "*" Indicates the end of the guided period.

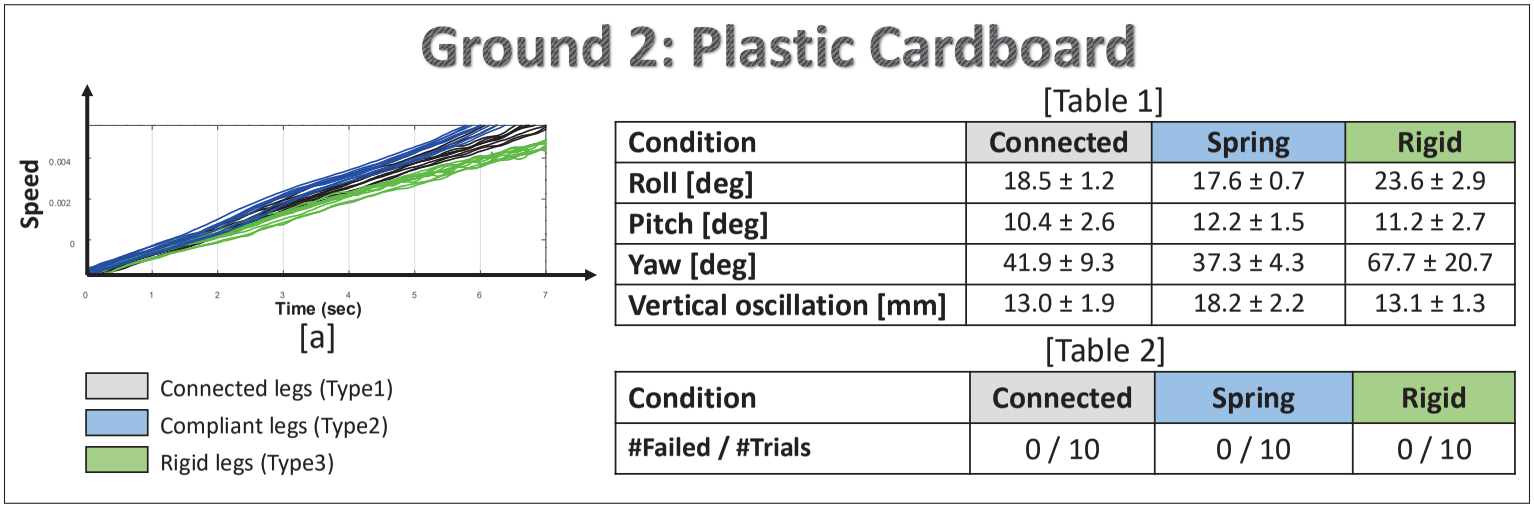

Figure 5.9: Results of the experiment on a plastic cardboard material.

[a] Comparison of the robot speed under the three types of legs. The vertical axis of figure [a] is an indication of the traveled distance after normalizing the lengths of the robot's legs. [Table 1] The average range (difference between the highest and lowest values) of the Roll, Pitch, Yaw motions [deg] ± S.D, and the Vertical oscillation of the robot's body [mm] ± S.D. [Table 2] The number of trials the robot fell down before reaching the target destination

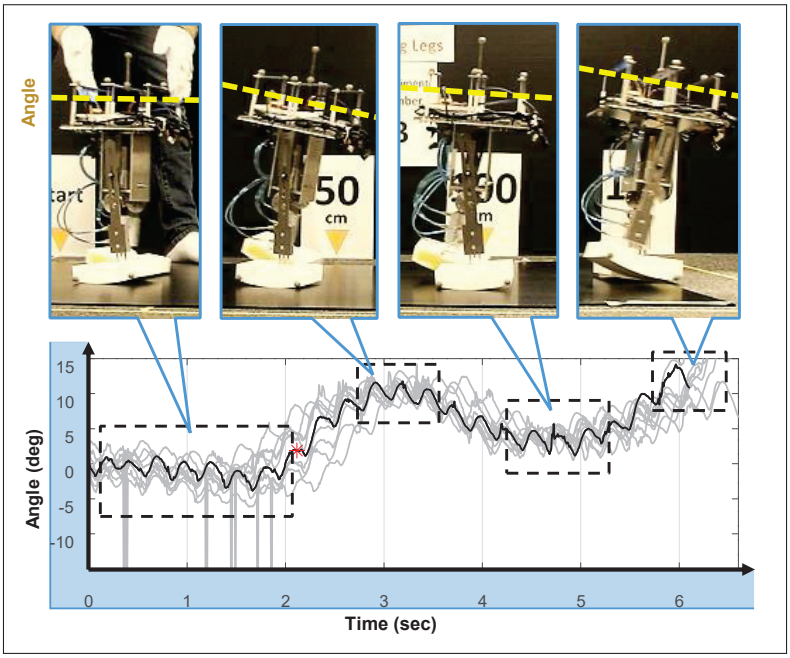

Figure 5.10: The corresponding body postures of the robot to its pitch angle oscillation during locomotion on Ground 2 with type 2 legs.

Results of the trials conducted on Ground 3

The trials conducted on a sponge material were to examine the robot's locomotion on a soft ground surface. By referring to the walking paths of figure 5.11, it seems that the robot on this ground material managed to maintain its walking direction by moving straight along the Z-axis regardless of the selected connection pattern. However, other differences still can be observed regarding the robot's stability, speed, and walking style.

It is evident from the motion graphs of the roll, pitch, yaw, and vertical oscillation of the robot's body that the robot with rigid legs had the shakiest walking behavior. As table 1 of figure 5.12 shows, it had the highest and most varying range of oscillation amplitudes of all motions compared to the other two types

of legs. For example, from the graphs of pitch motion, under this type of legs, the robot's body kept leaning forward and backward with a high oscillation range of (19.4 ± 3.7 deg) compared to (10.9 ± 2.0 deg) and (14.9 ± 2.7 deg) of type 1 and type 2 legs respectively. By contrast, as on the other ground materials, the robot with type 1 legs seemed to have the smoothest "most gentle" walking behavior. It showed the lowest range of oscillation amplitudes in all of the roll, pitch, yaw, and vertical oscillation of the robot's body as depicted in table 1.

From figure 5.12-a, the robot with rigid legs (type 3) still had the slowest gait speed to reach the target destination. However, this time, it exhibited the most stable behavior as table 2 of figure 5.11 shows. The rate in which the robot fell down before reaching the target destination was the smallest (6 / 11) compared to the other two types of legs, connected and compliant legs, which had the rates of (8 / 11) and (10 / 10) respectively.

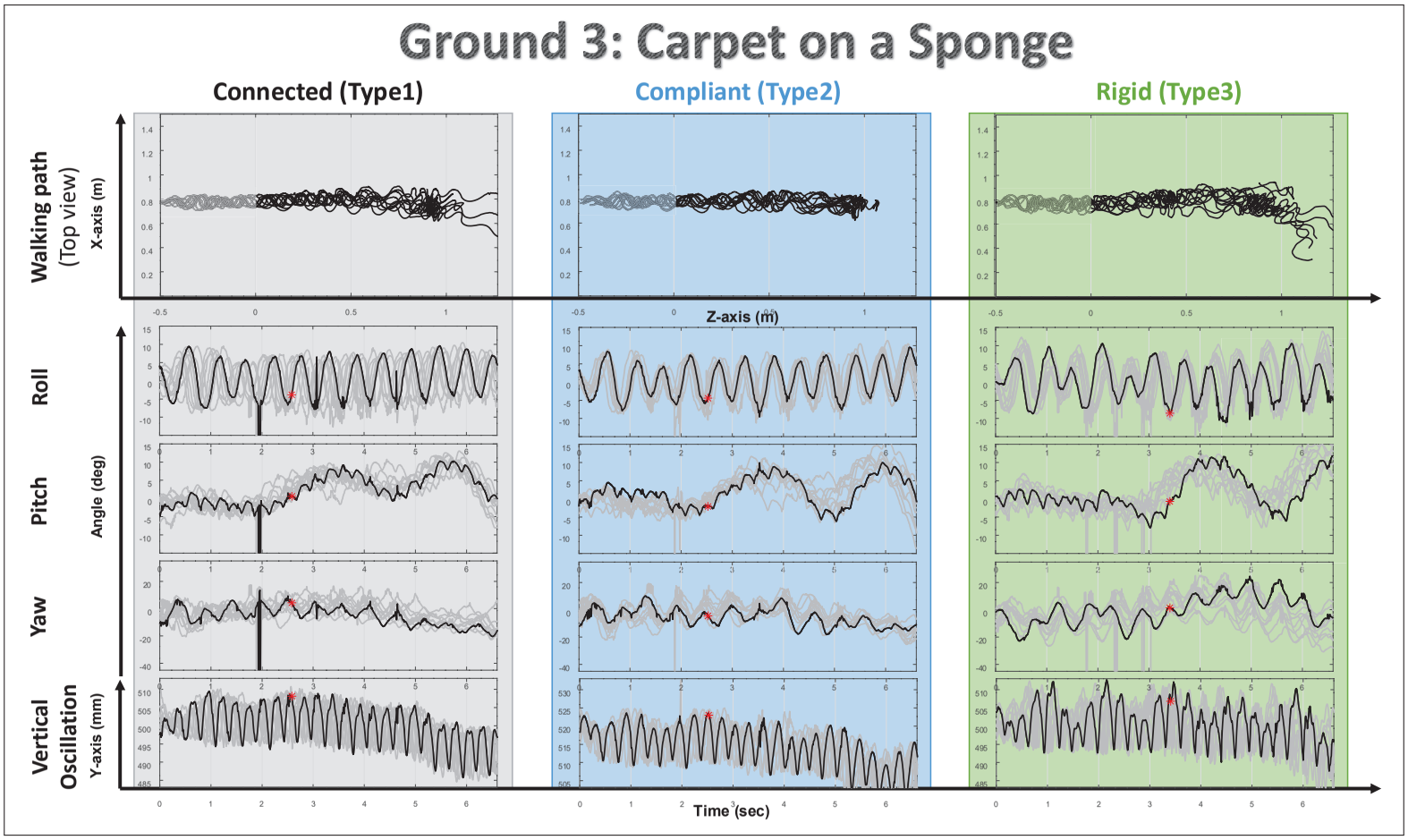

Figure 5.11: Results of the experiment on a sponge ground material.

Graphs of the Roll, Pitch, Yaw and Vertical oscillation of the robot's body under the three types of legs. The faded part at the beginning of walking path graphs represents the guided period of the robot. The highlighted black lines represent a typical behavior among the ten conducted trials under each type of legs. "$*$" Indicates the end of the guided period.

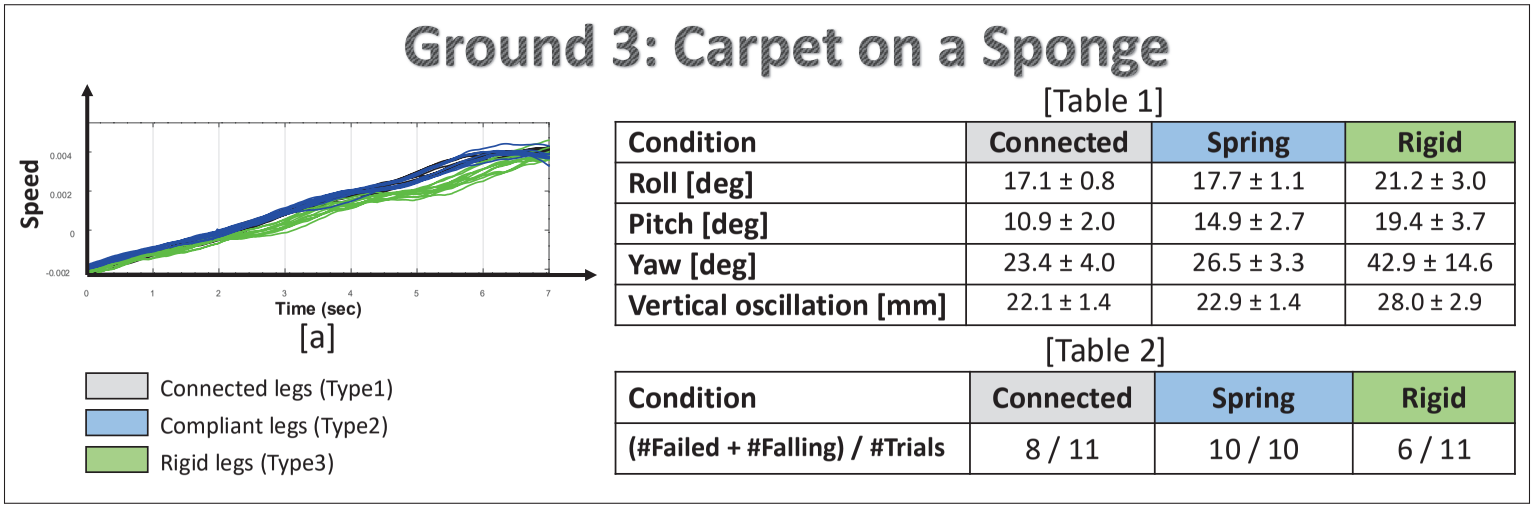

[Table 1]

Condition	Connected	Spring	Rigid
Roll [deg]	17.1 ± 0.8	17.7 ± 1.1	21.2 ± 3.0
Pitch [deg]	10.9 ± 2.0	14.9 ± 2.7	19.4 ± 3.7
Yaw [deg]	23.4 ± 4.0	26.5 ± 3.3	42.9 ± 14.6
Vertical oscillation [mm]	22.1 ± 1.4	22.9 ± 1.4	28.0 ± 2.9

[Table 2]

Condition	Connected	Spring	Rigid
(#Failed + #Falling) / #Trials	8 / 11	10 / 10	6 / 11

Figure 5.12: Results of the experiment on a sponge ground material.

[a] Comparison of the robot speed under the three types of legs. The vertical axis of figure [a] is an indication of the traveled distance after normalizing the lengths of the robot's legs. [Table 1] The average range (difference between the highest and lowest values) of the Roll, Pitch, Yaw motions [deg] ± S.D, and the Vertical oscillation of the robot's body [mm] ± S.D. [Table 2] The number of trials the robot fell down before reaching the upper limit of the target destination.

5.3 Supplementary experiment: switching connection pattern during locomotion to enhance the robot's behavior

So far, the conducted experiment examined the pros and cons of each connection pattern separately; where during each trial, a single type of legs was tested. However, by referring to table 5.1, which summarizes the results of all experiments, the robot's demands for a certain connection pattern to produce better behavior differ based on the surrounding environment. For example, the type of legs that showed the worst behavior on carpet ground material, it was the same type of legs that showed the most stable behavior on sponge ground material. Therefore, for this robot to operate on an actual unstructured environment, it should be enabled to switch between the different connection patterns during locomotion to better suit the given situation.

5.3.1 Procedure and experimental settings

For the purpose of testing how switching between different connection patterns will enhance the robot's behavior, here, in this supplementary experiment, we have updated the robot structure as shown in figure 5.13-a. The manually actuated valves were replaced with electronically actuated ones. A tank was also mounted on the robot's body to supply the actuator network system with the required air pressure.

The experiment was conducted on a carpet ground material as demonstrated in figure 5.14. To examine the effect of switching between connection patterns during the robot's locomotion, the experiment starts with the robot having rigid

Table 5.1: Summary results of section 5.2.3.

Ground	**Connection**	**Direction**	**Walking style**	**Speed**	**Stability**
Carpet	Type1	+	+	+	+
	Type2	-	**0**	-	**0**
	Type3	-	-	-	-
Plastic cardboard	Type1	+	+	**0**	+
	Type2	+	**0**	+	+
	Type3	-	-	-	+
Sponge	Type1	+	+	+	**0**
	Type2	+	**0**	+	-
	Type3	+	-	-	+

"+" Represents best behavior (maintains direction, gentle walking style, fastest, and most stable). "-" Represents worst behavior (changes direction, rough walking style, slowest, and least stable). "0" Represents intermediate behavior (between + and -).

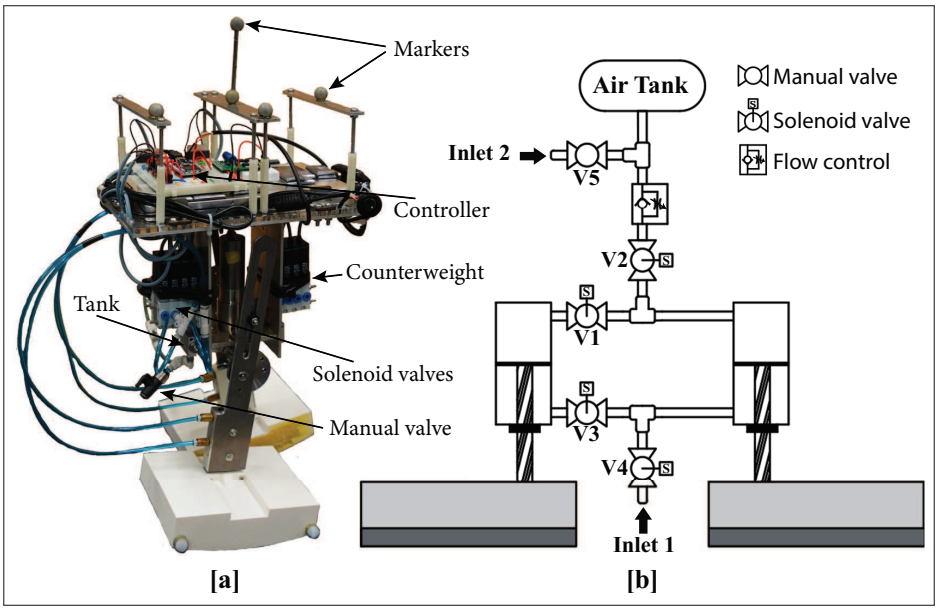

Figure 5.13: [a] The updated structure of "PedestriANS". [b] The updated ANS.

legs, which previously showed unstable behavior on this ground material. The robot then switches its connection to mutually connected legs, which already showed a stable walking behavior on this ground material.

Figure 5.13-b shows the updated actuator network system. Before starting the experiment, the lower chambers of both cylinders are pressurized through inlet 1. Afterwards, both valves V3 and V4 are closed to create rigid legs. While keeping V2 closed, the tank also gets pressurized through inlet 2. The robot will switch to connected legs during locomotion by opening both V1 and V2 valves.

The type of connected legs in this experiment slightly differs from the previously used connected legs. The former type of connected legs, shown in figure 5.2-a, connects the upper chambers of both cylinders, as well as the lower chambers. However, here, the upper chambers of both cylinders are connected while the lower chambers are not. Similar to the former type, once a robot's leg hits

Figure 5.14: Experimental environment.

the ground and enters the stance phase, it will fully retract; causing an expansion of the other leg. However, the difference here, once a robot's leg enters the swing phase; it will directly return to its equilibrium length, without the need to wait for the other leg to enter the stance phase to get expanded.

For this experiment, five trials with a duration of twelve seconds each were conducted. During each trial, the robot starts walking with rigid legs. To reduce the probability of the robot from falling down during the rigid legs period, the duration under this condition is set to be only four seconds. During the first second, the robot is guided. For the remaining three seconds, the robot is unguided. The robot then switches to mutually connected legs for the remaining eight seconds As demonstrated in figure 5.15 .

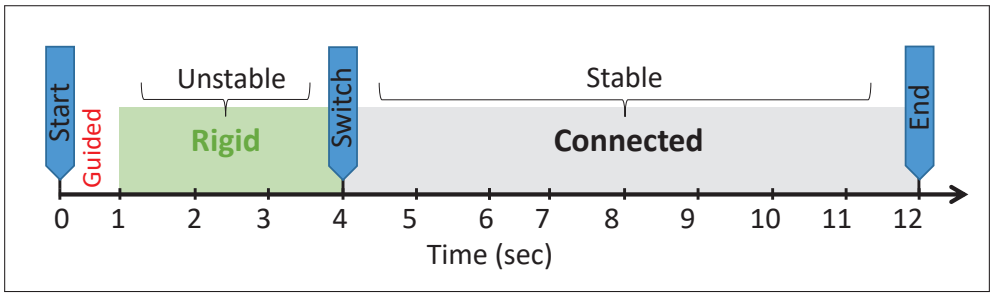

Figure 5.15: Experimental design: Switching connection pattern during locomotion.

5.3.2 Results

Similar to the previous experiment, the walking path, roll motion, pitch motion, yaw motion, and vertical oscillation of the robot's body were measured to evaluate the robot's behavior. By looking to the graphs of figure 5.16, we can notice the significant improvements that happened to the robot's gait after switching to connected legs.

The roll motion during the rigid legs period was oscillating with high range and variable amplitudes. However, once the robot switched to the connected legs as the figure shows, it started recovering from this unstable behavior to end up with a periodic oscillation that has lower and constant amplitudes.

The same thing can also be seen from the pitch motion graphs. During the rigid legs period, the robot was almost falling due to the high range of angle oscillation in the forward and backward directions. It's worth mentioning here that even with this short period for this part to prevent the robot from falling down before switching to the connected legs; almost 50 % (4 / 9) of the conducted trials the robot fell down and didn't make it to the connected legs. For the rest of the trials in which the robot made it to the connected legs without falling down;

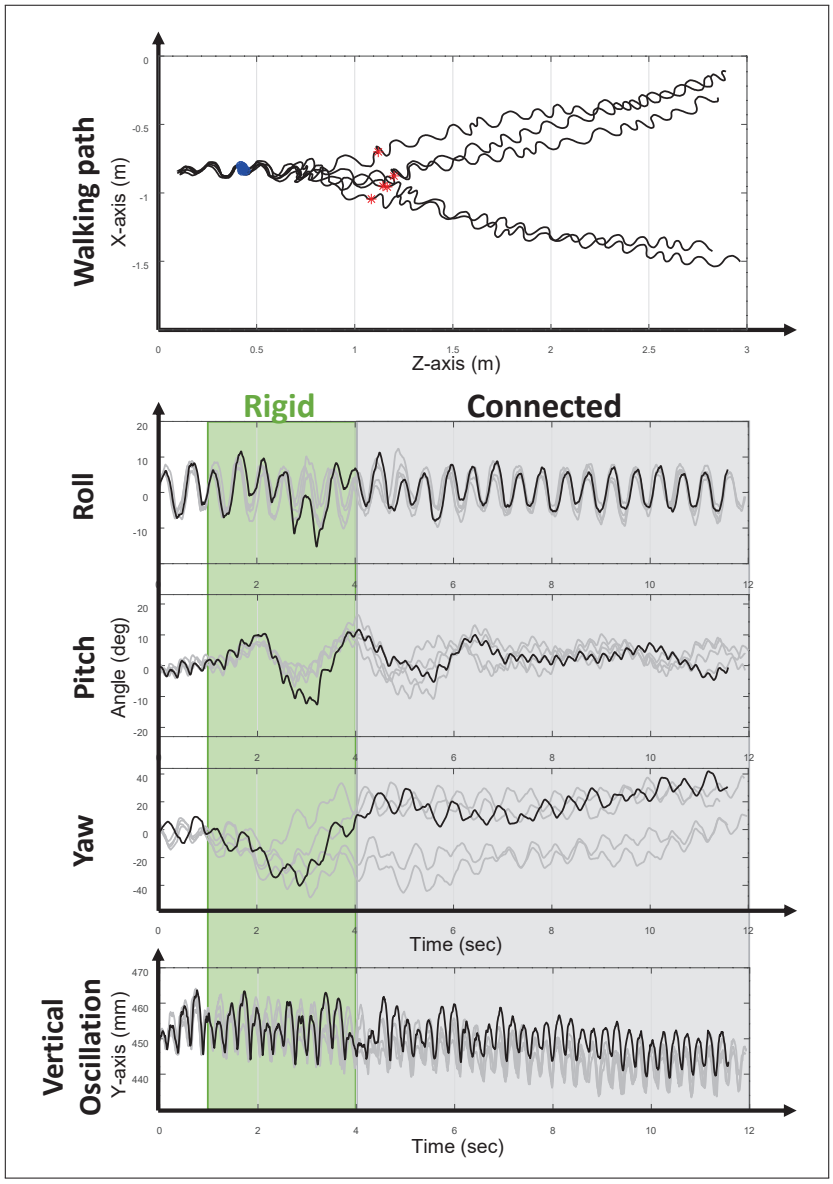

Figure 5.16: Results of the supplementary experiments. From top to bottom, the graphs are walking path, roll motion, pitch motion, yaw motion, and vertical oscillation of the robot's body. The green-shaded part (from 1 sec to 4 sec) represents the duration of the robot with rigid legs. The gray-shaded part (from 4 sec to 12 sec) represents the duration of the robot with mutually connected legs. The highlighted black lines represent one of the five conducted trials. "•" Indicates the end of the guided period. "*" Indicates the moment of switching.

the robot directly started correcting its behavior gradually until it maintained a stable behavior with an upright body posture.

From the yaw motion graphs, the unstable behavior of the robot during the rigid legs period is represented by the continuous changing of the walking direction. However, once the robot switched to the mutually connected legs, it started maintaining its direction. This behavior of the yaw motion reflects directly to what we see in the graphs of the walking path. The robot during the rigid legs period deviated into random moving directions. However, the robot maintained that direction, and kept moving straight after switching to the connected legs.

The changes happened to the vertical oscillation of the robot's body after switching to the connected legs may have the least noticeable improvement. However, with a closer look to the graphs, we can notice how at the end of all trials the robot achieved lower and constant oscillation amplitudes compared to the higher and variable oscillations at the beginning of the trials.

5.4 Discussion

For the conducted experiments on each of the ground materials, the robot's walking behavior has changed by changing the interaction between the actuators of the ANS. Based on these differences in the robot's walking behavior, as the results show, its demands for a certain connection pattern differ based on the given situation. For example, the connection pattern that better suits a certain ground material, it does not necessarily suit other ground materials, and what is bad for some ground materials, it might be the best for others. Exploiting

these various dynamics is the way to enable the robot from realizing adaptability to any given situation, and to develop an efficient gait pattern through all locomotion phases.

Each of the robot's feet has considerable weight; thus, a leg expansion during its swinging phase, in the case of types 1 and 2, directly affects the COM of the robot's body. In light of this, the difference in performance between mutually connected legs (type 1) and independent compliant legs (type 2) are not due to a mere difference in compliance. But also the time and manner of expansion affect the performance too. The expansion of a swinging leg, in case of type 1, depends on the stance leg since both legs are mutually connected. However, the expansion is independent of the stance leg in case of type 2. Therefore, the time for a swinging leg to get fully extended is different, and consequently has a different effect on positioning the COM of the robot, which in turn produces different body dynamics.

By looking at the vertical oscillation results of all experiments, there is a noticeable gradual decrease in the robot's height with time. The reasons behind this behavior are threefold. First, during the guided period, the robot's body is partially supported by the operator's hands; therefore, once the robot is left to walk by itself, its height slightly decreased as shown in the graphs. Second, by knowing that the height of the robot is being measured from the ground to the highest reflective marker placed on its body, its height will get directly affected by both roll and pitch motions. As leaning towards any direction (front, back, right, or left) during the robot's locomotion will result in a decrease in its height. Therefore, the vertical oscillation kept decreasing during some experiments in response to the increasing oscillation of either roll motion, pitch motion, or a

combination of both. The third and most important point, the used device for capturing these data, OptiTrack-V120: TRIO, uses a calibration square to define the ground plane. However, there is a difference between the defined plane and the actual floor surface, and they do not perfectly match. Although the difference between the two planes is very small and negligible, it is still visible in the graphs due to the used small scale of the Y-axis (millimeter). To measure this difference, we can refer to the trials conducted on Ground 2 (plastic cardboard) with rigid legs (type 3); because in this case the robot has a fixed leg length and never changes its height during locomotion. The difference in height between the beginning and end of the trial is 6 mm, and the robot traveled a distance of 1.9 m. Therefore, it is suggested that the angle between the defined horizontal plane of the sensor and the actual floor surface is at most 0.18°. A similar inclination line can be found on other ground materials as well.

Having different length for each of the three types of legs could affect the walking speed of the robot. To rule this out for the results of the conducted experiments, the speed graphs were made after normalizing the lengths of the robot's legs. However, even after this normalization, the graphs still show speed results that are independent of the leg's length. For example, the robot's walking speed with type 2 legs (longest legs) compared to type 1 legs was slower on Ground 1 as shown in figure 5.7-a, faster on Ground 2 as shown in figure 5.9-a, and similar on Ground 3 as shown in figure 5.12-a. Also, the speed results of the robot under type 2 and type 3 legs on Ground 1 is another example proving that the main factors affected the robot's behavior were the selected connection pattern between the robot's legs (mutually interconnected, independently compliant, or stiff), and the environment in which the robot is operating. The robot had relatively similar speeds, as figure 5.7-a shows, although type 2 has the longest

legs while type 3 has the shortest ones. There are many aspects that need to be looked at to understand the reasons behind these differences in the robot speed. The locomotion speed of a robot is influenced by many factors such as length of legs [35], [36], rotational slip that is caused by the yaw moment on the stance leg [37], elasticity of legs [38], the impact force between robot's feet and the ground [39], etc. Therefore, studying the effects of applying different connection patterns of the ANS on these factors would be an interesting area of study to be addressed in future work.

Furthermore, an additional experiment was also conducted on Ground 1 to exclude the effect of different legs lengths. The purpose of the experiment was to test the robot's behavior with Long rigid legs, then compare its performance with type 2 legs (similar length, different compliance). Despite having the same length for its rigid and compliant legs, the robot's behavior was still significantly different. The robot with rigid legs did not manage to complete any of the trials successfully as it kept falling before reaching the target destination. However, the robot with compliant legs, on the other hand, had much more stable behavior on the same ground material. It fell only one time out of the 11 conducted trials, as table 2 of figure 5.7 shows. Therefore, this clear difference in performance between the two types of legs is undoubtedly due to their different compliance as they both had the same length.

"PedestriANS" have shown an improvement in its behavior by changing the way its legs are interacting with each other. However, as mentioned earlier, the efficient, stable, and adaptive walking behavior of humans is not limited to the interaction between the two legs, but also a result of the interactions among the different parts of their bodies. Therefore, by expanding the ANS to include more

parts of the robot's body (which will be addressed in the next chapter), further enhancements will be realized in its behavior. This will increase the possible morphological changes, which in turn reflects on the robot's adaptability.

From the supplementary experiment, the robot managed to retrieve its stable behavior after switching to a different connection pattern during locomotion. However, with the current ANS, due to the limited pressurized air inside the tank, switching between two different connection patterns can only be done one time per trial. Therefore, to solve this problem in the future work, an air pump will be installed on the robot's body.

In this study, testing the robot's behavior under three types of legs, and on three different ground materials is just an example to show that the robot with ANS can adjust its whole body dynamics to adapt to a given environment. However, applications are not only restricted to these types of legs nor these ground materials. Moreover, although the results of the conducted experiments have only tackled the robot's behaviors in terms of the walking style, stability, speed, and moving direction, possible improvements could be much more than that.

Thus, the first step in the future work is to upgrade the robot's design. The upgrade will include expanding the ANS to cover more parts of the robot's body, installing an air pump to allow continuous ability of switching between the different connection patterns, and enabling the robot from autonomously choosing an adequate connection pattern to suit the given situation. The second step is to conduct experiments on terrains with various geometric properties (e.g., flat, sloped, rough, etc.) and different physical properties (e.g., slippery, hard, soft, etc.). The third step is to evaluate the robot's performance and its adaptability by checking its maneuverability, obstacles avoidance capability, and its ability

to recover stable behaviors after stumbling over sudden obstacles.

CHAPTER 6

THE INFLUENCE OF UPPER-BODY MOVEMENTS AND ITS INTERACTIONS WITH THE LOWER-BODY PARTS ON THE STABLE LOCOMOTION OF A BIPEDAL ROBOT

A human body functions optimally when all the parts operate together as a coherent unit [1]. Therefore, it is crucial to have an interaction among the various interconnected parts of the body to acquire balance during locomotion [40]. The stable walking behavior of humans is not merely a result of the dynamics generated by the lower-body parts; the various interactions with the different upper-body parts are involved as well. Several studies showed that the upper body's movements have a significant contribution to the dynamic balance during locomotion [41], [42], [43]. It even contributes to the stable walking to a similar extent as the lower-body, especially during challenging locomotion [41]. From this perspective, in this part of our study, we investigate the influence of adding an upper body to a bipedal robot, and examine how its movements will affect its stable walking behavior. In order to create a robot's body where all its parts are mutually interconnected, we utilize the principle of Actuator Network System (ANS).

From the necessity for a bipedal robot to have its parts mutually interconnected and realize direct interactions among each other to achieve more adaptable and stable walking behaviors, we have developed our bipedal robot PedestriANS (introduced in the previous chapter). This robot utilizes the principle of Actuator Network System (ANS) to manipulate its whole-body dynamics. It can adaptively change the type of interactions between its interconnected legs, as well as adjusting their physical characteristics such as compliance and stiffness.

The ANS of PedestriANS is composed of two linear actuators that are attached to its legs. These actuators are mutually interconnected through a network of tubes and valves. Therefore, due to the various possible interactions between the actuators, the robot was able to respectively adapt its whole-body dynamics to generate better walking behaviors over a variety of different environments.

Since all parts of the body should be involved during locomotion, in this chapter, we investigated the influence of adding an upper-body to PedestriANS. This upper-body forms a simple pendulum moving in the frontal plane of the robot; its oscillation direction and the magnitude of its rotational angle depend directly on the connection pattern type of the ANS. In the beginning, we conducted our experiments without including the upper-body with the robot's ANS. This means no mutual interactions between the robot's legs and the upper-body are involved, allowing us to understand the effects of adding an independent motionless upper body on the robot's walking behavior. After that, we extended the ANS to include the upper-body of the robot to create a body where all its parts are interconnected, and multiple interactions are now possible among all of them. Hence, conducting experiments under different connection patterns between the upper and lower body parts to examine how upper-body movements will enhance stability during locomotion.

6.1 The upper and lower body parts of the robot and their ANS connections

6.1.1 Structure of the robot

The lower-body parts of PedestriANS consist of two identical legs that are coupled at the crank with 180 deg out phase, as shown in figure 6.1-a. Each leg represents an inverted slider-crank mechanism, which is a four-bar linkage coordinated by a single degree of freedom. A dual rod pneumatic cylinder with a linear motion range of (20 mm) is fixed at the lower end of each leg; it creates an adjustable compliant leg and forms an element of the actuator network system. The robot's feet are attached to the legs through these pneumatic cylinders, as shown in the figure. The curved shape of the feet provides gentler gate patterns and reduces the collision strike against the ground. Knowing that the whole-body movement of the robot is generated by a single DC motor (24 V), and controlled by an Mbed microcontroller that is mounted on the robot's body as illustrated in the figure.

The upper-body of the robot was built to investigate the influence of its movements on the locomotion behavior of the robot. It consists of a swinging mass hanging down from a rotary actuator, as shown in figure 6.1-b. The actuator position on top of the robot allows the swinging to happen in the frontal plane above the robot's center of mass (COM). As demonstrated in figure 6.1-c, it is a double vane rotary actuator with an angular rotation range of (± 50 deg) from the vertical axis. Similar to the linear actuators fixed on the robot's legs, it is now associated with the robot's ANS. Therefore, the movement patterns of its

swinging mass (the way it oscillates) depends directly on the type of connection pattern among the actuators. Note that all actuators of the ANS are entirely passive, and no energy is supplied into the system; their movements and interactions during locomotion are simply caused by the collision impact forces of the robot's feet against the ground.

6.1.2 Valve system of the robot

The updated ANS of PedestriANS includes three actuators, as demonstrated in figure 6.1-c. Two linear actuators are attached to the robot's legs, and one rotary actuator is mounted on top of the robot and responsible for the oscillatory movement of the swinging mass. The linear actuator is composed of two chambers, proximal chamber (advancing) and distal chamber (retracting). The compliance adjustment and the movement of its rod (piston) depend on the air pressure difference between the two chambers. Higher pressure inside the proximal chamber compared to the distal one will cause an extension of the robot's leg, and the retraction happens once the distal chamber has a higher pressure. The same concept is applied to the rotary actuator too. However, the difference here, rotational movements are generated instead of the linear ones, and based on the pressure difference between the chambers, the mass will rotate in a clockwise (CW) direction or a counterclockwise (CCW).

The various arrangements of the valve system are what create the differences in the robot's behavior. With every set of switched valves (opened/closed), unique interactions among the actuators will affect the robot's dynamics. For example, closing all valves will create an independent movement of each body part. On

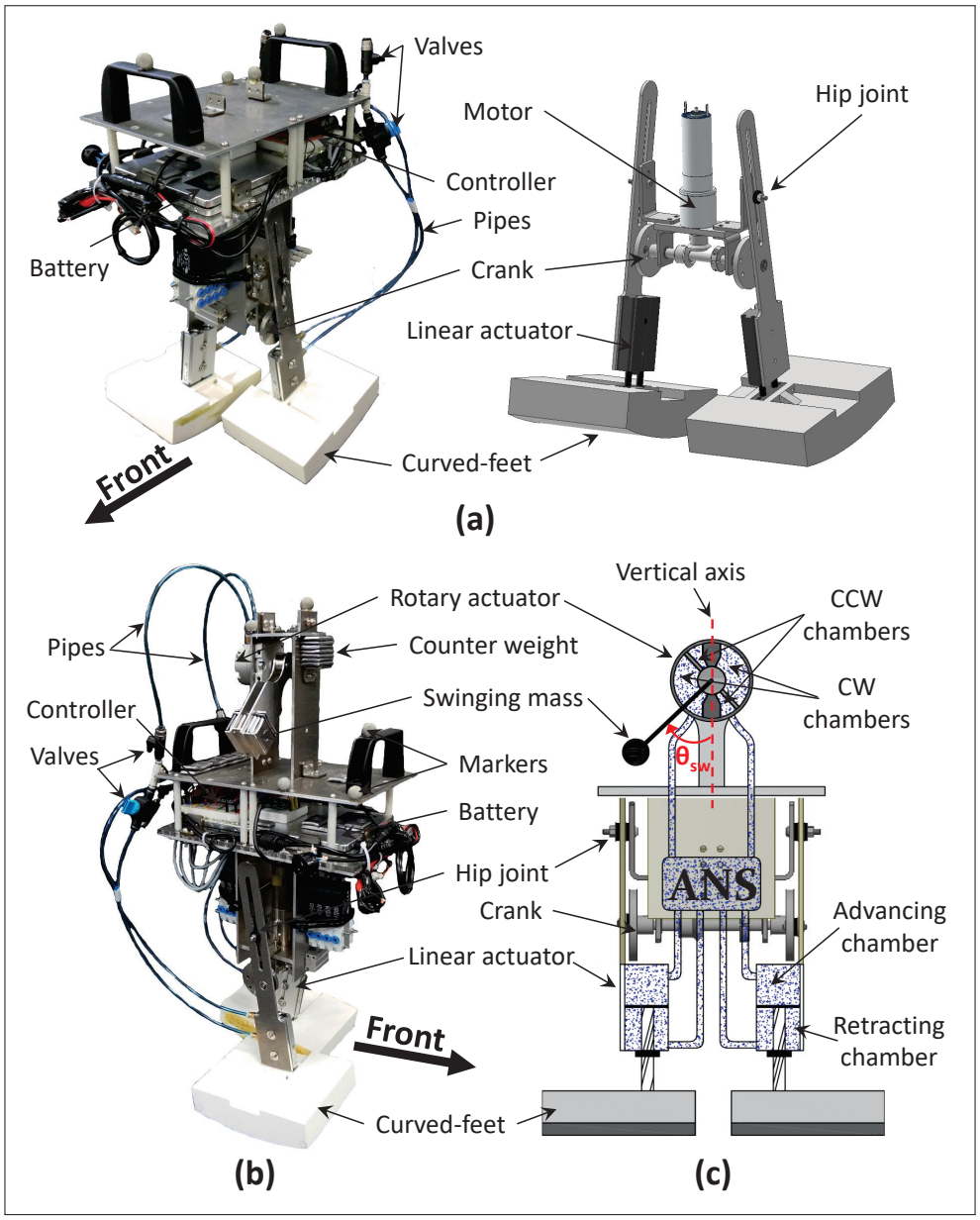

Figure 6.1: (a) Mechanical structure of the robot without an upper-body. (b) The updated robot with upper-body. (c) Illustration of the Actuator Network System (ANS). θsw: swing angle with respect to the vertical axis, positive in the clockwise direction.

the other hand, a specific combination of open valves will produce mutually interconnected parts with a particular way of interaction among them. Therefore, the whole-body dynamics of the robot are influenced by the type of in-

teractions among the actuators themselves, as well as their interaction with the surrounding environment during locomotion. And the compliance/stiffness of the actuators is adjusted by the air pressure value of the ANS.

More details about the different connection patterns of the ANS can be found in the next section.

6.2 Analyzing the effects of various interactions among the different body parts of the robot on its walking behavior

6.2.1 Connection patterns

To examine how the upper-body movements would affect the stable walking behavior of the robot, various connection patterns between the lower and upper body parts were tested throughout the experiments. The experiments were conducted under three groups of connection patterns, without an upper-body mass, with a motionless (fixed) upper-body mass, and with a moving upper-body. Note that a unique air pressure value of the ANS was selected for each connection pattern to get the best possible performance out of it.

Group 1, No Upper-Body mass (NUB)

Before adding an upper-body mass on top of the robot, experiments were conducted to set a baseline for our comparisons. Two types of connection patterns were tested within this group as shown in figure 6.2-a. Under type 1, mutually

connected legs, the air pressure inside the cylinders was adjusted to position the legs at their half-advanced lengths. Then, with a certain combination of open/close valves of the ANS, we allow force transfer between the two legs. In this case, the movement of one leg will affect the other one. For example, as the left leg fully retracts during its stance phase, the right leg will get fully expanded during its swing phase.

Under type 2 connection, independent compliant legs, both cylinders are fully extended by pressurizing the proximal (advancing) chambers with higher pressure value compared to the distal (retracting) ones. The valves of ANS are then kept closed to prevent any direct interaction between the two legs as demonstrated in the figure.

Group 2, Fixed Upper-Body mass (FUB)

The purpose of this group of connection patterns is to investigate the effects of adding a motionless upper-body mass to the robot. The stability performance of the robot will be compared to the connection patterns of Group 1 (NUB). During the experiments conducted within this group, no upper body movement was involved during the robot's locomotion. The swinging mass was mechanically fixed as illustrated in figure 6.2-b. Similar to Group 1, two types of connection patterns were tested, mutually connected legs (type 1) and independent compliant legs (type 2). Both types of connections have no direct interaction with the upper body as shown in the figures.

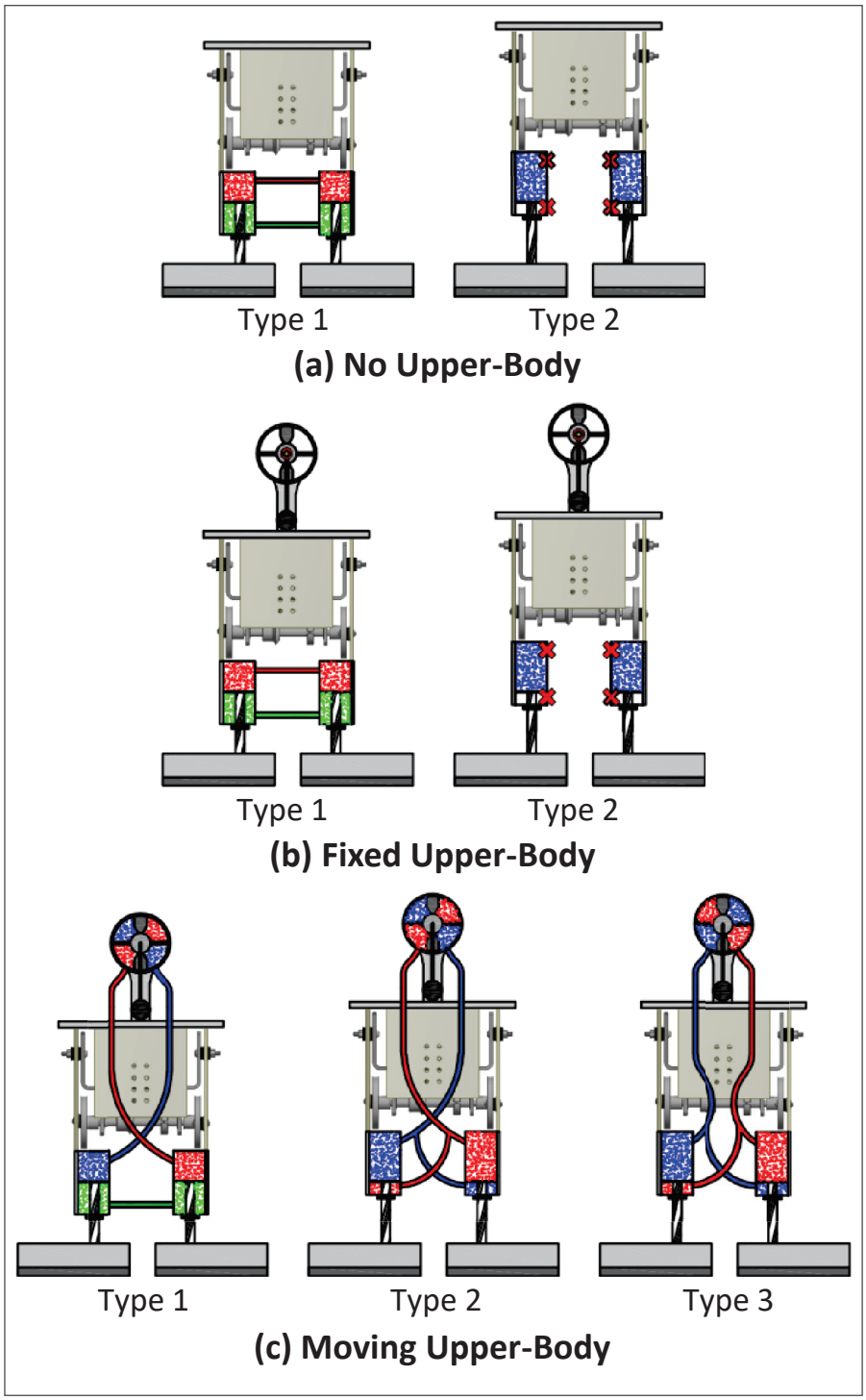

Figure 6.2: The applied connection patterns during experiments with their corresponding initial body posture of the robot. (a) Group 1 connections with no installed upper-body. (b) Group 2 connections with a motionless upper-body. (c) Group 3 connections with a moving upper-body.

Group 3, Moving Upper-Body mass (MUB)

In this group of connections, the movement of the swinging mass contributes to the whole-body dynamics of the robot and affects its walking behavior. The manner of its swinging relates directly to how the rotary actuator is connected with the rest of the ANS components. Three types of connection patterns belonging to this group were tested during the conducted experiment. Under type 1 of connections, the air pressure inside the ANS is adjusted to set the robot's legs at their half-advanced lengths, and the swinging mass is hanging down along the vertical axis (0 deg from the vertical axis). After that, the valve system of the ANS is switched in a way to create the connection pattern demonstrated in figure 6.2-c. In this case, mutual interactions are realized among all actuators of the ANS, between the two legs, as well as between each leg and the swinging mass. Their manner of interaction is demonstrated in figure 6.3-a. For example, as the left leg fully retracts during its stance phase, it will cause the right leg to fully expand and simultaneously rotates the swinging mass 27 deg in the clockwise direction (an opposing direction to the stance leg).

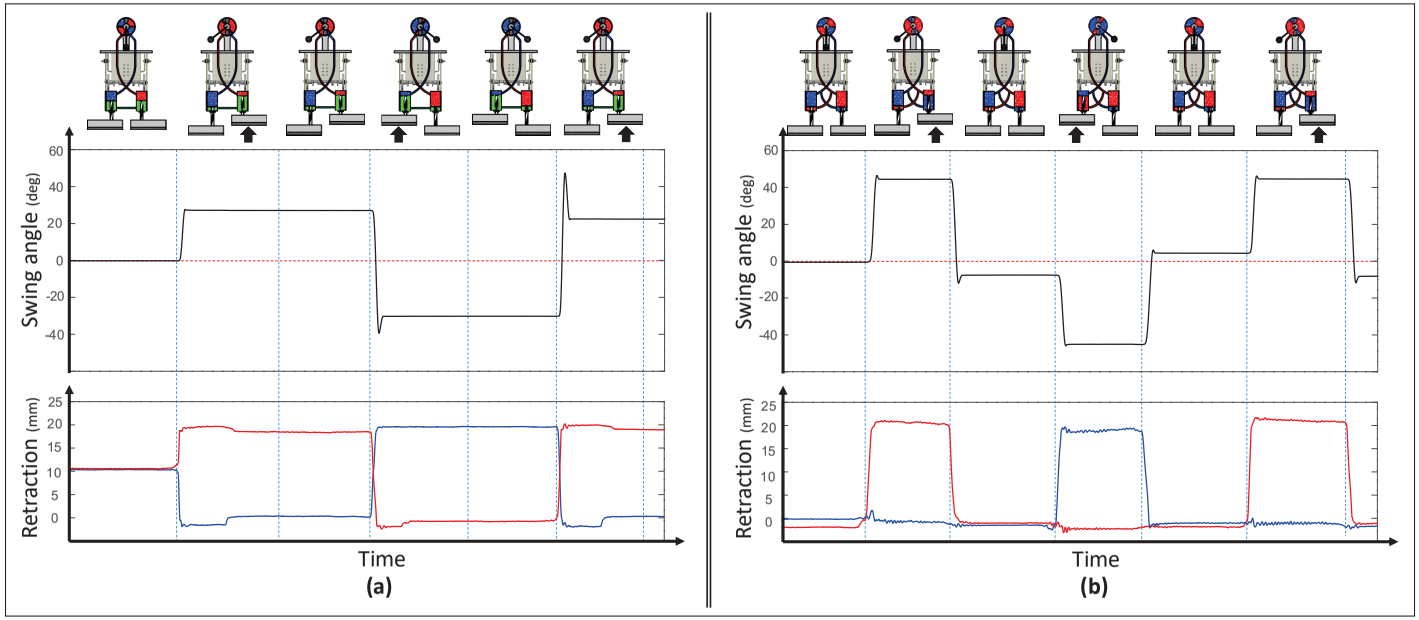

Figure 6.3: The manner of interaction between the lower and upper body parts for:

(a) under the type 1 connection of Group 3 (MUB), and (b) under type 2. The graphs at the bottom show the legs movements (expansion/retraction). The graphs in the middle show the response of the swinging mass to the legs movements. The figures on the top show the corresponding body postures of the robot; and are arranged from left to right as follows: initial posture, applying an external force to the left leg, removing the applied force, applying an external force to the right leg, removing the applied force, then repeat the cycle. The red line represents the left leg. The blue line represents the right leg. The horizontal dashed line at (angle = 0 deg) represents the vertical axis of the robot. A positive swing angle indicates rotation in the clockwise direction, while a negative angle means a counterclockwise rotation.

In the situation of type 2 connection, shown in figure 6.2-c, the air pressure of the ANS is adjusted to create fully expanded legs during the robot's initial posture while the swinging mass is hanging down along the vertical axis. Similar to type 1 of the same group, the interaction between each leg and the upper body will induce the swinging mass to rotate in the opposite direction of the stance leg. However, in this case, there is no "noticeable" interaction between the two legs as illustrated in figure 6.3-b. For example, the retraction of the left leg will cause the swinging mass to rotate 45 deg in the clockwise direction without any noticeable effect on the right leg.

Under type 3 connection, the legs are fully extended while the swinging mass is hanging down along the vertical axis during the initial posture of the robot. While there is no noticeable interaction between the two legs, contrary to type 2 connection, the swinging mass rotates in the same direction with respect to the stance leg. For example, as the left leg hits the ground during locomotion and fully retracts, the swinging mass will rotate 45 deg in the counterclockwise direction while no effect is observed on the movement of the right leg.

6.2.2 Experimental setups and procedures

The experiments were conducted to investigate how the different upper-body interactions with lower-body will influence the stable walking behavior of the robot. For each of the previously mentioned seven connection patterns, the following procedures were implemented during each trial:

1. Adjust the air pressure of the ANS, and manually switch the valves to one of the connection pattern types.

2. Operate the robot, put it on the ground, and then guide its movement direction for the first (0.5 meters) of its locomotion as shown in figure 6.4-b.
3. Release the robot and let it move by itself without guidance until it falls down.
4. Repeat the experiment three times for each type of connection patterns to ensure the reproducibility of the results.

The experiments were performed on a carpet ground material as shown in figure 6.4-a. Reflective markers were installed on the robot's body, as illustrated in figure 6.1, to analyze its dynamics during locomotion. An (OptiTrack-V120: TRIO) motion capture system was employed to record and track these markers.

6.2.3 Results

The evaluation of the robot's performance during the experiments was made by observing the distance traveled by the robot before falling down. This evaluation determines the effects of the applied connection patterns of the ANS on the stable walking behavior of the robot. The longer the distance traveled by the robot before falling down, the more stable it is.

Three trials were conducted for each of the previously mentioned seven types of connection patterns. The graphs of figure 6.5 show the walking paths of all experiments during the robot's locomotion. They show the distance traveled by the robot as well as the movement direction. As can be deduced from the graphs of Group 1 (NUB) connections, the robot without an upper-body mass

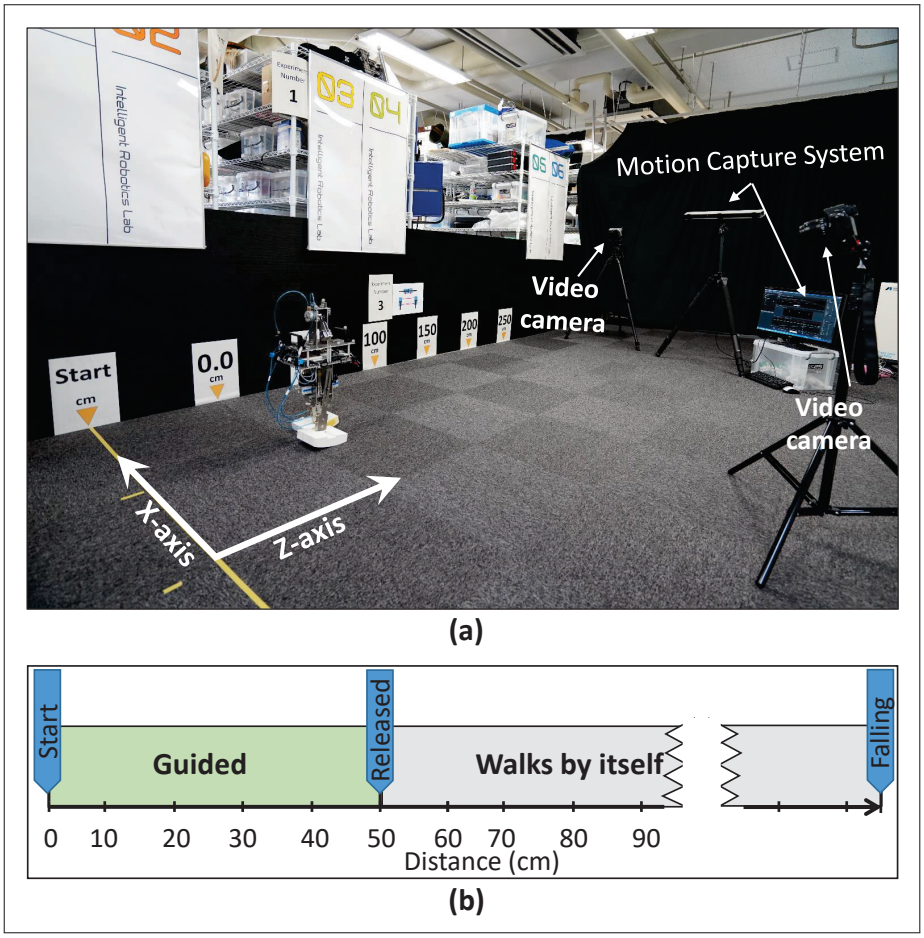

Figure 6.4: (a) Experimental environment. (b) Experimental design.

realized a stable walking behavior under its both types. Under type 1, mutually connected legs, the robot did not fall during any trial; while under type 2, with independent compliant legs, the robot traveled a distance of (2.12 ± 0.08 m) before falling down as depicted in table 6.1. However, both types of this group showed a deviation of their movement directions; type 1 turned (9.04 ± 0.57 deg) to the right during all trials, while type 2 kept turning to the left with a deviation angle of (7.94 ± 2.44 deg).

Once a motionless upper-body mass was added on top of the robot, the robot directly lost its stable behavior. This is evident from the graphs of Group 2 (FUB)

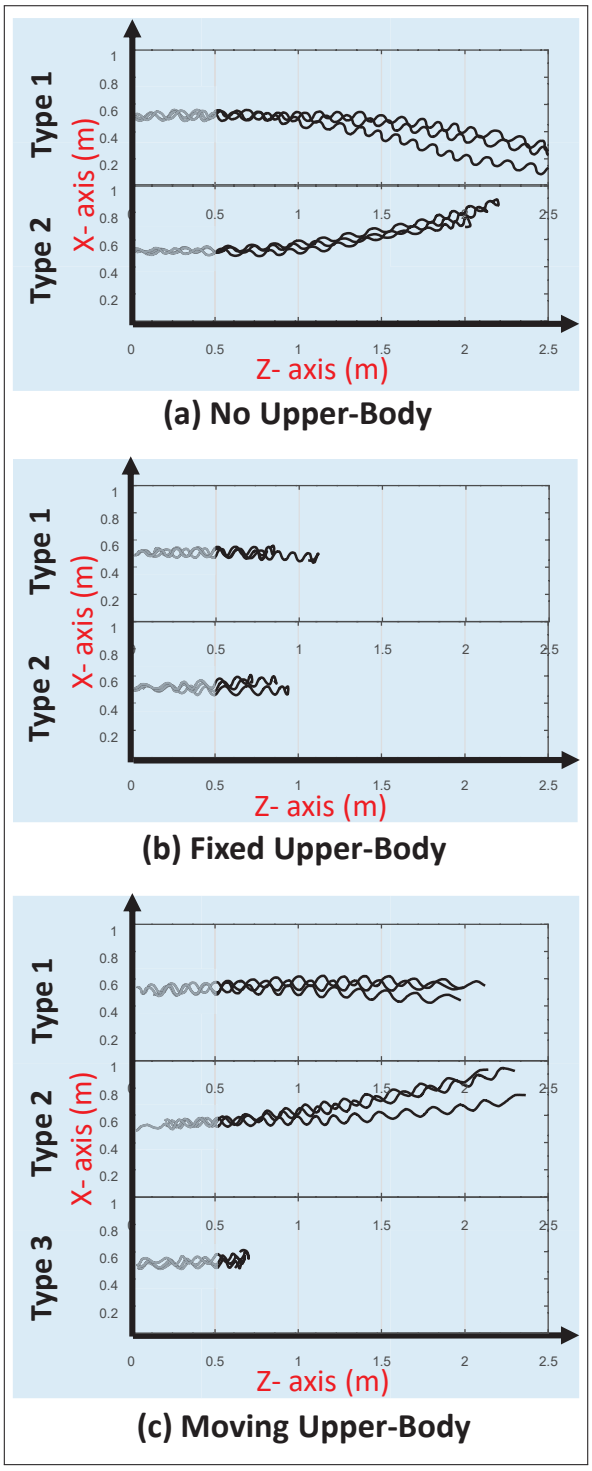

Figure 6.5: Graphs of the waking paths traveled by the robot during all trials for (a) Group 1 connections with no upper-body attached, (b) Group 2 connections with a fixed (motionless) upper-body, and (c) Group 3 connections with a moving upper-body. The faded part at the beginning of each graph (from 0 to 0.5 m) represents the guided period of the robot.

connections; regardless of the connection pattern used between the robot's legs, the robot was only able to move few steps before falling down after it was left to walk by itself without guidance as demonstrated in the table.

On the other hand, the robot retrieved its balance back and gained other preferences too after involving the swinging mass movement of its upper body. With mutually connected legs, and a swinging mass moving in an opposing direction to the stance leg, the robot under type 1 of Group 3 (MUB) connections managed to travel (2.03 ± 0.08 m) before falling down as table 6.1 shows. Not only that but also managed to maintain its moving direction and kept walking straight along the Z-axis as illustrated in the graphs of figure 6.5-c. Under type 2 of the same Group, where no noticeable interactions between the two compliant legs, the robot also exhibited stable behavior by walking (2.27 ± 0.12 m) before falling down. However, the robot during locomotion slightly deviated to the left side with an angle of (9.52 ± 2.70 deg) from the straight path direction. By contrast, with type 3 connection, the interaction between each leg and the upper body causes the swinging mass to oscillate in the same direction with respect to the stance leg. In this case, the robot showed the most unstable behavior among all connection patterns as shown in the table; it directly fell down after it was left to walk by itself without guidance.

Table 6.1: The average distance traveled by the robot, and the deviation angle of its movement from the straight direction

Group	**Connection**	**Traveled distance (m) ± S.D.**	**Deviation angle (deg) ± S.D.**
(1) No Upper-Body	Type1	Did not fall	- 9.04 ± 0.57
	Type2	2.12 ± 0.08	+ 7.94 ± 2.44
(2) Fixed Upper-Body	Type1	0.92 ± 0.17	- 0.04 ± 2.91
	Type2	0.84 ± 0.11	+ 2.92 ± 2.78
(3) Moving Upper-Body	Type1	2.03 ± 0.08	+ 0.14 ± 1.51
	Type2	2.27 ± 0.12	+ 9.52 ± 2.70
	Type3	0.68 ± 0.02	+ 4.02 ± 4.51

The traveled distance covers both the guided and unguided periods. The positive sign of the deviation angle indicates a deviation to the left side with respect to the movement direction, while the negative sign means turning to the right side.

6.3 Discussion

The conducted experiments show the importance of having interconnected parts to achieve stable walking behavior, as evident from the obtained results. By adding a fixed upper-body on top of the robot without being engaged in the interactions with other parts, the robot directly lost its stability. However, once the same upper-body was involved and interacted with the other parts, its movement helped to retrieve the stable behavior of the robot. The significance of having mutually connected parts was shown in the results of every group of connection patterns; the robot with mutually connected legs (type 1) showed better performance compared to independent legs (type 2) for both Groups 1 (NUB) and 2 (FUB). The same is also applied to Group 3 (MUB) of connection patterns; the robot realizes better performances with the proper selection of interactions among its parts.

The movement of the swinging mass in an opposing direction to the stance leg, as in type 1 and type 2 of Group 3 (MUB) connection patterns, reduces the total angular momentum of the body by balancing the rotational motion produced during locomotion. Therefore, we can see the robot generates more stable behaviors under these types of connection patterns. On the contrary, the robot with its upper-body moving in the same direction to its stance leg under type 3 of the same group showed the worst behavior due to the increased reaction moment exerted by stance leg to the ground.

Both type 1 and type 2 connections of Group 3 (MUB) caused the swinging mass to rotate in an opposing direction to the stance leg. However, the amplitude of their rotation angles is different, as can be seen in the graphs of figure 6.3.

These differences in the interactions among the body parts caused the robot to gain different benefits. The robot under type 2 connection relatively traveled longer distance, while under type 1, the robot maintained its moving direction. Therefore, selecting the way of interactions among the different parts should correspond to the gate requirements. And this is similar to what happens during human locomotion; the frequency and amplitude of the arms movements are adaptive to the gate conditions. For example, the amplitude of the arm swing increases proportionally to the walking speed [44].

The simple structure of the added upper-body has demonstrated the possible enhancements in performance that could be acquired by utilizing its interactions with other limbs. However, the advantages gained by the current upper-body are limited to the counterbalancing movement of the swinging mass with respect to the lower body. Therefore, we will upgrade the upper body in the future by expanding the ANS to include a trunk and two arms. This will increase the types of interactions among the interconnected parts, which in turn reflects on the adaptive walking behavior of the robot. For example, the robot would be able to maintain its equilibrium in challenging balancing tasks by bringing the COM back over the base of support.

Switching between the different connection patterns of the ANS was done manually prior to each experiment. Thus, the robot retained the predetermined connection pattern without being able to change it during locomotion. However, as mentioned earlier, the type of connection pattern among the body parts should be selected to suit the gait conditions. Therefore, in the future work, we will replace the manually actuated valves with electronically actuated ones, and realize a control system where the robot can autonomously choose an adequate

connection pattern and operate without continuous human input and guidance.

CHAPTER 7

DISCUSSION

The conducted experiments of the developed robots showed the importance of having interconnected parts to achieve adaptive walking behaviors. As evident from the obtained results, the robots' walking behaviors were changed by changing the interaction between the ANS actuators mounted on their bodies. Based on these differences in the robots' behaviors, their demands for a certain connection pattern differ based on the given situation. For example, the robot OCTANS required mutually connected legs to initiate its locomotion with the lowest driving force while demonstrated the most efficient performance during stationary gait under the condition of independent compliant legs. Pedestri-ANS, likewise, showed the best stability performance on stiff and soft ground surfaces under the conditions of mutually connected and independent rigid legs, respectively. Therefore, there is no Best Connection Pattern that better suits all locomotion conditions and environments. A connection pattern that generates the best performance for a certain gait condition does not necessarily suit other conditions, and vice versa. Thus, exploiting these various dynamics is the way to enable the robot to realize adaptability to any given situation and to develop an efficient gait pattern through all locomotion phases.

If the elements of high-speed processing, precise sensing, and accurate modeling of the surroundings are established, then having a supercomputer under the conventional approach of actively controlled actuators could be the best solution to realize robots able to interact properly with various environments. However, this is not a practical solution due to the high computational complexity. Therefore, to overcome this problem, we are using the principle of ANS to cre-

ate robotic systems capable of interacting with changing environments through passive interactions. Hence, with such systems, robots can spontaneously react to environmental changes passively without waiting for the controller to continuously process the surroundings and actively control the actuators at all times.

The enhancements in the adaptive performance of the developed robots are limited due to their simple mechanical structures that confined the size of the implemented Actuator Network Systems. Therefore, by expanding the ANS to include more parts of the robot's body (such as trunk and two arms), further improvements will be realized in its behavior. This will increase the possible morphological changes and broaden the body dynamics, which in turn reflects on the adaptive walking behavior of the robot and expand its ecological niche.

Automatic switching between different connection patterns during locomotion is an essential ability for these robots in order to operate in unstructured environments. However, changing the connection pattern of an ANS was done manually during most of the experiments conducted in this study. Thus, a robot would retain the predetermined connection pattern without being able to change it during locomotion. However, as mentioned earlier, the type of connection pattern among the body parts should be selected to suit the gait conditions. Therefore, it is crucial to upgrade the design of these robots. This could be done by replacing the manually actuated valves with electronically actuated ones, and realize a control system where a robot can autonomously choose an adequate connection pattern to operate without continuous human input and guidance.

In the current study, a pneumatic-based fluid system is used for force transmission between the actuators of ANS. However, the concept of ANS is not re-

stricted to pneumatic mediums only; it can be expanded to encompass other mediums as well, such as liquid-based fluid systems and electrical systems. For example, electric actuators (e.g., electric motors) can be used for the electric ANS instead of the currently used pneumatic actuators (e.g, air cylinders), the network of valves will be replaced by an array of logic gates to switch the connections, and PWM signals will be used instead of the compressed air.

Implementing an ANS provides a subtle equilibrium between robustness and controllability. It allows easier control of large systems of actuators by creating various passive interactions through different connection patterns and adjusting large quantities of actuators with few input signals (e.g., using pneumatic multiplexer). Therefore, these features of the ANS can be utilized in diverse areas of research besides improving the locomotion gate of a bipedal robot. Possible fields of research with ANS could include the development of shapeshifting robots, kinetic arts, modular robots with remote force transmission, and building human-like robots able to interact with humans by generating designated motions through structural constraints and passive interactions with the inevitable physical contact with the surroundings.

7.1 Various behavioral factors affected by ANS connections

Unlike other mechanical systems that create fixed relations and constraints among links/ joints (e.g., parallel mechanism), ANS can generate various types of interactions among neighboring and distant links/ joints alike by its changeable connection patterns. Therefore, this will widen the domain of applications by increasing the range of adjustability performed on the system. Something similar to the ”Anti-Roll Bar” in automobile suspension systems that connects

opposite wheels together to stabilize vehicles over road irregularities, but on a bigger scale that connects all links of a massive system. Therefore, the different connection patterns of an ANS affect the robot's dynamics in various ways by changing the type of interaction between its body parts. For instance, in the case of PedestraiANS under spring-like legs, the retraction/ expansion of a swinging leg is independent of the other stance leg. On the other hand, in the case of mutually connected legs, the retraction/expansion movement of a swinging leg depends directly on the other stance leg. In light of this, the difference in performance between mutually connected legs and independent compliant legs is not due to a mere difference in compliance; the manner and timing of expansion affect the performance too. Therefore, each of these types of legs shows distinct effects on the gait cycle (e.g., the periods of single and double limb support), angular momentum, rotational slip caused by the yaw moment on the stance leg, ground reaction forces, and so on. In addition to this, the different manners and timing for a swinging leg to get fully extended will consequently have a different effect on positioning the COM of the robot since each of the robot's feet has a considerable mass, which in turn produces different body dynamics.

In order to have a better understanding of the role of ANS in realizing adaptable behaviors and explain why a certain connection pattern is more suitable for a given ground material, the next section attempts to provide some insights to answer these questions based on results obtained from a simulation environment.

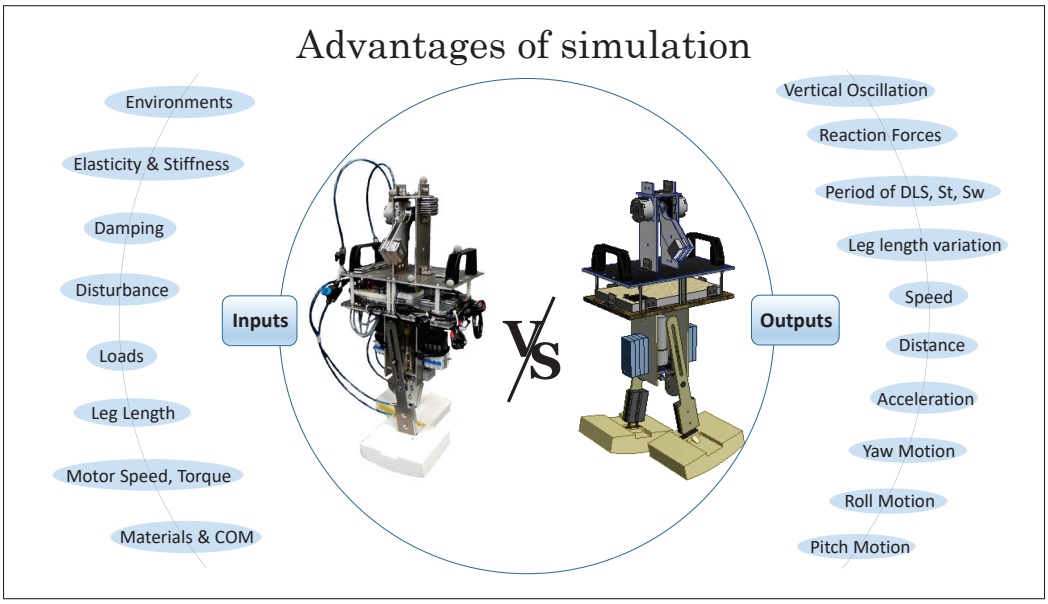

Figure 7.1: Advantages of the dynamic simulation environment.

7.2 Investigating the relationship between a robot's body characteristics and its surroundings through simulation

Having a dynamic simulation environment to analyze the robot's behavior will allow us to extend the tested input parameters, and at the same time, it will provide more data to describe the robot's performance. For example, as shown in figure 7.1, various environmental conditions can be adjusted (e.g., friction, damping, stiffness, etc.) before running the experiments, and a wide range of results can be obtained during and after the experiments. Therefore, with more data in hand, we can further investigate the relationship between the robot's body characteristics and the environment in which the robot is operating.

For this purpose, we are using the Dynamic Simulation environment in Autodesk Inventor, shown in figure 7.2. The theory and methods used to perform dynamic analysis of a mechanical system using this software can be sum-

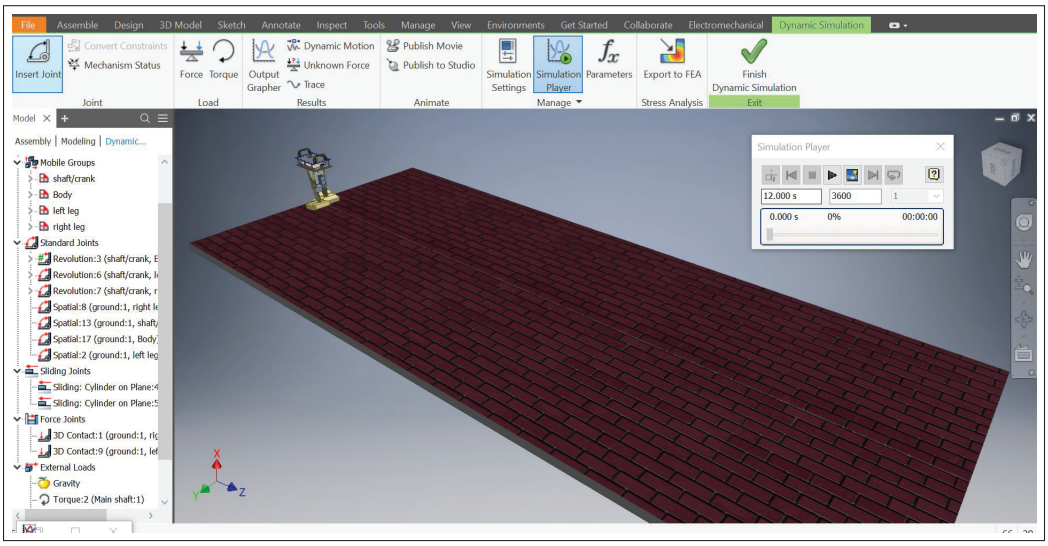

Figure 7.2: The Dynamic Simulation environment of Autodesk Inventor.

marised as follows. Dynamic Simulation is based on multi-body dynamics theory. In this theory, the components of a mechanical system are modeled as rigid bodies interconnected by joints. The constraint equations for each joint are used in conjunction with Lagranges equation of motion to create a system of differential-algebraic equations. The solution of these equations provides the position, velocity, and acceleration of each part, as well as the reaction forces at each joint. Each part is in dynamic equilibrium at each time step of the solution process. This allows the position, velocity, acceleration, and reaction force information at a specific instance to be used as boundary conditions for finite element analysis.

7.2.1 Experimental settings

Simulation experiments were conducted in this section to examine the reasons behind the different effects of ANS's connection patterns to environmental changes. The applied settings to the dynamic simulation environment and the tested parameters are demonstrated through the following points:

- The behavior of the robot PedestriANS with No Upper-Body was investigated.
- The speed of the motor attached to the robot's body was fixed at 120 RPM (similar to the actual robot).
- Three types of legs were tested. 1) Mutually connected legs. 2) Independent spring-like legs. 3) Rigid legs.
- Experiments were conducted on a leveled ground surface with different values of friction, stiffness, and damping.
- The time period of each trial is 12 seconds.
- At the begging of each trial, the robot was guided by external forces to overcome the effect of inertia.

7.2.2 Experimental results

In order to analyze the robot's behavior, two sets of experiments were conducted. The first set of experiments were conducted on a leveled ground with a fixed stiffness (1000 N/mm), fixed damping (1 N s/mm), and variable friction values (0.15, 0.20, 0.25, 0.30, 0.35, 0.40). The second set of experiments were conducted on a ground with a fixed friction (0.25 selected based on the results of

the first experiments), fixed damping (1 N s/mm), and variable stiffness values (20, 40, 50, 100, 500, 1000 N/mm). The effect of different connection patterns of the ANS on the robot responses to environmental changes was investigated by looking into six factors:

1. Movement direction of the robot.
2. Stability performance of the robot (The longer the distance traveled by the robot, the more stable it is).
3. Ground reaction forces.
4. Changes of legs' lengths.
5. Periods of stance phase, swing phase, and double limp support.
6. Robot's speed.

First set of experiments (variable friction)

At a fixed stiffness value and fixed damping between the robot's feet and the ground surface, the robot's requirements for mutually connected legs increase as the friction between the robot's feet and the ground increase. This is evident from the walking path trajectories of the conducted experiments with variable friction values, as shown in figure 7.3. The robot was able to maintain its balance on a high friction surface (frection= 0.35) with only mutually connected legs, where the robot fell down with rigid and independent compliant legs. On the other hand, as the friction decreases, the robot realizes stable behavior (does not fall) regardless of the selected connection pattern between its legs. However, this doesn't mean that the robot's performance is the same. At low values of

friction (0.20, 0.15), the robot with rigid legs was less capable of maintaining its walking direction compared to the other two types of legs.

Changing the friction value affected various aspects of the robot's gait cycle although all other parameters remained unchanged for each connection pattern. For example, these differences in the friction affected the ground reaction forces, the period of stance phase, swing phase, double-limb support, and the robot's speed as shown in the graphs of figures 7.4, and 7.5. The low friction surface of the ground caused an increase in the walking cycle period of the robot, increased the double-limb support (both in time and as a percentage of step duration), and consequently reduced the robot speed. It seems that this increase in the period of DLS caused the robot to maintain its stability (didn't fall down); however, it prevented the robot from maintaining its walking direction as illustrated in the figures.

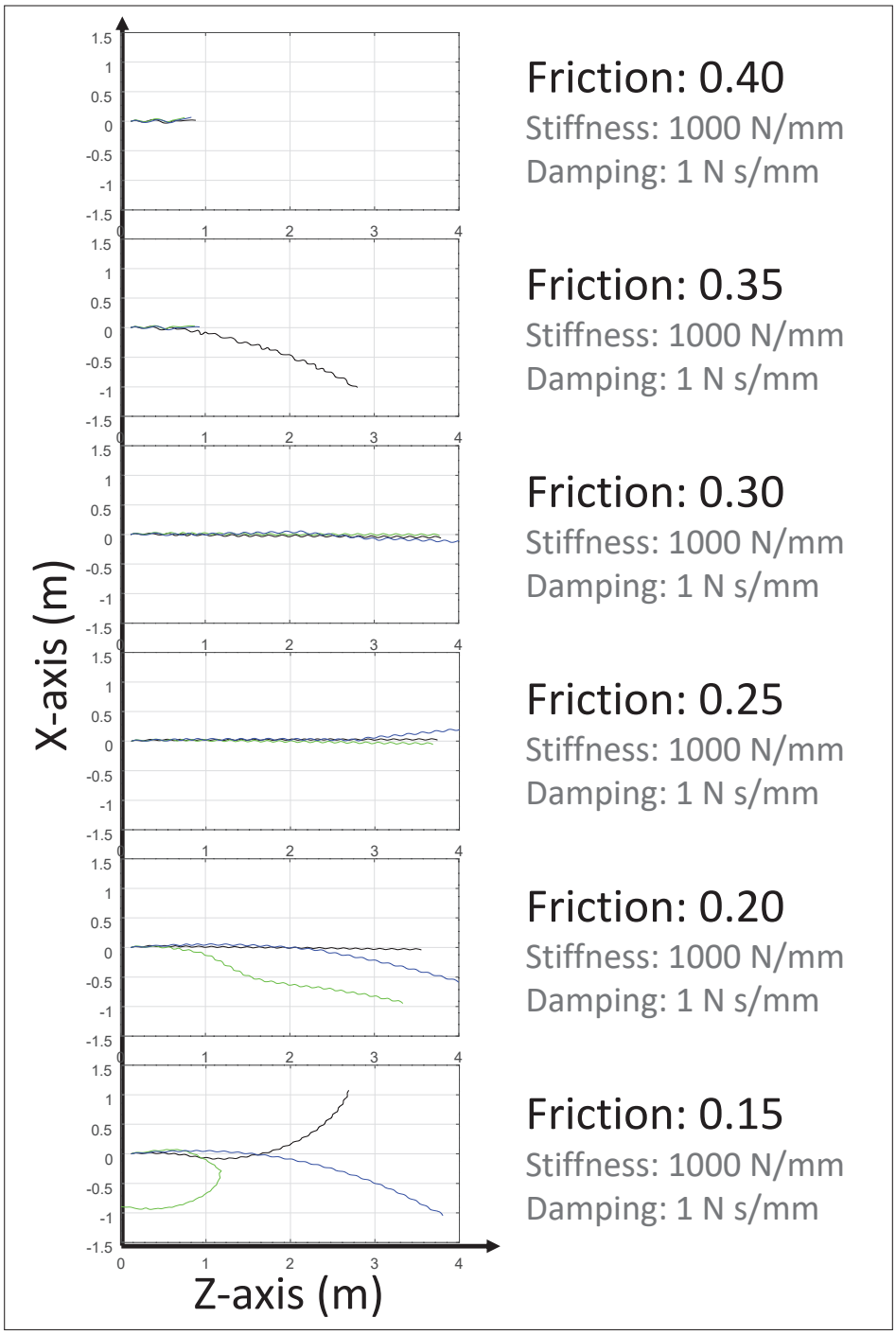

Figure 7.3: Graphs of the walking path trajectories for the experiment conducted on a ground with variable friction values, fixed stiffness (1000 N/mm), and fixed damping (1 N s/mm). The black, blue, and green curves represent the robot with mutually connected, independent compliant, and rigid legs respectively.

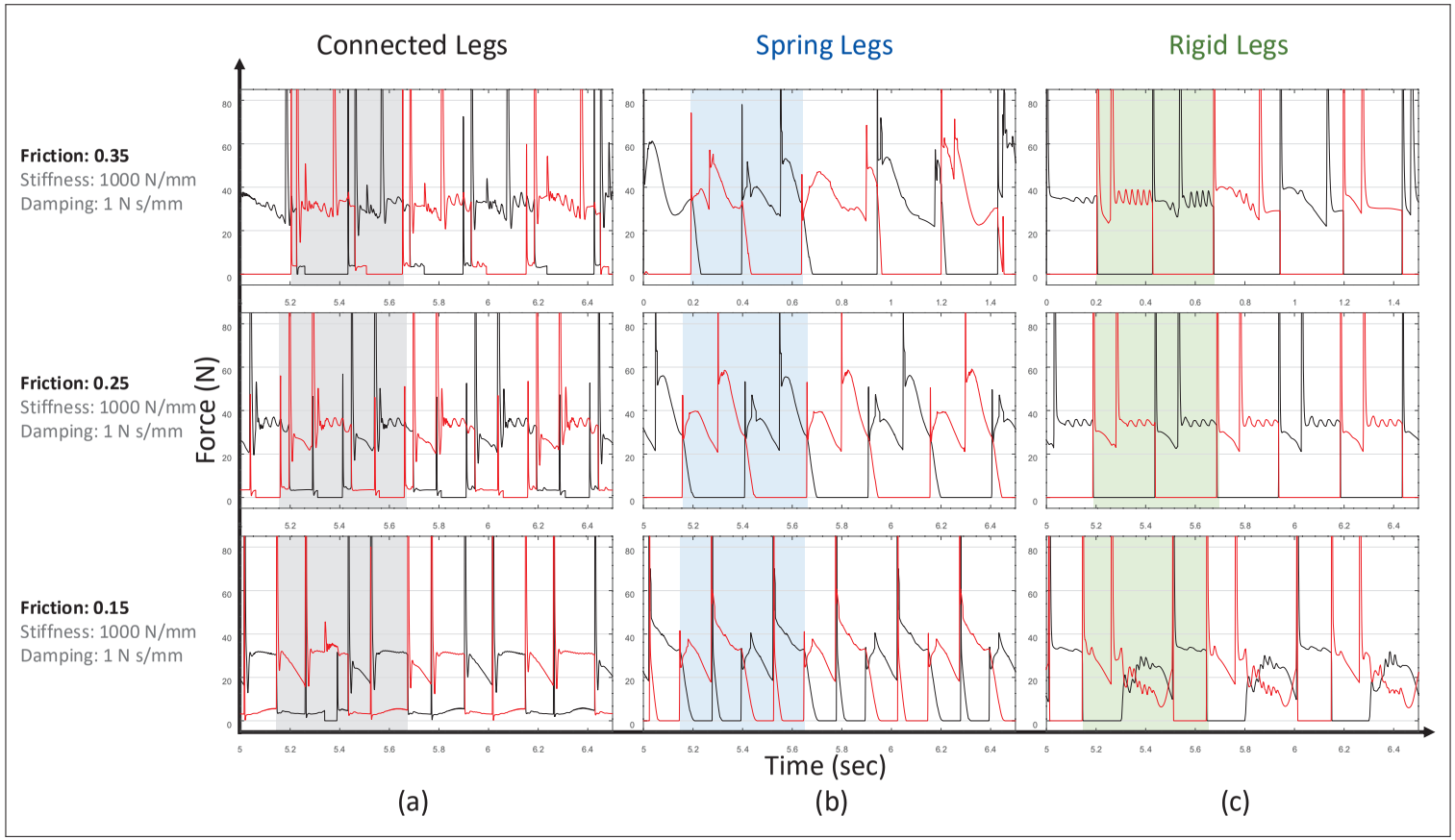

Figure 7.4: Graphs of the ground reaction force of the three types of legs on grounds with three friction values (0.15, 0.25, 0.35). Black curves represent the GRF of the right legs. Red curves represent the GRF of the left legs. The shaded areas indicate one gate cycle (the time period in which one foot contacts the ground to when that same foot again contacts the ground).

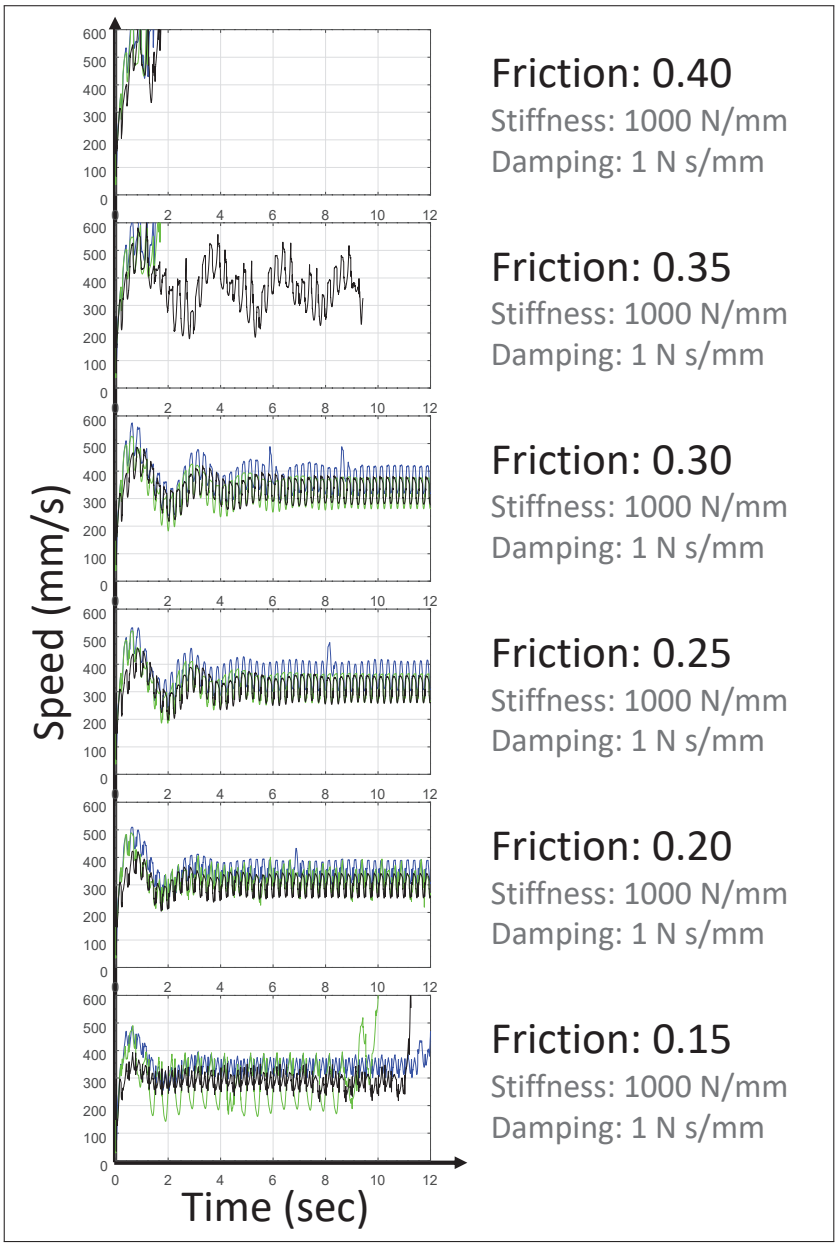

Figure 7.5: Speed graphs of the robot for the experiment conducted on a ground with variable friction values, fixed stiffness (1000 N/mm), and fixed damping (1 N s/mm). The black, blue, and green curves represent the robot with mutually connected, independent compliant, and rigid legs respectively.

Second set of experiments (variable stiffness)

In order to examine the effects of the different connection patterns of the ANS on the robot performance while operating on ground materials with variable stiffness, this section discusses the results obtained from conducting simulation experiments on grounds with variable stiffness at fixed friction and damping. The friction value of (0.25) was selected for this set of experiments based on the results of the variable friction experiments, where the robot under all types of legs showed good performance.

As the stiffness decreases beneath the robot's feet, it becomes more difficult for the robot to attain stable behavior as shown in the walking path graphs of figure 7.6. The robot with independent compliant legs, for instance, directly fell down when operated on a relatively soft ground surface with stiffness values less than 50 N/mm. On the contrary, the robot with rigid legs retained its stability on ground surfaces with stiffness values less than 20 N/mm as it completed the whole operation period without falling down. The robot's performance with mutually connected legs was also better than the independent spring-like legs; however, on grounds with stiffness less than 40 N/mm, the robot fell down after moving a few steps as the graphs show.

Reducing the ground surface's stiffness caused a distortion in the ground reaction force of the robot with spring-like legs as shown in figure 7.7. The robot on the soft ground surface couldn't reproduce the M-shaped ground reaction force (one early and one late peak separated by a minimum around the mid-stance) generated during the stance phase on stiff grounds. The robot's speed decreased as the ground's stiffness decreased beneath the robot's feet as evident from the speed graphs of figure 7.8. However, the robot with spring-like legs

was the fastest, while the robot with rigid and connected legs approximately had the same speed.

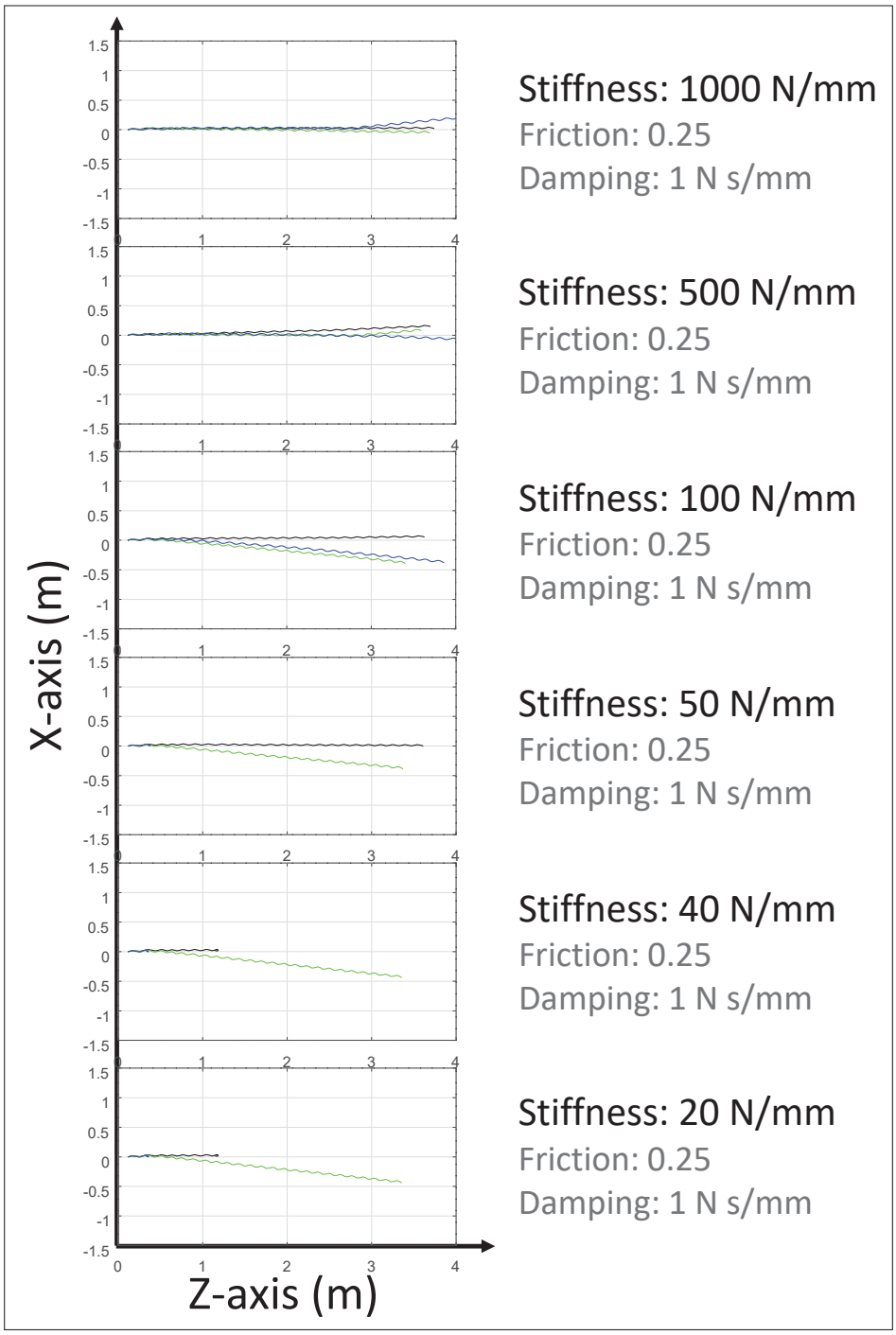

Figure 7.6: Graphs of the walking path trajectories for the experiment conducted on a ground with variable stiffness values, fixed friction (0.25), and fixed damping (1 N s/mm). The black, blue, and green curves represent the robot with mutually connected, independent compliant, and rigid legs respectively.

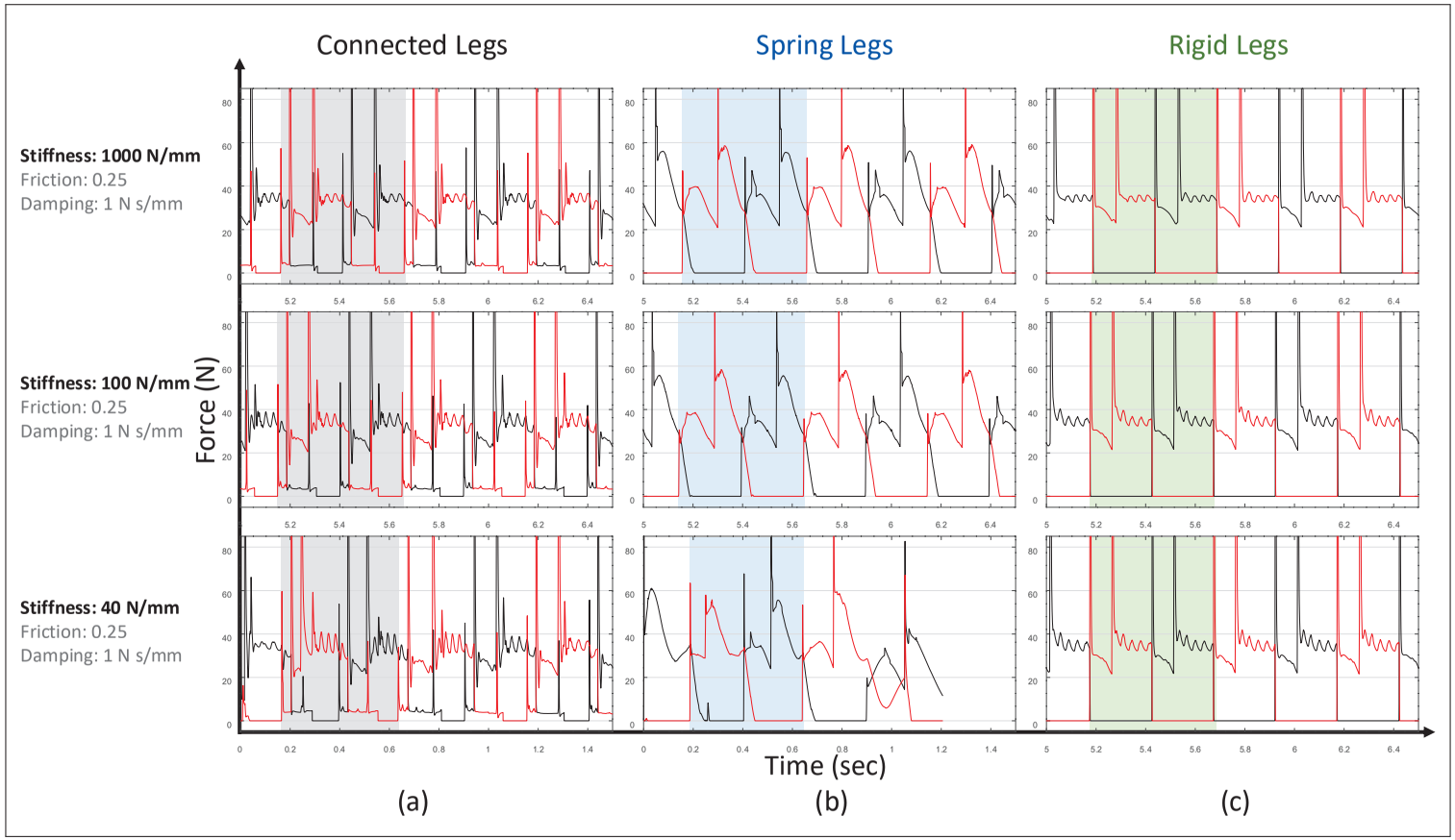

Figure 7.7: Graphs of the groud reaction force of the three types of legs on grounds with three stiffness values (40, 100, 1000 N/mm). Black curves represent the GRF of the right legs. Red curves represent the GRF of the left legs. The shaded areas indicate one gate cycle (the time period in which one foot contacts the ground until that same foot contacts the ground again).

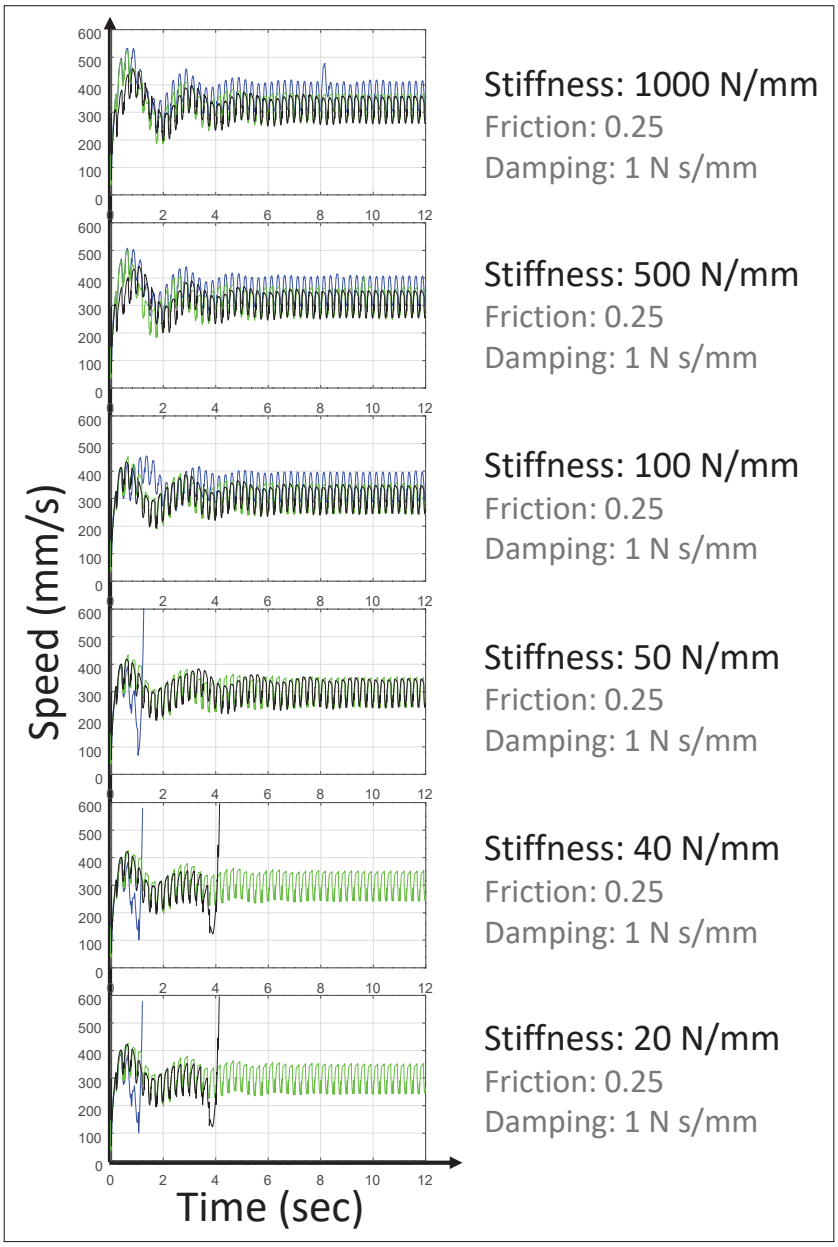

Figure 7.8: Speed graphs of the robot for the experiment conducted on a ground with variable stiffness values, fixed friction (0.25), and fixed damping (1 N s/mm). The black, blue, and green curves represent the robot with mutually connected, independent compliant, and rigid legs respectively.

7.3 Notes

In this chapter, we have only addressed the effects of adjusting two input parameters (friction and stiffness) separately while fixing everything else; and discussed the role of ANS in realizing adaptive behaviors by only considering the results obtained from the walking path trajectories, ground reaction forces, and the robot speed. However, the possible adjustments of input parameters are much more (e.g., compliance adjustment of legs, corresponding force transmission based on the air pressure value, leg lengths, motor speed and torque, applying various loads, the contribution of upper-body, handling disturbances, etc.). The obtained results to examine the relationship between the robot's characteristics and the environment could also include roll motion, pitch motion, yaw motion, vertical oscillation, angular momentum, changes in leg lengths, acceleration, etc.

The simulation findings match the real-world results obtained from the conducted experiments with the PedestriANS robot in almost all aspects. The range of stable locomotion obtained with mutually connected legs is wider compared to the other types of legs as shown in the graphs of figures 7.9, and 7.10. However, there were times where other connection patterns showed better performances; the robot with rigid legs, for instance, was the only robot that had a stable behavior on a low stiffness ground material, and the robot with spring-like legs showed better performance on a slippery ground surface (low friction) since it had a relatively smaller deviation angle from the straight direction during locomotion.

One of the differences between the simulation and real-world results is the

Friction coefficient	Connected Legs		Spring-like legs		Rigid legs	
	Stability	Direction	Stability	Direction	Stability	Direction
0.40						
0.35						
0.30						
0.25						
0.20						
0.15						

Figure 7.9: Summary results of the first set of experiments (variable friction). A shaded cell represents a stable/ maintained straight direction. A light-shaded cell represents a relatively stable/ maintained straight direction. A white (unshaded) cell represents unstable/ didn't maintain a straight direction.

robot's speed. In the simulation experiments, the robot with independent spring-like legs is always faster compared to the other two types of legs. This is due to the fact that this type of legs is the longest. On the other hand, the speed results from the real-world experiments were independent of the legs' length. This is because the speed graphs of the real-world experiments represented the time needed for the robot to reach the target destination; in such a case, the robot with shorter legs could reach the target destination faster than the robot with longer legs if kept moving straight.

Stiffness (N/mm)	Connected Legs		Spring-like legs		Rigid legs	
	Stability	Direction	Stability	Direction	Stability	Direction
1000						
500						
100						
50						
40						
20						

Figure 7.10: Summary results of the second set of experiments (variable stiffness). A shaded cell represents a stable/ maintained straight direction. A light-shaded cell represents a relatively stable/ maintained straight direction. A white (unshaded) cell represents unstable/ didn't maintain a straight direction.

CHAPTER 8

CONCLUSION

This study aims to eventually realize robust robots that can accompany humans, robots that can handle disturbances, and walk effectively over various types of terrains such as grass and gravel. For this purpose, here in our research, we are following the morphological computation approach. This will allow us to exploit the different characteristics of the robot's body, such as elasticity, stiffness, and the various interactions among the different parts of the robot's body itself, and their interactions with the surrounding environment. In order to leverage adaptive morphology in robotic systems, we are implementing the principle of Actuator Network System (ANS). As the term implies, ANS consists of actuators that are mutually interconnected through a network of pipes and valves. Corresponding to each connection pattern among the actuators, distinct dynamics of the robot's body will come out.

To reach the goal of developing robust robots, here in this research, we have built four different legged robots with ANS. Each of these robots represents a step forward towards the target. Therefore, in this dissertation, a full chapter was assigned to present each one of these robots separately. And below is the summary:

CHAPTER 3 presented the development of an eight-legged rimless wheel robot "OCTANS" that uses passive interactions among the air cylinders attached to its legs to transfer energy from one leg to another. With a focus on the role of ANS in transferring energy among the robot's legs, two experiments were conducted to test the effects of different connection patterns on the robot's walking behavior. In the Traveling Distance experiment, we investigated the

distance traveled by the robot after leaving an inclined board as an indication of the robot's efficiency. The results showed that the robot with independent spring-like legs was able to travel a significantly longer distance compared to the robot with mutually interconnected legs. In the Driving Force experiment, we investigated the Motion Initiation Slope Angle needed to trigger the robot's movement as an indication of the minimum driving force required for the robot to start its locomotion. The results showed that the robot with mutually interconnected legs, which realizes energy transfer among its legs during locomotion, needed a smaller MISA to initiate motion compared to the robot with independent spring-like legs.

From the results of both experiments, the robot's demands differ based on the given situation. i.e. Based on the DF experiment, the robot needed a connection pattern that realizes a mutual interaction between its legs to start locomotion with lower driving force, while for a stationary gait pattern, as can be inferred from the TD experiment, the robot required a different connection pattern that prevents any interaction among its legs to reduce energy dissipation during locomotion, and as a result, the robot traveled longer distance. Therefore, by enabling the robot to proactively choose an adequate connection pattern and autonomously change it during locomotion, the robot can realize adaptability to any given situation and develop an efficient gait pattern through all locomotion phases.

CHAPTER 4 introduced the development of a bipedal robot prototype. The robot uses an ANS to transfer energy between its legs through the passive interaction between the pneumatic cylinders mounted on its legs. To examine the effect of the three different types of legs on the stable walking behavior of the

robot, both of the roll motion, and the vertical oscillation of the robot's body were examined during the conducted experiments. As the results showed, having direct interaction with the ability to transfer energy from one leg to the other, the robot was able to move smoother with stable behavior as it realizes low oscillation amplitude of both the roll motion and the vertical oscillation of the robot's body. The robot with rigid legs, by contrast, had the highest oscillation amplitudes of both the roll motion and the vertical oscillation of the robot's body, which led to a noticeable vibration of the robot during locomotion. However, the robot with compliant independent legs showed a behavior in-between the other two types of legs.

CHAPTER 5 demonstrates the development of a bipedal robot with adaptive morphology, called PedestriANS. By using an Actuator Network System (ANS) coupled with the robot's body, the robot is able to adjust the physical characteristics of its legs (compliance and stiffness), as well as changing the way its legs are interacting with each other's and the environment.

To test our hypothesis that a robot performance on varying environments cannot be at its best with a single body morphology, but it needs to respectively change its whole body dynamics for better adaptation, two experiments have been conducted, main and supplementary experiments. The purpose of the main experiment is to examine how effective is changing the robot's morphology on its behavior. Therefore, trials have been conducted on three different ground materials (rigid, slippery, and soft), and under three different connection patterns between the robot's legs (rigid legs, compliant legs, and mutually connected legs). The robot's behavior was evaluated by taking into consideration four aspects, the waking style of the robot, stability, moving direction,

and speed. With every connection pattern on each of the ground materials, as the results showed, the robot generated various dynamics and locomotion behaviors due to the different interactions between the robot's legs themselves, and the environment. These results came to support our hypothesis; the robot required different connection patterns between its legs to show better performances based on the given ground material. For example, a connection pattern that produced stable behavior on a certain ground material, showed unstable behavior on other ground materials, and vice versa.

For the supplementary experiment, the robot's ANS was updated. The robot now is able to switch between the different connection patterns during locomotion. The purpose of this experiment is to put the idea of implementing ANS to the test, and check whether it will enhance the robot's performance during locomotion or not. For this purpose, we used the results obtained from the main experiment. For example, on a rigid ground material, the robot with rigid legs showed unstable behavior; however, on the same ground material, the robot with mutually connected legs established stable behavior. Therefore, by using the same ground material for the supplementary experiment, the robot started its locomotion with rigid legs for a few seconds. Then, it switched to mutually connected legs. Similar to what it was expected; the robot managed to rectify its behavior during locomotion. The robot started its locomotion with unstable behavior. However, after switching its connection pattern, the robot directly started correcting its locomotion to end up with stable behavior.

CHAPTER 6 studied the influence of adding an upper-body to a bipedal robot on its stable walking behavior. The added upper-body forms a swinging mass that oscillates in the frontal plane above the robot's COM. Its movement

pattern (the way it oscillates) depends on the type of interactions created with other limbs since all body parts are mutually interconnected through an Actuator Network System (ANS). Although it has a simple structure and restricted to move in a single plane, the experimental results clearly demonstrated the significance of engaging upper-body movements through its interaction with other body parts during locomotion. Throughout the experiments, the robot with a fixed (motionless) upper-body exhibited unstable walking behaviors, however, once the same upper-body was involved and interacted properly with other body parts, its movement helped to retrieve the stable behavior of the robot.

ACKNOWLEDGMENTS

Alhamdulillah; All praise is due to Allah for giving me the ability to accomplish this work.

First and foremost, I would like to express my sincere thanks to Professor Hiroshi Ishiguro for his invaluable advice and guidance throughout my studies. I would also like to thank my supervisors Dr. Yutaka Nakamura and Dr. Yoshihiro Nakata, for their assistance, patience, and dedicated involvement in every step of this project. They provided a great deal of support and input on my work, and I could not have done it without their help. I would also like to thank all the professors who increased my knowledge in many areas and gave insightful responses to my questions and concerns. I would like to thank my fellow labmates in the ”Smart Mechanics and Machine Learning” group who always offered their help. Even the smallest discussion would always introduce new ideas on how to overcome a problem. I would also like to thank my family and friends for providing me with unfailing support and continuous encouragement throughout my years of study and through the process of researching and writing this dissertation. This accomplishment would not have been possible without them.

APPENDIX A

THE SETUPS AND PROCEDURES OF THE EXPERIMENTS CONDUCTED WITH THE OCTANS ROBOT

The following steps are the detailed procedure performed before and during conducting the experiments of section 3.5.1:

1. Setting cylinders to their half advancing length.

   To get the cylinders advanced to their half stroke, the forces applied on both sides of the piston should have the same value. To get equal forces on both of the piston sides, the amount of pressure needed inside both of the cylinders chambers are measured using the following formula:

$$p = \frac{F}{\mathrm{A}}$$

$$\Rightarrow \quad F = p * A$$

$$\text{if:} \quad F1 = F2$$

$$\Rightarrow \quad p1 * A1 = p2 * A2$$

Where: p: $Pressure$, F: $Force$, A: $Area$.

   And the following steps were performed to get all of the robot legs to their half advanced length before conducting each trial.

   a. Make All of the retracting chambers connected to each other by opening all the valves of group (b) (see figure 3.3-b)

   b. Make all of the advancing chambers connected to each other by opening all the valves of group (a) (see figure 3.3-b)

   c. Using air compressor, pump air into retracting chambers with pressure of p1.

d. Pump air into advancing chambers with pressure of p2.

2. Before starting the experiment, measure the air pressure inside the chambers (p1_pre) and (p2_pre) and record it.
3. Change the connection pattern.
4. Put the robot on the inclined board.
5. Setting the slope angle of the inclined board.

   a. Change the angle of the inclined board step by step by increasing the height of the jack 1cm each time.

   b. Wait for 10 seconds.

   c. Check whether the robot start to move or not

   d. If the robot doesn't move, repeat from (5). Otherwise, move to next step
6. After each trial, measure the air pressures inside the cylinders.

   a. Make All of the retracting chambers connected to each other by opening all the valves of group (b) (see figure 3.3-b)

   b. Make all of the advancing chambers connected to each other by opening all the valves of group (a) (see figure 3.3-b)

   c. Measure the air pressure inside the chambers (p1_post) and (p2_post) and record it.
7. Compare the pressure values pre and post the experiment. If the pressure values are the same, record the experiment result (traveled distance or MISA) and go to (1) to do next trial. Otherwise go to (1) and repeat the same trial.

BIBLIOGRAPHY

[1] N. A. Bernstein, (translated from the Russian by M.L. Latash and edited by M.L. Latash and M.T. Turvey). Dexterity and Its Development. Lawrence Erlbaum Associates, Mahmash, New Jersey, 1996.

[2] S. Aoi, P. Manoonpong, Y. Ambe, F. Matsuno, & F. Wrgtter, Adaptive Control Strategies for Interlimb Coordination in Legged Robots: A Review. Frontiers in Neurorobotics, 11, 39, 2017.

[3] S. Collins, A. Ruina, R. Tedrake, & M. Wisse, Efficient bipedal robots based on passive-dynamic walkers. Science, 307, 1082-1085, 2005.

[4] D. Torricelli, J. Gonzalez, M. Weckx, R. Jimenez-Fabia n, B. Vanderborght, M. Sartori, & . . . J. L. Pons, Human-like compliant locomotion: State of the art of robotic implementations. Bioinspiration & Biomimetics, 11, Article 051002, 2016.

[5] R. Pfeifer, & J. Bongard, How the body shapes the way we think: A new view of intelligence. Cambridge, MA: The MIT Press, 2006.

[6] K. Kaneko, F. Kanehiro, M. Morisawa, K. Akachi, G. Miyamori, A. Hayashi, & N. Kanehira, Humanoid robot HRP-4 Humanoid robotics platform with lightweight and slim body. Proceedings of the 2011 IEEE/RSJ International Conference on Intelligent Robots and Systems (IROS2011), 2011.

[7] M. Hirose, & K. Ogawa, Honda humanoid robots development. Philosophical Transactions of the Royal Society A, 365, 11-19, 2007.

[8] S. Mintchev, & D. Floreano, Adaptive morphology: A design principle for multimodal and multifunctional robots. IEEE Robotics & Automation Magazine, 23, 3, 4254, 2016.

[9] R. Pfeifer, M. Lungarella, & F. Iida, Self-organization, embodiment, and biologically inspired robotics. Science, 318, 5853, 10881093, 2007.

[10] T. McGeer, Passive dynamic walking. The International Journal of Robotics Research, 9(2), 62-82, 1990.

[11] S. H. Collins, M. Wisse, & A. Ruina, A three dimensional passive-dynamic walking robot with two legs and knees. The International Journal of Robotics Research, 20, 607-615, 2001.

[12] R. Tedrake, T. W. Zhang, M. Fong, & H. S. Seung, Actuating a simple 3D passive dynamic walker. Proceedings of IEEE International Conference on Robotics and Automation, New Orleans, LA, 2004.

[13] G. A. Pratt, & M. M. Williamson, Series elastic actuators. Proceedings of IEEE International Conference on Intelligent Robots and Systems, Pittsburgh, PA, 1995, August 5-9.

[14] R. V. Ham, S. Thomas, B. Vanderborght, K. Hollander, & D. Lefeber, Compliant actuator designs: Review of actuators with passive adjustable compliance/controllable stiffness for robotic applications. IEEE Robotics and Automation Magazine, 16,3,8194, 2009.

[15] B. Vanderborght, A. Albu-Schaeffer, A. Bicchi, E. Burdet, D. G. Caldwell, R. Carloni, & . . . S. Wolf, Variable impedance actuators: A review. Robotics and Autonomous Systems, 61, 1601-1614, 2013.

[16] M. Wisse. Essentials of Dynamic Walking : Analysis and Design of Two-Legged Robots. PhD thesis, Technische Universiteit Delft, 2004.

[17] D. Hobbelen, T. De Boer, & M. Wisse, System overview of bipedal robots flame and TUlip: Tailor-made for limit cycle walking. IEEE/RSJ International Conference on Intelligent Robots and Systems, Nice, France, 2008.

[18] K. Hosoda, T. Takuma, A. Nakamoto, & S. Hayashi, Biped robot design powered by antagonistic pneumatic actuators for multi-modal locomotion. Robotics and Autonomous Systems, 56, 46-53, 2008.

[19] H. Ryu, Y. Nakata, Y. Nakamura, & H. Ishiguro, Adaptive whole-body dynamics: An actuator network system for orchestrating multijoint movements. Robotics & Automation Magazine, 14(8), 85-92, 2015.

[20] H. Ahmad, Y. Nakata, Y. Nakamura, & H. Ishiguro, A Bipedal Robot with an Energy Transfer Mechanism between Legs: A Pilot Study. IEEE International Conference on Robotics and Biomimetics (ROBIO) 2018, Kuala Lumpur, Malaysia.

[21] H. Ahmad, Y. Nakata, Y. Nakamura, & H. Ishiguro, A study on energy transfer among limbs in a legged robot locomotion. Adaptive Behavior, 26, 6, 309-321, 2018.

[22] S. Yu, Y. Nakata, Y. Nakamura and H. Ishiguro, "A design of robotic spine

composed of parallelogram actuation modules," *Artificial Life and Robotics*, vol.22, no.4, pp.477-482 (2017).

[23] T. Hashizume, Y. Nakata, Y. Nakamura and H. Ishiguro, "Adjustable response of a robotic arm by switching paths of an actuator network system," *International Symposium on Artificial Life and Robotics*, Beppu, Japan, 416-419 (2017).

[24] D. Gouaillier, V. Hugel, P. Blazevic, C. Kilner, J. Monceaux, P. Lafourcade, etl.(2009). Mechatronic design of NAO humanoid. IEEE International Conference on Robotics and Automation-Kobe-Japan

[25] Collins, A. Ruina, R. Tedrake, & M. Wisse. (2005). Efficient Bipedal Robots Based on Passive-Dynamic Walkers. Science, vol. 307, no. 5712, pp. 1082-1085.

[26] Scott Miller, Rico Jovanni Ulep, Ezra Ameperosa, Kyle Seay, & Pranav Bhounsule. (2015). The Roadrunner: A 2-D Powered Rimless Wheel Robot for Energy-efficient and Rough Terrain Locomotion. Conference: Dynamic Walking Columbus, Ohio

[27] Ryosuke Inoue, Fumihiko Asano, Daiki Tanaka & Isao Tokuda. (2011). Passive Dynamic Walking of Combined Rimless Wheel and Its Speeding-up by Adjustment of Phase Difference. IEEE/RSJ International Conference on Intelligent Robots and Systems

[28] Diego Torricelli, Jose Gonzalez, Maarten Weckx, Ren Jimnez-Fabin, Bram Vanderborght, Massimo Sartori, etl.(2016). Human-like compliant locomotion: state of the art of robotic implementations. IOP publishing- Bioinspir. Biomim. 11 (2016) 051002

[29] Fumihiko Asano and Junji Kawamoto. (2012). Passive Dynamic Walking of Viscoelastic-legged Rimless Wheel. IEEE International Conference on Robotics and Automation

[30] Coleman, M. J., Chatterjee, A., & Ruina, A. (1997). Motions of a rimless spoked wheel: a simple three-dimensional system with impacts. Dynamics and Stability of Systems 12:139159.

[31] D. Neumann. (2009). kinesiology of the musculoskeletal system foundation for rehabilitation. second edition page.656. Mosby.

[32] Anthony J. Blazevich. (2007). Sports Biomechanics: The Basics: Optimising Human Performance.A&C Black.

[33] H. Kim, J. Choi, & T. Seo, Optimal Design of Klann-based walking Mechanism for Water-running Robots. The 14th IFToMM World Congress, Taipei, Taiwan, 2015.

[34] V. S. Karelin, On the synthesis of the inverted slider-crank mechanisms for approximate straight-line motion. Mechanism and Machine Theory, 21, I, 13-18, 1986.

[35] R. Ringrose, Self-stabilizing running. Proceedings of International Conference on Robotics and Automation IEEE, 1, 487-493, 1997.

[36] D. Webb, Maximum walking speed and lower limb length in hominids. American Journal of Physical Anthropology.101,4,515-525, 1996.

[37] F. Zhao, & J. Gao, Anti-Slip Gait Planning for a Humanoid Robot in Fast Walking. Applied Sciences. 9, 13, 2657, 2019.

[38] J.C. Dean, & A.D. Kuo. Elastic coupling of limb joints enables faster bipedal walking. Journal of the Royal Society Interface. 6, 35, 561573, 2009.

[39] M. Luneckas, T. Luneckas, & D. Udris. Leg placement algorithm for foot impact force minimization. International Journal of Advanced Robotic Systems. 15, 1, 2018.

[40] J. L. Baird, "The role of the upper body in human locomotion," *Electronic Doctoral Dissertations for UMass Amherst*. Paper AAI3545899 (2012).

[41] K. J. Bostrm, T. Dirksen, K. Zentgraf and H. Wagner, "The Contribution of Upper Body Movements to Dynamic Balance Regulation during Challenged Locomotion," *Front. Hum. Neurosci.* 12:8 (2018). doi: 10.3389/fnhum.2018.00008.

[42] H. Herr and M. Popovic, "Angular momentum in human walking," *J. Exp. Biol.* 211, 467481 (2008). doi: 10.1242/jeb.008573.

[43] A. K. Silverman, J. M. Wilken, E. H. Sinitski and R. R. Neptune, "Whole-body angular momentum in incline and decline walking," *J. Biomech.* 45, 965971 (2012). doi: 10.1016/j.jbiomech.2012.01.012.

[44] S. F. Donker, T. Mulder, B. Nienhuis and J. Duysens, "Adaptations in arm movements for added mass to wrist or ankle during walking," *Experimental Brain Research*, 146, 1, 2631 (2002).

LIST OF PUBLICATIONS

- Huthaifa Ahmad, Yoshihiro Nakata, Yutaka Nakamura, and Hiroshi Ishiguro, "The influence of upper-body movements and its interactions with the lower-body parts on the stable locomotion of a bipedal robot," [Article under review].

- Huthaifa Ahmad, Yoshihiro Nakata, Yutaka Nakamura, and Hiroshi Ishiguro, "PedestriANS: a bipedal robot with adaptive morphology," *Adaptive Behavior*, Article first published online February (2020). doi: 10.1177/1059712320905177.

- Huthaifa Ahmad, Yoshihiro Nakata, Yutaka Nakamura, and Hiroshi Ishiguro, "A Bipedal Robot with an Energy Transfer Mechanism between Legs: A Pilot Study," *IEEE International Conference on Robotics and Biomimetics (ROBIO)*, Kuala Lumpur, Malaysia, 1256-1261 (2018).

- Huthaifa Ahmad, Yoshihiro Nakata, Yutaka Nakamura, and Hiroshi Ishiguro, "A study on energy transfer among limbs in a legged robot locomotion," *Adaptive Behavior*, 26, 6, 309321 (2018).

- Huthaifa Ahmad, Yoshihiro Nakata, Yutaka Nakamura, and Hiroshi Ishiguro, "Switching locomotion of a four-legged robot by changing the connection patterns of an actuator network system," *The 22nd International Symposium on Artificial Life and Robotics (AROB)*, Beppu, Japan, 338-341 (2017).